APPENDIX 1

Report of the 2000 Planning Workshop on Designing the Iron Fertilization Experiment in the Subarctic Pacific

Table of Contents

A1.1 2000 WORKSHOP SUMMARY

The workshop on "Designing the Iron Fertilization Experiment in the Subarctic Pacific" was held October 19–20, 2000 in Tsukuba, Japan. The workshop was co-sponsored by PICES and CRIEPI (Central Research Institute of Electric Power Industry, Japan).

The specific objectives of the workshop were to:

1. Establish the current knowledge about the role of iron in limiting phytoplankton production in the subarctic Pacific;
2. Identify the specific questions that should be answered by the *in situ* iron fertilization experiment in the subarctic Pacific;
3. Initiate planning for the experiment, including logistics and funding, *etc*.

The workshop had the following scientific sessions:

1. General overview of IronEx and SOIREE, iron chemistry and biology in seawater;
2. Chemisty in the North Pacific and IronEx;
3. Biology in the North Pacific and IronEx;
4. Physics in the North Pacific and iron addition techniques.

The workshop was very successful thanks to 19 excellent presentations and the spirited discussion from the 39 participants.

A1.1.1 Proposed experiment summary

Background

The North Pacific is one of the three large high nitrate, low chlorophyll (HNLC) regions, along with the equatorial Pacific and the Southern Ocean that has been identified to be iron-limited (Martin *et al.*, 1991). Large-scale iron enrichment experiments have been conducted in the equatorial Pacific (IronEx II; Coale *et al.*, 1996) and in the Southern Ocean (SOIREE; Boyd *et al.*, 2000).

There are two prominent gyres in the North Pacific, the Alaska Gyre (hereafter called the Eastern Subarctic Gyre (ESG) with Station P on its southern edge) and the Western Subarctic Gyre (WSG). The input of iron for the North Pacific is thought to come mainly from the atmospheric deposition of Asian dust from the Gobi Desert (Duce and Tindale, 1991). Hence, there is a strong zonal gradient in iron deposition with the WSG receiving more dust than the eastern gyre. Evidence for this gradient in atmospheric iron deposition can be seen in the concentration gradient of soluble iron (0.85 nM in the WSG versus 0.53 nM in the ESG), and in the phytoplankton community (the WSG has more centric diatoms and a spring bloom, while the ESG has smaller cells (prymnesiophytes and prasinophytes) and more pennate diatoms and no spring bloom (Kudo, pers. comm.)). Opal dominates the carbon flux in the WSG while $CaCO_3$ dominates the flux in the ESG (Kudo, pers. comm.). The WSG has been studied mainly by Japanese scientists, while one site in the ESG (Station P) has been studied mainly by Canadian scientists (*e.g.*, see *Deep-Sea Research II,* Vol. **46** on Canadian JGOFS). An extensive comparison of the different trophic levels in the WSG and the ESG has recently been summarized in a special volume of *Progress in Oceanography* (Vol. **43** (2/3) and in particular, see Harrison *et al.*, 1999; Banse and English, 1999) and hence, a thorough background of information exists for designing our proposed iron enrichment experiments. We are proposing to continue this previously successful collaboration between Japan and Canada and invite international collaborators to join us in these intensive large-scale iron enrichment experiments where we have gaps in our expertise.

There are several strong reasons to conduct two large-scale iron enrichment experiments along this large-scale iron deposition gradient in the WSG (with high deposition) and in the ESG (with low deposition). These two sites are located in a quiescent area of the ocean with a shallow mixed layer depth in summer (20–30 m), a strong relatively shallow pycnocline (~100 m), weak and well defined surface currents, few frontal areas, and an excellent long-term time series (spanning more than 40 years in the case of Station P in the ESG).

Furthermore, each site can be reached in 2 to 3 days' travel time from major oceanographic laboratories in Japan and Canada. Therefore, this proximity will facilitate a revisit to the sites to determine the fate of the bloom and the associated response of grazers, climate change biogas production, and ligand production by the microbial community.

Shipboard iron enrichment experiments have revealed that centric diatoms grow in WSG water (Kudo, pers. comm.), in contrast to a pennate diatom-dominated community in the ESG (Martin *et al.*, 1991). This difference in the final phytoplankton community will allow comparisons in the response of grazers, carbon flux, the production of climate change biogasses and a wide range of other parameters.

The iron enrichment experiment in the WSG in particular, will represent a simulation of the annual episodic dust input from the Asian continent. Future plans of the Japanese **S**urface **O**cean **L**ow **A**tmosphere **S**tudy (SOLAS) program are to determine the input and effects of one of these dust events on the WSG. Therefore, it is important that a simulated, controlled addition of iron proceed after assessing the response of the WSG to a natural episodic dust event.

The iron enrichment experiment in the WSG and ESG will be conducted with the same methods and key principal investigators (Kenneth H. Coale, Phillip W. Boyd, and Cliff S. Law) as used in IronEx II and the **S**outhern **O**cean **I**ron **RE**lease **E**xperiment (SOIREE). Therefore, these two iron enrichment experiments and IronEx and SOIREE will offer an important contrast along a latitudinal gradient. The subarctic North Pacific represents a site where biological and chemical reactions (based on surface water temperature) should be intermediate between the previous tropical and polar iron enrichment sites. For example, the bloom developed very quickly in IronEx II (Coale *et al.*, 1996) while in SOIREE, the bloom appeared to last >40 days according to SeaWiFS images (Boyd *et al.*, 2000).

Hypotheses

The North Pacific has two prominent gyres, the western and eastern subarctic gyres (WSG and ESG). These two gyres are characterized by relatively uniform distributions in temperature, salinity, macronutrients, and light, yet they have strong zonal gradients in atmospheric iron deposition between the WSG and the ESG.

We hypothesize that:

1. the difference in episodic iron deposition gives rise to distinct phytoplankton communities (*e.g.*, centric diatoms in the WSG versus pennates in the ESG) which characterize these biogeochemical provinces;
2. the biogeochemical response of any given province (air–sea fluxes in biogases, export flux of carbon, *etc.*) is driven by episodic events such as atmospheric iron deposition.

To test these hypotheses, an iron enrichment experiment, on the scale of the entire community, is required in each gyre such that the biological community response and the resultant geochemical signals can be measured. These iron enrichment experiments will simulate natural episodic dust deposition events that occur annually, especially in the WSG.

In addition to measuring the response of a wide range of biogeochemical parameters to a large-scale iron enrichment, we hypothesize that:

- the WSG will have a higher carbon flux dominated by an opal flux, in contrast to the ESG which will have a lower carbon flux dominated by a $CaCO_3$ flux. Thus the efficiency of the biological pump will be higher in the WSG than in the ESG;
- there will be a larger response (more grazing) by the mesozooplankton in the WSG than in the ESG, which could lead to an increase in carbon flux through fecal pellet production;
- there will be more biogas production, especially dimethyl sulphide (DMS) production, due to the larger number of prymnesiophytes in the ESG compared to the WSG;
- there will be more ligands produced by the microbial community in the ESG than in the WSG because the microbial loop is more dominant in the ESG than in the WSG.

Scientific questions

- What is the fate/longevity of the bloom with an emphasis on ligand production and the response of the grazers (micro and mesozooplankton)?

- What is the magnitude and characteristics of particles (carbon flux) sinking at the end of the bloom?
- What is the production of various climate change biogases (DMS, N_2O, methane, *etc.*) during and after the bloom?

References

Banse, K. and English, D.C. 1999. Comparing phytoplankton seasonality in the eastern and western subarctic Pacific and the western Bering Sea. *Prog. Oceanogr.* **43**: 235–288.

Boyd, P.W., Wong, C.S., Merrill, J., Whitney, F., Snow, J., Harrison, P.J. and Gower, J. 1998. Atmospheric iron supply and enhanced vertical flux in the NE subarctic Pacific: Is there a connection? *Global Biochem. Cycles* **12**: 429–441.

Boyd, P.W., Watson, A.J., Law, C.S. *et al.* 2000. A mesoscale phytoplankton bloom in the polar Southern Ocean stimulated by iron fertilization. *Nature* **407**: 695–701.

Coale, K.H., Johnson, K.S., Fitzwater, S.E. *et al.* 1996. A massive phytoplankton bloom induced by an ecosystem-scale iron fertilization experiment in the equatorial Pacific Ocean. *Nature* **383**: 495–501.

Duce, R.A. and Tindale, N.W. 1991. Atmospheric transport of iron and its deposition in the ocean. *Limnol. Oceanogr.* **36**: 1715–1726.

Harrison, P.J., Boyd, P.W., Varela, D.E., Takeda, S., Shiomoto, A. and Odate, T. 1999. Comparison of factors controlling phytoplankton productivity in the NE and NW subarctic Pacific gyres. *Prog. Oceanogr.* **43**: 205–234.

Martin, J.H., Gordon, R.M. and Fitzwater, S.E. 1991. The case for iron. *Limnol. Oceanogr.* **36**: 1793–1802.

Other useful references

Data of the M/V *Skaugran* is available at: http://www.mirc.jha.or.jp/minnano/CGER_NIES/skaugran/index.html

Harrison, P.J. Unpublished. Station Papa time series: insights into ecosystem dynamics. In particular, see the summary table of various parameters.

Hashimoto, S. and Shiomoto, A. 2000. High-west and low-east in April and no trend in August in chlorophyll a concentration and standing stock in the subarctic Pacific in 1999. *Bull. Jpn. Soc. Fish. Oceanogr.* **64**: 161–172.

Kuma, K., Katsumoto, A., Kawakami, H., Takatori, F. and Matsunaga, K. 1998. Spatial variability of Fe(III) hydroxide solubility in the water column of the northern North Pacific Ocean. *Deep-Sea Res. I* **45**: 91–113.

Kuma, K., Nishioka, J. and Matsunaga, K. 1996. Controls on iron(III) hydroxide solubility in seawater: the influence of pH and natural organic chelators. *Limnol. Oceanogr.* **41**: 396–407.

Nojiri, Y., Fujinuma, Y., Zeng, J. and Wong, C.S. 1999. Monitoring of pCO_2 with complete seasonal coverage utilizing a cargo ship M/S *Skaugran* between Japan and Canada/US. Proceedings of the Second International Symposium on CO_2 in the Oceans, pp. 17–23.

Shiomoto, A. and Asami, H. 1999. High-west and low-east distribution pattern of chlorophyll-a, primary productivity and diatoms in the subarctic North Pacific surface waters, midwinter 1996. *J. Oceanogr.* **55**: 493–503.

Shiomoto, A. and Ishida, Y. 1998. Primary production and chlorophyll *a* in the northwestern Pacific Ocean in summer. *J. Geophys. Res.* **103**: 24,651–24,661.

SUPER 1993. (National Science Foundation Project) See special volume of *Progress in Oceanography* **32** on results from Station P.

Taniguchi, A. 1999. Differences in the structure of the lower trophic levels of pelagic ecosystems in the eastern and western Pacific. *Prog. Oceanogr.* **43**: 289–315.

Tsuda, A., Saito, H. and Kasai, H. 2001. Geographical variation of body size of *Neocalanus cristatus*, *N. plumchrus* and *N. flemingeri* in the subarctic Pacific and its marginal seas: Implication of the origin of large form *N. flemingeri* in Oyashio area. *J. Oceanogr.* **57**: 341–352.

Zeng, J., Nojiri, Y. and Wong, C.S. 1999. Seasonal analysis of pCO_2 along the high latitude route of *Skaugran* monitoring in the north Pacific. Proceedings of the Second International Symposium on CO_2 in the Oceans, pp. 25–29.

Summary of the Canadian program

We are proposing to fertilize a 64-km^2 patch of ocean near Station P in the subarctic NE Pacific during July–August 2002. Iron will be added three or four times during the 3-week experiment and a wide variety of physical, chemical and biological parameters will be measured. In particular, we will carefully document the expected increase in phytoplankton biomass and the subsequent carbon flux out of the photic zone, the drawdown in CO_2, and the production of other climate change gases such as DMS.

There are several reasons why an iron enrichment experiment should be conducted at Station P in the NE subarctic Pacific. Station P, or Ocean Station Papa (50ºN and 145ºW), has a 40-year time series of physical, chemical, and biological parameters and thus has one of the longest open ocean time

series in the world. Three large intensive sampling programs have provided detailed information, especially on biological rate process studies (SUPER, WOCE, and Canadian JGOFS). This large published data set/time series will provide an excellent background to assess the annual and interannual natural variability for evaluating the magnitude of the response to the iron addition experiment. The subarctic North Pacific represents a latitudinal gradient between the polar (Southern Ocean) and equatorial regions and therefore, an iron addition experiment at Station P will allow a comparison among the three large HNLC regions and between the eastern and western gyres in the subarctic Pacific.

The subarctic NE Pacific has physical, chemical and biological properties different from the other two HNLC regions (Southern Ocean and equatorial Pacific). In particular, it has a very shallow summer mixed layer depth, a strong, shallow pycnocline and low currents which should help to keep the iron patch intact and ensure the success of the experiment. The biodiversity of the plankton is also different from the equatorial Pacific and Southern Ocean and therefore, the response to the iron addition and the flux of carbon out of the photic zone may be different.

Unlike the equatorial Pacific, Station P is in close proximity (3 days steaming) to major research laboratories at the Institute of Ocean Sciences and the University of British Columbia and therefore, it should be easier to document the longer-term recovery from the iron addition. If the detailed documentation of the ecosystem response to a single iron addition is successful, it will allow us to proceed to the next phase — repeated iron additions and longer-term monitoring that this will require.

Key questions that have not been entirely resolved by previous iron enrichment experiments are:

- How does the change in biodiversity and foodweb structure differ for markedly different ecosystems which have been perturbed by an iron additon?
- What is the drawdown of CO_2 and, especially, the flux of carbon to the deep ocean?
- How does the production of ligands influence the iron chemistry and the longevity of the phytoplankton bloom?
- How does zooplankton grazing influence the formation of the bloom and the carbon flux (*e.g.*, fecal pellet production)?
- What is the long-term response and recovery of the ecosystem following an iron addition?
- What is the magnitude of production of other climate change gases, such as DMS, during the bloom and how is the production influenced by phytoplankton species, microbial processes and grazing?

Objectives will be to:

- measure the response of bacteria, phytoplankton and zooplankton in terms of species, standing stocks and rate processes to the iron addition;
- measure the drawdown of CO_2 and the flux of carbon to depth;
- study the relationship between ligand production and the associated changes in iron chemistry and their influence on the longevity of the phytoplankton bloom;
- assess the influence of zooplankton grazing on phytoplankton bloom formation and carbon flux;
- follow the long-term response and recovery of the phytoplankton bloom;
- quantify the production of various climate change gases during the iron enrichment experiment and assess the factors which influence the production of these biogases.

Biological oceanographic sampling

The upper 150 m will be sampled vertically (6–8 depths) each day using 12 acid-cleaned PVC samplers on a CTD/water sampler rosette system at the patch centre (determined by SF_6 levels) and in the surrounding waters. Real-time vertical profiling of temperature, salinity, transmissivity, chlorophyll *a* fluorescence and underwater irradiance (PAR, 400–700 nm) will be carried out. Discrete water samples will be analysed for: chlorophyll *a* (size-fractionated, >20, 5–20, 2–5 and 0.2–2 µm), heterotrophic bacterial abundance, microzooplankton abundance, and phytoplankton abundance (flow cytometry, epifluorescence and light microscopy). Additional samples will be incubated on deck to measure rates of primary production (^{14}C, 24 h incubation, simulated *in situ* and size-fractionated as for chlorophyll *a*, bacterial production, and microzooplankton grazing. Mesozooplankton abundance will be assessed from

150–0 m vertical hauls. The Th:U activity ratio of particles in the upper water column will be collected using a submersible pumping system.

Geochemical measurements

Two types of sampling will be done: hydrocasts and underway sampling from the vessel's non-toxic seawater supply (intake 5-m subsurface) and analysed by fluorometry (calibrated with discrete chlorophyll *a* samples every 2 days, corrected for quenching during daylight hours), and using a bubble-segmented automated nutrient analysis system, respectively. Underway samples for dissolved iron will be conducted from a clean towed batfish sampling system, and samples for pCO_2 will be drawn from the vessel's non-toxic seawater system. Phytoplankton samples for the single-cell flavodoxin assay will be pre-concentrated onboard ship and later analysed shoreside.

Sampling will be conducted by:

- towed batfish with a clean pump and tubing (this is not a pumping undulating fish): conductivity/salinity sensor, SF_6, fCO_2, pH, nitrate, iron, Chlorophyll *a* (fluorometer) (measurments will be sampled continuously);
- hydrocasts by rosette CTD/Niskin samplers: T, S, O_2, Chlorophyll *a*, macronutrients (N, P, Si) by auto-analyzer, iron by chemiluminescence, particulate iron size-fractions, total iron, dissolved iron, SF_6, DIC, TA, pH, DOC, DON, POC, DMS;
- free-drifting sediment traps (at 50-m intervals, 50–600 m) deployed and retrieved at 3-day intervals to obtain samples for detritus organic C, N, P, Si, PIC, Fe, Cd, Al, rare earth elements, Th:U ratios, coccolithophore counts and planktonic species, and scanning electron microscope pictures;
- deckboard perturbation experiments: algal carbon, growth rates and C:Chl-*a* ratios, *etc*.

We (Drs. C.S. Wong and Paul J. Harrison) hope to have one or two strings of moored sediment traps, plus free floating traps. Moored traps would be at the control site. Floating traps would hopefully follow the patch. It will be difficult to keep the patch and traps together, but there is a real need for trap data to try to quantify and characterize export. Free-floating sediment traps may perform differently than moored traps. Therefore, we should have free-floating traps in and out of the iron patch. There is a need to know more about microzooplankton, the effects of ligands, and also climate change biogases, including but not limited to, DMS, CO_2, and N_2O. SOIREE showed enhancement of nitrous oxide at the top of the thermocline, so this is one gas that should be studied. There will be aircraft-based sampling of gases and aerosols above the iron patch. We hope to sample over a longer time, possibly by back-to-back cruises extending over 6 weeks. We expect to have the CCGS *J.P. Tully* for 4 weeks and will need another ship for one of these two cruises. Cruises could be separated by several weeks if the patch could be found on second cruise. Iron limitation at Station P in July and August is severe, so the project will need to take place during this time. The project will be part of the Canadian SOLAS program.

Summary of the Japanese programs

A preliminary experiment of about 40 days is proposed during June–August 2001 on board the R/V *Kaiyo-Maru* in the WSG (45–50°N, 160–165°E), with next effort in August to mid-September 2003 with the T/S *Oshoro-Maru* or R/V *Kaiyo-Maru*) to initiate the SF_6/Fe patch and conduct the basic study. In October 2003 the R/V *Hakuho-Maru* will be used for intensive sampling and measurements. From analyzing long-term responses, we hope to:

- measure responses of bacteria, phytoplankton and zooplankton in terms of species, standing stocks and rate processes to the iron addition;
- measure the drawdown of CO_2 and the flux of carbon export;
- study the interaction between biogeochemical processes in the surface water during the phytoplankton bloom and the production of climate gases in the atmosphere;
- study the relationship between phytoplankton (diatom) production and higher trophic levels (salmon);
- assess the influence of iron supply on the characteristics of the plankton ecosystem in the western subarctic Pacific.

Proposals will be submitted to the Science and Technology Agency (2001–2005), Ministry of Education, Science and Culture (2001 Basic Science, 2002–2004 Scientific project with high priority) and NEDO grant.

A1.1.2 Discussions on experimental design

What do we know from IronEx I and IronEx II and SOIREE, *etc.*?

Japan SOLAS is still in the preparation stage. A study of the influence of natural atmospheric iron supply on the characteristics of the plankton ecosystem in the western subarctic Pacific will be one of the important topics. (A long cruise is expected to stay at a station in the spring high dust season.)

- Iron limitation is clearly present in populations of phytoplankton in HNLC regions.
- Iron enrichment de-couples larger phytoplankton from the mesozooplankton community.
- Evidence for carbon export in SOIREE is not clear. There may have been an export of carbon, yet a retention of iron. Evidence for carbon export in IronEx is clearer.
- The response rate in SOIREE was much slower than that in IronEx.
- There is now more interest in the effect of iron enrichment in different macronutrient-limited regimes, specifically low NO_3 where N-fixation dominates N-uptake.
- A ship-based study of light limitation of iron enrichment in the SOIREE region showed that light limitation is present at 100 m.
- There is some interest in long-term addition experiments using low levels of iron.
- The role of mesoscale eddies at Station P is intriguing. They may offer a way to track a patch of water for years, but the phytoplankton community in an eddy may be untypical of the Gulf of Alaska. Also, eddies have no surface water expression, so their relevance to an iron enrichment experiment is not clear.
- The European community has just sent (November 2000) the R/V *Polarstern* to the Southern Ocean (in the Atlantic sector) to do a SOIREE-type experiment over a longer time, such as the **CAR**bon Dioxide **U**ptake by the **S**outhern **O**cean (CARUSO) experiment.

What do we still need to know?

- There is a need to study Station P, and the NW Pacific, but other regions need to be studied too.
- What is the fate of primary production (carbon) on POC export flux, DOC, respiration and response of higher trophic levels (is there an increase in fish production?). The time scale is over a year, so a model approach is needed.
- What are the roles of ligands? What members of the community produce and take up ligands?
- Does zinc affect other enzyme processes?
- There is a need to study DMS/DMSP and other climate change biogases. Previous iron enrichment studies have measured DMS production. There should be both ships and aircraft for sampling. At Station P, ocean levels of DMS are very high; atmospheric levels are low.
- We need to know what factors influence the carbon-to-nutrient and other trace metal export ratios.
- Iron might end up below the mixed layer during long-term commercial projects. Will it become available the next summer after winter mixing?
- Would long-term iron enrichment drive a system toward another limitation (N, Si, Zn, Co, *etc.*)?
- What is the impact of long-term iron enrichment on fish? Governments may see fish production as a secondary benefit of iron enrichment, so this question will be asked of us. The public may see this as a problem, due to “wrong” species benefiting, such as pennate diatoms that produce domoic acid. (These are not questions that can be addressed with the current experiment.)
- What are the chemical processes associated with iron saturation and super-saturation of seawater?
- How does Fe(II) stay around so long in iron enrichment patches?
- What are the major grazers on diatoms and how do they respond when diatom (pennate/centric) abundance increases?
- Understanding the dynamics of the plankton ecosystem, export carbon flux and climate-related gases to iron enrichment is appropriate for the requests of Government and Industry who are seeking scientific information to asses the effects on future global atmospheric CO_2 and environmental impacts.

What do we hope to learn from an iron enrichment experiment at Station P and WSG?

- What are the similarities and differences in the plankton ecosystem response to iron fertilization in the subarctic Pacific?
- There is a special interest in the east–west North Pacific comparison which includes differences in dominant species (pennate/centric diatoms) and export flux (Org-C/Opal/$CaCO_3$).

Methodology

- There is a need to standardize sampling methods to enable comparison among experiments in different HNLC regions. A list of dominant species and their biomass is useful for the comparison.
- The first step is the application of previous IronEx methodology ($FeSO_4$, initial concentration level, iron infusion timing, *etc.*). Then we may go to a new method such as the use of chelated iron (iron lignite), long-period and low-level iron supply, *etc*.
- We should add DMSP to list of samples.
- Microzooplankton are important grazers and dilution experiments are necessary to quantify the coupling of primary production and grazing.
- Iron organic ligand studies have technical problems but how are they to be solved?
- Analyses of biogases in the atmosphere are important, but how are they to be done?
- Bag experiments have limitations. Small bags might not represent the ocean. Large bags are too difficult to manage. However, there should be some role for bag experiments.
- The use of organic chelated iron (iron lignite) may provide carbon source for heterotrophic organisms.
- A stable isotope study will be done in SOFeX to see the proxy of the paleo-oceanographic environment.
- After silicate in the surface water will be used up, a re-infusion of iron will give us some idea of the long-term change in dominant species.

Logistics

- The Station P project needs a second ship. Kenneth Coale recommended that a U.S. ship may be available if a group of American scientists were to propose to participate. The U.S. SOLAS program would be one way to generate support. It would help to have a Canadian–Japanese proposal ready. U.S. scientists must start to prepare proposals now for the Station P 2002 cruise.
- Canadian or U.S. aircraft would be useful for tracking the iron patch. An airplane with a hyperspectral sensor would be really helpful.
- ADIOS-2 will be launched soon. Similar to SeaWiFS, it will be useful.

A1.2 EXTENDED ABSTRACTS OF THE 2000 IFEP PLANNING WORKSHOP

A1.2.1 General overview of IronEx and SOIREE, iron chemistry and biology in seawater

Open ocean iron fertilization for scientific study and carbon sequestration

Kenneth H. Coale

Moss Landing Marine Laboratories, 8272 Moss Landing Road, Moss Landing, CA, U.S.A. 95039
E-mail: coale@mlml.calstate.edu

Abstract

Through initial enrichment experiments in the subarctic Pacific and a series of recent large-scale iron fertilization experiments in the equatorial Pacific and the Southern Ocean, strong correlations in atmospheric iron deposition, marine production and climate change have now been mechanistically linked to iron limitation in the global ocean. These experiments have been significant in a number of ways: (1) they have advanced the importance of iron in regulating phytoplankton production on global scales, (2) they have demonstrated the utility of open ocean enrichment experiments for the study of ecological and physiological processes, and (3) they have suggested that anthropogenically induced eutrophication through open ocean iron fertilization may be useful in controlling atmospheric carbon dioxide. Although the latter remains an issue of current study and debate, the utility of iron fertilization in examining a variety of biological and geochemical processes has been unequivocally demonstrated.

The ability to perform such experiments, however, is not trivial and involves many demanding capabilities. Here, we report the theoretical and practical considerations of creating a patch of seawater enriched with iron, then detecting this patch and the biological and chemical signal which developed, in an area dominated by advective processes. Physical and chemical models were used to predict the speciation, solubility, and the final concentration of iron in surface waters injected with acidic iron sulfate. A Lagrangian coordinate system was established using a drogued buoy, and the iron-enriched area was tagged with the inert chemical tracer sulfur hexafluoride (SF_6).

This method has proven useful on four experiments conducted by Moss Landing Marine Laboratories (MLML) researchers in the equatorial Pacific and in the Southern Ocean. Shipboard analysis and airborne observations confirmed good spatial agreement between the Lagrangian drifter and the biological and chemical signatures in the patch.

The biological response, upon addition of iron to high nitrate, low chlorophyll (HNLC) systems, is becoming more predictable. Although the inert tracer allows for an estimate of the physical mixing of the enriched waters, a well constrained budget of carbon export is more difficult to calculate.

Experimental strategy

The mechanics of producing an iron-enriched experimental patch and following it over time has been worked out in four release experiments in the equatorial Pacific (IronEx I and II, Martin *et al.*, 1994; Coale *et al.*, 1996) and more recently in the Southern Ocean (SOIREE, Boyd *et al.*, 2000). A similar strategy will be employed in the CARUSO (**CAR**bon Dioxide **U**ptake by the **S**outhern **O**cean) experiments now underway in the Atlantic sector of the Southern Ocean and will be similar to the methods used by the SOFeX (Southern Ocean Iron Experiment) group in an upcoming experiment.

Form of iron

Based upon the IronEx experiments, these all involve the injection of an iron sulfate solution into the ship's wake where it is rapidly diluted and dispersed throughout the mixed layer. The rationale for using ferrous sulfate is given in Coale *et al.* (1998) and involves the following thinking: (1) Ferrous sulfate is the most likely form of iron to enter the oceans via atmospheric deposition, (2) it is readily soluble (initially), (3) it is available in a relatively pure form so as to reduce the introduction of other potentially bioactive trace metals and

(4) its counter ion (sulfate) is ubiquitous in seawater and not likely to produce confounding effects. Although mixing models indicate that iron (II) carbonate may reach insoluble levels in the ship's wake, rapid dilution reduces this possibility.

New forms of iron are now being considered by those who would seek to reduce the need for subsequent infusions. Our laboratory has investigated the bioavailability of iron lignosite to phytoplankton in the California Current. These results indicate that, on an equimolar basis, iron lignosite may be as effective or better in promoting phytoplankton growth. Because this is a chelated form of iron, problems of rapid precipitation are reduced. In addition, Fe-lignosite is about 15% Fe by weight making it a space-efficient form of iron to transport. As yet untested is the extent to which such a compound would reduce the need for re-infusion.

Inert tracer

Concurrent with the injection of iron is the injection of the inert chemical tracer, SF_6. By presaturating a tank of seawater with SF_6 and employing an expandable displacement bladder, a constant molar injection ratio of Fe:SF_6 can be achieved. In this way, both conservative and non-conservative removal of iron can be quantified. In addition, the relatively rapid shipboard detection of SF_6 can be used to track and map the enriched area (Upstill-Goddard *et al.*, 1991; Watson *et al.*, 1991). Addition of Helium-3 to the injected tracer can provide useful information regarding gas transfer. These experiments have been further developed (Law *et al.*, 1998; Nightingale *et al.*, 2000).

Fluorometry

Because the biophysical response of the phytoplankton is rapid and readily detectable, shipboard measurements of relative fluorescence (F_v/F_m) using fast repetition rate (FRR) fluorometry is a useful tactical tool and gives nearly instantaneous mapping and tracking feedback (Greene *et al.*, 1991; Kolber *et al.*, 1994; Behrenfeld *et al.*, 1996).

Shipboard iron analysis

Because iron is rapidly lost from the system (at least initially), the shipboard determination of iron is necessary to determine the timing and amount of subsequent infusions. Several shipboard methods, using both chemiluminescent and catalytic colorimetric detection have proven useful in this regard (Elrod *et al.*, 1991; Obata *et al.*, 1993; Johnson *et al.*, 1994).

Lagrangian drifters

A Lagrangian point of reference has proven to be very useful in every experiment to date. Depending upon the advective regime, this is the only practical way to achieve rapid and precise navigation and mapping of the enriched area (Stanton *et al.*, 1998).

Remote sensing

A variety of airborne and satellite-borne active and passive optical packages provide rapid, large-scale mapping and tracking of the enriched area (Hoge *et al.*, 1998). Although SeaWiFS was not operational during IronEx I and II, AVHRR was able to detect the IronEx II bloom and airborne optical LIDAR was very useful during IronEx I. SOIREE (**S**outhern **O**cean **IR**on **E**nrichment **E**xperiment) has made good use of the more recent SeaWiFS images which have markedly extended the observational period and led to new hypotheses regarding iron cycling in polar systems (Abraham *et al.*, 2000).

What we (think we) know

Biophysical response

The experiments to date have focused on the HNLC areas of the world's oceans, primarily in the subarctic, equatorial Pacific and Southern Ocean. In general, when light is abundant many researchers find that HNLC systems are iron limited. The nature of this limitation is similar between regions but manifests itself at different levels of the trophic structure in some characteristic ways. In general, all members of the HNLC photosynthetic community are physiologically limited by iron availability. This observation is based primarily on the examination of the efficiency of photosystem II, the light-harvesting reaction centers. At ambient levels of iron, light harvesting proceeds at sub-optimal rates. This has been attributed to the lack of iron-dependent electron carrier proteins at low iron concentrations. When iron concentrations are increased by

sub-nanomolar amounts, the efficiency of light harvesting rapidly increases to maximum levels. Observations using FRR fluorometry and non-heme iron proteins have been described in detail (Greene *et al.*, 1991; Kolber *et al.*, 1994; Behrenfeld *et al.*, 1996; La Roche *et al.*, 1996). What is notable about these results is that iron limitation seems to affect the photosynthetic energy conversion efficiency of even the smallest of phytoplankton (Cavender-Bares *et al.*, 1999). This has been a unique finding which stands in contrast to the hypothesis that, because of diffusion, smaller cells are not iron limited, but larger cells are.

Nitrate uptake

Iron is also required for the reduction (assimilation) of nitrate. In fact, a change of five oxidation states is required between nitrate and the reduced forms of nitrogen found in amino acids and proteins. Such a large and energetically unfavorable redox process is only possible by substantially reducing power (in the form of NADPH) made available through photosynthesis (see above) and active nitrate reductase, an iron-requiring enzyme. Without iron, plants cannot take up nitrate efficiently. This provided original evidence implicating iron deficiency as the cause of the HNLC condition. When phytoplankton communities are relieved from iron deficiency, specific rates of nitrate uptake increase. Cochlan *et al.* (2002) have observed this in both the equatorial Pacific and the Southern Ocean using isotopic tracers of nitrate uptake and conversion.

Growth response

When relieved from resource-based physiological limitation, phytoplankton growth rates increase dramatically (Coale *et al.*, 1996; Fitzwater *et al.*, 1996). In several experiments, over widely differing oceanographic regimes, we have demonstrated that when light and temperature are favorable phytoplankton growth rates in HNLC environments increase to their maximum at dissolved iron concentrations generally below 0.5 nM. This observation is significant in that it indicates that phytoplankton are adapted to very low levels of iron, that is, they do not grow faster if given more than half a nanomolar of iron. Given the disagreement within the scientific community about the validity of iron measurements, these phytoplankton provide a natural environmental and biogeochemical benchmark against which to compare results.

Heterotrophic community

As the primary trophic level producers, it appears that these consumers of recently fixed carbon (both particulate and dissolved) respond to the food source and not necessarily to the iron. Because their division rates are fast, heterotrophic bacteria, ciliates and flagellates can rapidly respond to increasing food availability to the point where the growth rates of the smaller phytoplankton can be almost balanced by grazing (Barbeau *et al.*, 1996; Hall and Safi, 2001). Thus there is a much more rapid turnover of fixed carbon and nitrogen in iron-replete systems. Landry *et al.* (2000) have documented this in dilution experiments conducted during IronEx II. These results also appear to be consistent with the recent SOIREE experiments.

Nutrient uptake ratios

An imbalance in production and consumption, however, can arise at the larger trophic levels. Because the reproduction rates of the larger micro- and mesozooplankton are long with respect to diatom division rates, iron-replete diatoms can escape the pressures of grazing on short time scales (weeks). This is thought to be the reason why, in every iron enrichment experiment, diatoms ultimately dominate in biomass. This result is important for a variety of reasons. It suggests that transient additions of iron would be most effective in producing net carbon uptake and it implicates an important role of silicate in carbon flux. The role of iron in silicate uptake has been studied extensively by Franck *et al*. (2000). Our results, together with those of Takeda and Obata (1995), show that iron alters the uptake ratio of nitrate and silicate at very low levels.

Organic ligands

Consistent with the role of iron as a limiting nutrient in HNLC systems is the notion that organisms may have evolved competitive mechanisms to increase iron solubility and uptake. In terrestrial systems this is accomplished using extracellularly excreted or membrane-bound siderophores. Similar compounds have been shown to exist in seawater where the competition for iron may be as fierce as it is on land. In open

ocean systems where it has been measured, iron-binding ligand production has increased with the addition of iron. Whether this is a competitive response to added iron or a function of phytoplankton biomass and grazing is not yet well understood. However, this is an important natural mechanism for reducing the inorganic scavenging of iron from the surface waters and increasing iron availability to phytoplankton. Several studies (Trick and Wilhelm, 1995; Van den Berg, 1995; Rue and Bruland, 1997; Croot *et al.*, in prep.) have advanced considerably our understanding of these ligands, their distribution and their role in ocean ecosystems.

Carbon flux

It is this imbalance in the community structure which gives rise to the geochemical signal. Whereas iron stimulation of the smaller members of the communtures, such as an increased production of dimethylsulfionproprionate (DMSP) occurs (Turner *et al.*, 1996), it is the stimulation of the larger producers which decouples the large cell producers from grazing and results in a net uptake and export of nitrate, CO_2 and silicate. The extent to which this imbalance results in carbon flux, however, has yet to be adequately constrained. This has been primarily a problem of experimental scale. Even though mesoscale experiments have, for the first time, given us the ability to address the effect of iron on communities, the products of surface water processes have been difficult to track. For instance, on the IronEx II experiment, a time series of the enriched patch was diluted by 40% per day and is described by Nightingale *et al.* (2000). The dilution was primarily in a lateral (horizontal/isopycnal) dimension. Although some correction for lateral dilution can be made, our ability to quantify carbon export is dependent upon the measurement of a signal in waters below the mixed layer, or from an uneroded enriched patch. Current data from the equatorial Pacific showed that the IronEx II experiment advected over six patch diameters per day. This means that at no time during the experiment were the products of increased export reflected in the waters below the enriched area. Our results from the equatorial Pacific, when corrected for dilution, suggest that about 2,500 tons of carbon were exported from the mixed layer over a 7-day period. These results are preliminary and subject to more rigorous estimates of dilution and export production, but they do agree favorably with estimates based upon both carbon and nitrogen budgets.

Experimental scale

Given these considerations, the most feasible way to understand and quantify carbon export from an enriched water mass is to increase the scale of the experiment such that both lateral dilution and sub-mixed layer relative advection is small with respect to the size of the enriched patch. For areas such as the equatorial Pacific, this would be very large (100s of kilometers on a side). For other areas, this could be much smaller. From the acoustic Doppler current profiler (ADCP) data presented, it appears that lateral advection was not as much of a problem during SOIREE as during the IronEx experiments. The relative advection of the enriched patch over the underlying waters will be a function of wind stress and regional hydrodynamics. In the subarctic Pacific, this can be severe. It is this author's opinion that an uncontained enrichment experiment in this region should be large (1000 km^2 or greater) to avoid lateral mixing and slippage relative to the sub-mixed layer.

What we need to know

There are a multitude of questions remaining regarding the role of iron in shaping the nature of the pelagic community. Some of these topics involve the role of the heterotrophic bacterial community in cycling iron and carbon, the extent to which the smaller phytoplankton contribute to flux, the partitioning of light isotopes of carbon and nitrogen in biomarker compounds and in the bulk plankton and their use in establishing paleo-isotopic tracers of growth rate and trophic structure, the use of single cell FRR fluorometry to study species specific response to iron, the use of sediment traps and radioisotopic disequilibrium to measure and infer carbon export. Many of the remaining questions will be the subject of the CARUSO and SOFeX experiments as well as future experiments in the subarctic Pacific. The focus of the IronEx and SOFeX experiments has been from the scientific perspective, but this focus is shifting towards the application of iron enrichment as a carbon sequestration strategy. We have come about rapidly from the perspective of trying to understand how the world works, to one of trying to make the world work for us.

Several basic questions remain regarding the role of natural or anthropogenic iron fertilization on carbon export. Some of the most pressing questions are: What are the best proxies for carbon export? How can carbon export best be verified? What are the long term ecological consequences of iron enrichment on: (1) surface water community structure? (2) midwater processes? (3) benthic processes? And what is the response of the community structure and biological pump to iron enrichment in low nutrient low chlorophyll (LNLC) systems where nitrogen fixation may be iron limited? Even with these answers, there are others which would need to be addressed prior to any serious consideration of iron fertilization as an ocean carbon sequestration option (see below).

Technology

Simple technology is sufficient to produce a massive bloom. The technology required for either a large-scale enrichment experiment or for purposful attempts to sequester carbon, is readily available. Ships, aircraft (tankers and research platforms), tracer technology, a broad range of new AUVs (autonomous underwater vehicles) and instrument packages, Lagrangian buoy tracking systems, together with aircraft and satellite remote sensing systems and a new suite of chemical sensors/*in situ* detection technologies are all available, or are being developed at this time. The big questions, however, are larger than the technology.

Resources

With a slow start, the notion of both scientific experimentation through manipulative experiments, as well as the use of iron to purposefully sequester carbon, is gaining momentum. There are now national, international, industrial, and scientific concerns willing to support larger-scale experiments. The materials required for such an experiment are inexpensive and readily available even as industrial byproducts (paper, mining, steel processing).

Feasibility

Given the concern over climate change and the rapid modernization of large underdeveloped countries (China, India, *etc.*), there is a pressing need to address the increased emission of greenhouse gasses. Through the implementation of the Kyoto accords or other international agreements to curb emissions (Rio), financial incentives will reach into the multi-billion dollar level annually. Certainly there will soon be an overwhelming fiscal incentive to investigate, if not implement purposeful open ocean carbon sequestration trials.

Questions

The question is not whether we have the capability of embarking upon such an engineering strategy, the question is whether we have the collective wisdom to responsibly negotiate such a course of action. Posed another way: If we do not have the social, political and economic tools or motivation to control our own population and greenhouse gas emissions, what gives us the confidence that we have the wisdom and ability to responsibly manipulate and control large ocean ecosystems without propagating yet another massive environmental calamity? Have we, as an international community, first tackled the difficult but obvious problem of overpopulation and implemented alternative energy technologies for transportation, industry and domestic use?

There are other social questions which arise as well, such as: Is it appropriate to use the ocean commons for such a purpose? What individuals, companies or countries would derive monetary compensation for such an effort and how would this be decided?

It is clear that there are major science investigations and findings which can only benefit from large-scale open ocean enrichment experiments, but certainly a large-scale carbon sequestration effort should not proceed without a clear understanding of both the science and the answers to the questions above.

References

Abraham, E.R., Law, C.S., Boyd, P.W., Lavender, S.J., Meldenado, M.T. and Bowle, A.R. 2000. Importance of stirring in the development of an iron-fertilized phytoplankton bloom. *Nature* **407**: 727–730.

Barbeau, K., Moffett, J.W., Caron, D.A., Croot, P.L. and Erdner, D.L. 1996. Role of protozoan grazing in relieving iron limitation of phytoplankton. *Nature* **380**: 61–64.

Behrenfeld, M.J., Bale, A.J., Kobler, Z.S., Aiken, J. and

Falkowski, P.G. 1996. Confirmation of iron limitation of phytoplankton photosynthesis in the Equatorial Pacific Ocean. *Nature* **383**: 508–511.

Boyd, P.W., Watson, A.J., Law, C.S. *et al.* 2000. A mesoscale phytoplankton bloom in the polar Southern Ocean stimulated by iron fertilization. *Nature* **407**: 695–702.

Cavender-Bares, K.K., Mann, E.L., Chishom, S.W., Ondrusek, M.E. and Bidigare, R.R. 1999. Differential response of equatorial phytoplankton to iron fertilization. *Limnol. Oceanogr.* **44**: 237–246.

Coale, K.H., Johnson, K.S., Fitzwater, S.E. *et al.* 1996. A massive phytoplankton bloom induced by an ecosystem-scale iron fertilization experiment in the equatorial Pacific Ocean. *Nature* **383**: 495–501.

Coale, K.H., Johnson, K.S., Fitzwater, S.E., Blain, S.P.G., Stanton, T.P. and Coley, T.L. 1998. IronEx-I, an in situ iron-enrichment experiment: Experimental design, implementation and results. *Deep-Sea Res. II* **45**: 919–945.

Cochlan, W.P., Bronk, D.A. Coale, K.H. 2002. Trace metals and nitrogenous nutrition of Antarctic phytoplankton: experimental observation in the Ross Sea. *Deep-Sea Res. II* **49**: 3365–3390.

Elrod, V.A., Johnson, K.S. and Coale, K.H. 1991. Determination of subnanomolar levels of iron (II) and total dissolved iron in seawater by flow injection analysis with chemiluminescence detection. *Anal. Chem.* **63**: 893–898.

Fitzwater, S.E., Coale, K.H., Gordon, R.M., Johnson, K.S. and Ondrusek, M.E. 1996. Iron deficiency and phytoplankton growth in the equatorial Pacific. *Deep-Sea Res. II* **43**: 995–1015.

Franck, V.M., Brzezenski, M.A., Coale, K.H. and Nelson, D.M. 2000. Iron and silicic acid concentrations regulate Si uptake north and south of the Polar Frontal Zone in the Pacific Sector of the Southern Ocean. *Deep-Sea Res. II* **47**: 3315–3338.

Greene, R.M., Geider, R.J. and Falkowski, P.G. 1991. Effect of iron limitation on phytosyntheses in a marine diatom. *Limnol. Oceanogr.* **36**: 1772–1782.

Hall, J. and Safi, K. 2001. The impact of in situ Fe fertilization on the microbial food web in the Southern Ocean. *Deep-Sea Res. II* **48**: 2591–2613.

Hoge, E.F., Wright, C.W., Swift, R.N., Yungel, J.K., Berry, R.E. and Mitchell, R. 1998. Fluorescence signatures of an iron-enriched phytoplankton community in the eastern equatorial Pacific Ocean. *Deep-Sea Res. II* **45**: 1073–1082.

Johnson, K.S., Coale, K.H., Elrod, V.A. and Tinsdale, N.W. 1994. Iron photochemistry in seawater from the Equatorial Pacific. *Mar. Chem.* **46**: 319–334.

Kolber, Z.S., Barber, R.T., Coale, K.H., Fitzwater, S.E., Green, R.M., Johnson, K.S., Lindley, S. and Falkoski, P.G. 1994. Iron limitation of phytoplankton photosynthesis in the Equatorial Pacific Ocean. *Nature* **371**: 145–149.

Landry, M.R., Ondrusek, M.E., Tanner, S.J., Brown, S.L., Constantinou, J., Bidigare, R.R., Coale, K.H. and Fitzwater, S.E. 2000. Biological response to iron fertilization in the eastern equatorial Pacific (IronEx II). I. Microplankton community abundances and biomass. *Mar. Ecol. Prog. Series* **201**: 27–42.

LaRoche, J., Boyd, P.W., McKay, R.M.L. and Geider, R.J. 1996. Flavodoxin as an in situ marker for iron stress in phytoplankton. *Nature* **382**: 802–805.

Law, C.S., Watson, A.J., Liddicoat, M.I. and Stanton, T. 1998. Sulfur hexafloride as a tracer of biogeochemical and physical processes in an open-ocean iron fertilization experiment. *Deep-Sea Res. II* **45**: 977–994.

Martin, J.H., Coale, K.H., Johnson, K.S. *et al.* 1994. Testing the iron hypothesis in ecosystems of the equatorial Pacific Ocean. *Nature* **371**: 123–129.

Nightingale, P.D., Liss, P.S. and Schlosser, P. 2000. Measurements of air-gas transfer during an open ocean algal bloom. *Geophys. Res. Lett.* **27**: 2117–2121.

Obata, H., Karatani, H. and Nakayama, E. 1993. Automated determination of iron in seawater by chelating resin concentration and chemi-luminescence detection. *Anal. Chem.* **65**: 1524–1528.

Rue, E.L. and Bruland, K.W. 1997. The role of organic complexation on ambient iron chemistry in the equatorial Pacific Ocean and the responce of a mesoscale iron addition experiment. *Limnol. Oceanogr.* **42**: 901–910.

Stanton, T.P., Law, C.S. and Watson, A.J. 1998. Physical evolution of the IronEx I open ocean tracer patch. *Deep-Sea Res. II* **45**: 947–975.

Takeda, S. and Obata, H. 1995. Response of equatorial phytoplankton to subnanamolar Fe enrichment. *Mar. Chem.* **50**: 219–227.

Trick, C.G. and Wilhelm, S.W. 1995. Physiological changes in costal marine cyanobacterium *Syenechoclccus* sp. PCC 7002 exposed to low ferric ion levels. *Mar. Chem.* **50**: 207–217.

Turner, S.M., Nightingale, P.D., Spokes, L.J., Liddicoat, M.I. and Liss, P.S. 1996. Increased dimethyl sulfide concentrations in seawater from *in situ* iron enrichment. *Nature* **383**: 513–517.

Upstill-Goddard, R.C., Watson, A.J., Wood, J. and Liddicoat, M.I. 1991. Sulfur hexafloride and helium-3 as sea-water tracers: deployment techniques and continuous underway analysis for sulphur hexafloride. *Anal. Chim. Acta* **249**: 555–562.

Van den Berg, C.M.G. 1995. Evidence for organic complexation of iron in seawater. *Mar. Chem.* **50**: 139–157.

Watson, A.J., Liss, P.S. and Duce, R. 1991. Design of a small-scale *in situ* iron fertilization experiment. *Limnol. Oceanogr.* **36**: 1960–1965.

Dissolved iron speciation in seawater

Eden L. Rue and Ken Bruland

Department of Ocean Sciences, University of California, 1156 High Street, Santa Cruz, CA, U.S.A. 95064
E-mail: elrue@cats.ucsc.edu or bruland@cats.ucsc.edu

Introduction

The role of iron in limiting oceanic productivity and influencing community structure has been demonstrated for the high nitrate, low chlorophyll (HNLC) waters of the subarctic Pacific, equatorial Pacific, the Southern Ocean, and even some coastal upwelling regimes. As a consequence, iron has been elevated to the same status as nitrogen, phosphorus and silicon as important nutrients influencing global biogeochemical cycles. In oceanic surface waters, concentrations of dissolved iron (defined as the iron concentration in the filtrate passing through a conventional 0.2 or 0.4µm filter) commonly range from 0.02 nM (20 pM) to 1 nM. In remote HNLC regimes (such as the equatorial Pacific, subarctic Pacific, and parts of the Southern Ocean) iron can be a limiting nutrient with dissolved iron concentrations in surface waters on the order of 0.02 to 0.05 nM (20 to 50 pM). These concentrations are low enough for dissolved iron to be diffusion limiting with respect to growth rates for all but the smallest phytoplankton cells (Hudson and Morel, 1990; Sunda and Huntsman, 1995). Measurements of total dissolved iron concentrations alone, however, are insufficient for understanding the accessibility of iron to phytoplankton. Knowledge of the chemical speciation of iron is critical for examining the mechanisms by which phytoplankton are fulfilling their iron requirements and is important for addressing the question of how the lack of iron limits phytoplankton productivity in certain regions of the oceans.

Discussion

The majority of this dissolved iron in remote low-iron, HNLC regimes appears to be chelated (as FeLi) with organic ligands (Li) which resemble siderophores in their conditional stability constants and molecular weight (Rue and Bruland, 1997). In HNLC areas such as the equatorial Pacific, it appears that these chelated forms of iron are primarily less than 1000 in relative molar mass (molecular weight) (Rue and Bruland, 1997), with only a small fraction existing as larger, colloidal size material. In these low-iron waters, both Li and FeLi appear to exist primarily in the soluble fraction and colloidal forms do not appear to be a significant fraction of the dissolved iron. Results on the chemical speciation of iron in central gyre regions of the North Pacific and North Atlantic both indicate that the bulk of the dissolved iron exists as organic Fe(III)-chelates (Rue and Bruland, 1995; Wu and Luther, 1995). Even though the data are very limited, it even appears that iron in the deep ocean exists primarily as Fe(III)-chelates (Rue and Bruland, 1995; Nolting *et al*., 1998) although it is uncertain to what extent the iron is soluble or colloidal in form. The higher concentrations of dissolved iron in coastal waters also appear to be associated with organic ligands (Gledhill and van den Berg, 1994; van den Berg, l995). In contrast to the low-iron open ocean, however, the high-iron Narragansett Bay (Rhode Island, United States) has the bulk of what seems to be organically complexed dissolved iron existing as a colloidal Fe fraction, with only a small amount found in the relative molar mass <1000 ultrafiltrate (Rue and Bruland, pers. comm.). Powell *et al*. (1996) used ultrafiltration to carry out a size-fractionation study of dissolved iron and dissolved organic carbon in the Ochlockonee estuary (Florida, United States). They showed that in high-iron, low-salinity regions of the estuary the vast majority of iron was in the high molecular weight fraction (relative molar mass >10,000), but that this component was only a minimal fraction in higher salinity regions. Thus, the chemical form of dissolved iron appears to change dramatically from being primarily associated with a complex, higher molecular weight, colloidal fraction in estuarine and fresh waters, to being in the form of low molecular weight, water soluble, strong Fe(III)-organic chelates in oceanic surface waters.

Although the identity, origin, and chemical characteristics of these organic compounds are largely unknown, it has been implied that some

component of these natural ligands are siderophores (Rue and Bruland, 1995). Macrellis *et al*. (2001) report the first direct evidence from natural seawater to support this theory. Large volume seawater collection and solid phase extraction employing Biobeads SM-2 and Amberlite XAD-16 resins were conducted in the California coastal upwelling system. Electrochemical analyses using competitive ligand equilibration/adsorptive cathodic stripping voltammetry (CLE-ACSV) showed that extracted groups of compounds had conditional iron-binding affinities (with respect to Fe') of $K^{cond}_{FeL,Fe'}$ = $10^{11.5}$–$10^{11.9}$ M^{-1}, identical to those constants measured for purified marine siderophores produced in laboratory cultures. In addition, 63% of the extracted compounds fall within the defined size range of siderophores (300–1000 Daltons). Hydroxamate or catecholate iron-binding functional groups were responsible for iron complexation in all isolated extracts, illustrating that the functional groups previously shown to be active in marine and terrestrial siderophores extracted and purified from laboratory cultures are active in a natural marine community milieu. Thus, these data provide the first evidence from natural marine systems that a significant fraction of the organic iron-binding compounds that control the availability of iron and therefore, influence the global biogeochemical cycling of this micronutrient, are biologically produced siderophores.

Much of the current interest in the marine chemistry of iron stems from its role as a limiting micronutrient affecting plankton productivity and biological species composition. The high degree of organic complexation of iron makes it critically important to re-evaluate our perceptions of the marine biogeochemistry of iron and the mechanisms by which biota can access this chelated iron. Trace metal assimilation by phytoplankton has historically been modeled using the free ion concentration (or activity) model (Morel and Hering, 1993), with iron uptake by phytoplankton typically correlated with free, hydrated Fe^{3+} concentrations (using EDTA buffered solutions). It is now realized, however, that it is the far more abundant, kinetically labile, hydrolysis species comprising Fe(III)' (such as $Fe(OH)^{2+}$) that actually control uptake rates of inorganic iron (Hudson and Morel, 1990; Hudson, 1998). As a result, recent papers dealing with iron limitation in laboratory culture media correlate effects with [Fe(III)'] rather than [Fe^{3+}] (Sunda and Huntsman, 1995).

A recent example (Rue and Bruland, 1997) of an iron speciation study in a low-iron HNLC area was performed as part of the IronEx II mesoscale iron addition experiment (Coale *et al*., 1996). Rue and Bruland (1997) observed two classes of Fe(III)-binding organic ligands: a strong ligand class (L1) with a conditional stability constant $K^{cond}_{FeL1,Fe(III)'}$ = 5×10^{12} L mol^{-1} and a mean concentration of 310 pM, and a weaker class (L2) with a conditional stability constant $K^{cond}_{FeL2,Fe(III)'}$ = 6×10^{11} L mol^{-1} and a mean concentration of 190 pM. The total Fe(III)-binding organic ligand concentrations were ~25 times higher than total dissolved iron concentrations of only 20 pM. Thermodynamic equilibrium calculations suggest that 99.9% of the ambient dissolved Fe(III) would be complexed with these organic ligands and results from ultra filtration experiments indicated that they exist as low molecular weight Fe(Ill) chelates. Upon the initial mesoscale iron injection of ~2nM, the total iron-binding ligand concentration increased by 400% to 2 nM within a day. Most of this increase was due to the stronger ligand class, L1, which increased from 0.3 to 1.3 nM. Results obtained from samples collected throughout the entire course of the iron enrichment experiments suggest that these iron-binding organic ligands are produced rapidly in response to small iron additions to this low-iron regime. The chelated iron appears to somehow be directly or indirectly accessible for growth. The presence of these chelators causes the labile inorganic species (Fe(III)') to exist at extremely low concentrations, perhaps requiring photochemical or other redox mechanisms to provide an adequate supply of Fe' (Rue and Bruland, 1997; Price and Morel, 1998). At this point, we are just beginning to understand how chelated iron might be accessible by the biological community (Maldonado and Price, 1999, 2000; Wells and Trick, 2004). Prokaryotes and even unicellular eukaryotes, such as diatoms, appear to be able to utilize some of the chelated iron (Price *et al*., 1994; Price and Morel, 1998; Hutchins *et al.*, 1998, 1999). There are suggestions that eukaryotic phytoplankton, such as diatoms, can access this chelated Fe(III) by using cell surface-bound reductases to reduce the chelated Fe(III) to Fe(II) which then dissociates and is subsequently assimilated either as Fe(II)' or, after

re-oxidation, as Fe(Ill)' (Maldonado and Price, 1999). There are some data to suggest that the protozoan grazers of the microbial community can utilize and solubilize colloidal iron (Barbeau *et al*., 1996), and there is also evidence that particulate iron associated with the plankton community can be remineralized and reused as regenerated iron much in the same way as nitrogen is recycled (Hutchins *et al*., 1993; Hutchins and Bruland, 1994). Price and Morel (1998) estimated that 83% of the iron uptake by microorganisms within the euphotic zone of the equatorial Pacific was from such biological regeneration, while the remaining 17% was supplied from external sources such as eolian deposition and upwelling. In addition, it has been suggested that various members of the phytoplankton and microplankton community can utilize phagocytosis to engulf and partially digest particulate iron (Raven, 1997), thereby rendering a fraction of the particulate iron available over an extended time scale. Recent evidence suggests that the photosynthetic phytoplankton *Ochromonas* can obtain iron directly in particulate form by ingesting bacteria (Maranger *et al*., 1998). As a result of the diversity of iron uptake strategies employed by various marine microorganisms, some of the "non-available" iron is likely recycled by various mechanisms and at various rates into biologically available forms (Wells and Mayer, 1991; Wells *et al*., 1995). Therefore, most of the dissolved iron and part of the particulate iron may eventually be made available to the plankton community.

Conclusions

Addressing the processes responsible for the role of iron forces us to look more closely at its marine chemistry. The majority of dissolved iron exists as Fe(III)-chelates with relatively specific and strong Fe(III)-binding ligands. Results from iron fertilization experiments have raised a number of questions that point to the need for more research. What are these iron-binding ligands? Are the stronger class of ligands, apparently produced in rapid response to increased iron levels, siderophores? Are they inducible, excreted, and regulated? What about the weaker class of ligands? Are these simply photochemical degradation products or cell lysis products (from zooplankton grazing or viral lysing) containing porphyrin groups such as those in cytochromes, chlorophylls, and haem proteins? Very little information exists, however, as to the chemical nature of these iron-binding ligands or the mechanisms involved in their production, function or fate. The need for future research elucidating the molecular structure and character of the strong iron-binding ligands observed in seawater has been recognized and has begun. In addition, research into the biological availability of the various chelated forms of iron, and the mechanisms various microorganisms utilize to access these iron species, will continue to be a research area of great importance in the next decade.

References

Barbeau, K., Moffett, J.W., Caron, D.A., Croot, P.L. and Erdner, D.L. 1996. Role of protozoan grazing in relieving iron limitation of phytoplankton. *Nature* **380**: 61–64.

Coale, K.H., Johnson, K.S., Fitzwater, S.E. *et al*. 1996. A massive phytoplankton bloom induced by ecosystem-scale iron fertilization experiment in the equatorial Pacific Ocean. *Nature* **383**: 495–501.

Gledhill, M. and van den Berg, C.M.G. 1994. Determination of complexation of Fe(III) with natural organic complexing ligands in seawater using cathodic stripping voltammetry. *Mar. Chem.* **47**: 41–54.

Hudson, R.J.M. and Morel, F.M.M. 1990. Iron transport in marine phytoplankton: Kinetics of cellular and medium coordination reactions. *Limnol. Oceanogr.* **35**: 1001–1020.

Hudson, R.J.M. 1998. Which aqueous species control the rates of trace metal uptake by aquatic biota? Observations and predictions of non-equilibrium effects. *Sci. Total Environ.* **219**: 95–115.

Hutchins, D.A., Witter, A.E., Butler, A. and Luther III, G.W. 1999. Competition among marine phytoplankton for different chelated iron species. *Nature* **400**: 858–861.

Hutchins, D.A., DiTullio, G.R., Zhang, Y. and Bruland, K.W. 1998. An iron limitation mosaic in the California upwelling regime. *Limnol. Oceanogr.* **43**: 1037–1054.

Hutchins, D.A. and Bruland, K.W. 1994. Grazer-mediated regeneration and assimilation of Fe, Zn, and Mn from planktonic prey. *Mar. Ecol. Prog. Ser.* **110**: 259–269.

Hutchins, D.A. 1993. Iron and the marine phytoplankton community. pp. 1–49. *In* Progress in Phycological Research, Vo1. II. *Edited by* D. Chapman and F. Round, Biopress Ltd.

Macrellis, H.M., Trick, C.G., Rue, E.L., Smith, G.J. and Bruland, K.W. 2001. Isolation of natural iron-binding ligands from seawater. *Mar. Chem.* **76**: 175–187.

Maldonado, M.T. and Price, N.M. 2000. Nitrate regulation of Fe reduction and transport by

Fe-limited *Thalassiosira oceanica*. *Limnol. Oceanogr.* **45**: 814–826.

Maldonado, M.T. and Price, N.M. 1999. Utilization of iron bound to strong organic ligands by phytoplankton communities in the subarctic Pacific Ocean. *Deep-Sea Res. II* **46**: 2447–2474.

Maranger, R., Bird, D.F. and Price, N.M. 1998. Iron acquisition by photosynthetic marine phytoplankton from injected bacteria. *Nature* **396**: 248–251.

Morel, F.M. and Hering, J.G. 1993. Principles and Applications of Aquatic Chemistry. Wiley, New York, 588 pp.

Nolting, R.F., Gerringa, L.J.A., Swagerman, M.J.W., Timmermans, K.R. and de Baar, H.J.W. 1998. Fe(III) speciation in the high nutrient, low chlorophyll Pacific region of the Southern Ocean. *Mar. Chem.* **62**: 335–352.

Powell, R.T., Landing, W.M. and Bauer, J.E. 1996. Colloidal trace metals, organic carbon and nitrogen in a southeastern U.S. estuary. *Mar. Chem.* **55**: 165–176.

Price, N.M. and Morel, F.M.M. 1998. Biological cycling of iron in the oceans. pp. 1–36. *In* Metal Ions in Biological Systems, Vol. 35: Iron Transport and Storage in Microorganisms, Plants and Animals. *Edited by* A. Sigel and H. Sigel, Marcel Dekker, New York.

Price, N., Ahner, M.B.A. and Morel, F.M.M. 1994. The Equatorial Pacific Ocean: grazer-controlled phytoplankton populations in an iron-limited ecosystem. *Limnol. Oceanogr.* **39**: 520–534.

Raven, J. 1997. Phagotrophy in phototrophs. *Limnol. Oceanogr.* **42**: 198–205.

Rue, E.L. and Bruland, K.W. 1995. Complexation of iron(III) by natural organic ligands in the Central North Pacific as determined by a new competitive ligand equilibration/adsorptive cathodic stripping voltammetric method. *Mar. Chem.* **50**: 117–138.

Rue, E.L. and Bruland, K.W. 1997. The role of organic complexation on ambient iron chemistry in the equatorial Pacific Ocean and the response of a mesoscale iron addition experiment. *Limnol. Oceanogr.* **42**: 901–910.

Sunda, W.G. and Huntsman, S.A. 1995. Iron uptake and growth limitation in oceanic and coastal phytoplankton. *Mar. Chem.* **50**: 189–206.

van den Berg, C.M.G. 1995. Evidence for organic complexation of iron in seawater. *Mar. Chem.* **50**: 139–157.

Wells, M.L. and Trick, C.G. 2004. Controlling iron availability to phytoplankton in iron-replete coastal waters. *Mar. Chem.* **86**: 1–13.

Wells, M.L. and Mayer, L.M. 1991. The photoconversion of colloidal iron oxyhydroxides in seawater. *Deep-Sea Res.* **38**: 1379–1395.

Wells, M.L., Price, N.M. and Bruland, K.W. 1995. Iron chemistry in seawater and its relationship to phytoplankton: A workshop report. *Mar. Chem.* **48**: 157–182.

Wu, J. and Luther III, G.W. 1995. Complexation of Fe(III) by natural organic ligands in the Northwest Atlantic Ocean by a competitive ligand equilibration method and a kinetic approach. *Mar. Chem.* **50**: 159–178.

Fundamental differences in the iron acquisition systems among phytoplankton

Charles G. Trick

Department of Plant Sciences, The University of Westem Ontario, London, Ontario, Canada N6A 5B7
E-mail: cyano@julian.uwo.ca

Abstract

Laboratory and shipboard "grow-out" experiments have provided the foundation of our understanding of how different members of the phytoplankton community access "free iron" versus iron bound in natural or artificial ligands. While the mechanism(s) is not fully established, these laboratory and natural population experiments have provided insights into how different members of a community compete for iron supplied either as a xenosiderophore–iron complex or as a ligand–iron complex. We make the distinction between known siderophores added to the system (xeno-siderophores, in this case) and the natural ligands that have been isolated and/or described by the van den Berg and Rue/Bruland research groups. To investigate the role of each of these iron–organic complexes on the shaping of the phytoplankton community, natural populations were exposed to increasing levels of organic iron complexing agents during three recent cruises. The growth and composition of the population were monitored to assess the impact of individual ligands on the eukaryotic and prokaryotic communities. Flow cytometric analysis offered unique insights into the effects of a range of levels of available iron on the phytoplankton community from contrasting oceanographic regimes, including high nutrient, low chlorophyll (HNLC) areas and the oligotropbic central gyres.

Introduction

There are two dichotomies that must be considered when evaluating the methods by which natural phytoplankton communities acquire iron. First, there is a dichotomy on how we view the different population "adaptations". Second, how do we view the source material — the form of iron? The most important question in assessing the relationship between the cellular physiological processes with the ecological processes is based on how we combine these two dichotomies.

In the traditional cellular view, the accessibility of specific forms of iron is different between the two most prominently discussed groups of phytoplankton: the cyanobacteria and the diatoms. Considerable research on the iron acquisition system by diatoms clearly indicates that the prime form of available iron is that of the free ionic form (often referred to as Fe'). When physiologically available forms of iron are reduced to a specific level, the cell accommodates with alterations in the cell quota for iron (by altering the cellular composition: reduction in the iron demands in the photosystem (ferridoxin:flavodoxin), reducing the demands for iron in chlorophyll biosynthesis, perhaps reducing the iron demands for nitrate acquisition). All of these changes occur in direct response to the level of Fe'.

In contrast, the physiological status of cyanobacteria is equally dependent on the availability of free inonrganic iron (Fe') until the levels of iron are reduced significantly to induce the low-iron physiology of these cells. The low-iron physiological state induces a slight reduction in the iron quota of the cell, but the magnitude of the change is not as pronounced as in the diatom model. The primary alteration in cell physiology when Fe' is low is the induction (through depression) of the high-affinity iron acquisition system. This system is a two (or more) part acquisition system comprising of an extracellular-released iron binding ligand (termed: siderophore) and the equally specific iron–ligand membrane receptor for the transport of the ligand-bound iron.

From the cellular perspective, we can refer to these as the FIT (Free Iron Transport) model and the LIT (Ligand Iron Transport) model and we note that our view of iron availability in the oceans in many ways now parallels these two models. Rue and Bruland (this workshop) have just outlined the importance of the naturally formed ligands in marine waters in comparison with the level of newly advected or introduced iron within an ecosystem. Thus, how iron is provided in an

ecosystem is the next dichotomy: some systems are dominated by "fresh" inorganic iron (paralleling the FIT model) whereas others have significant levels of natural ligand binding the iron (paralleling the LIT model). The origin of this natural ligand remains unknown but appears to be a collection of potentially active compounds (Macrelis *et al*., 2001).

In this presentation I would like to propose whether we are accurate in implying the ecological and physiological descriptions of the FIT and LIT models hold true, based on our laboratory and shipboard grow-out experiments. For this presentation I will limit myself to the use of the addition of artificial ligands. In this case, the artificial ligands are siderophores produced by, and isolated from, microorganisms other than the ones we are studying in these experiments. I will use the term "xenosiderophore" to denote these ligands since they are produced in response to iron stress by the host cell ("siderophore") that is foreign ("xeno") to the ecosystem. I will consider the influence of two xenosiderophores on four phytoplankton cultures and on natural communities from a HNLC region of the Eastern Pacific Ocean.

Materials and methods

Laboratory experiments

Experiments were performed in the laboratory using the following cultures: *Synechococcus* sp. PCC7002, *Talassiosira weissflogii* CCMP1051, *Heterosigma akashiwo* NEPCC560R, and *H. akashiwo* NEPCC764R. All cells were maintained in four separate modifications of artificial seawater (ASM) (Harrison *et al.*, 1980) supplemented with f/2 nutrients, metals (except iron) and vitamins. Cells were maintained at four different levels of iron ranging from 0.1 μM to 1 μM. Cells were grown at l8ºC under continuous light flux of 65–80 μmol photons m^{-2} s^{-1}.

The batch culture experiments of 50 mL cultures were prepared in 250 mL acid-washed Erlenmeyer flasks. Cultures were preconditioned in the appropriate medium using the stock culture maintained at the nearest iron concentration. All media contained 1 μM $FeCl_3$ plus the indicated level of either desferal or rhodotorulic acid (Sigma). The induction of iron stress was monitored using F_v/F_m measurements of photosynthetic efficiency (for diatom and flagellate) cultures or chlorophyll/ zeaxanthin levels for the cyanobacterium. Cell densities were monitored at intervals of 6 to 8 h with a Neurembauer hemocytometer and regression analysis of the experimental growth phase was used to calculate the growth rates.

Iron uptake rates were performed using 72 h old cultures, spiked with 2 nM $^{59}FeCl_3$. Cells were allowed to accumulate the radiotracer and sub-fractions harvested at 2, 4, 6 and 24 h. Titanium chloride-EDTA was used to remove unincorporated isotopes. Rates of iron accumulation were calculated using the linear portion of isotope burden versus time.

Field-based sampling

Sampling sites were located off the shelf break on a transect between the Galapagos Islands and the western coast of Peru. All sample water was collected by pumping from surface waters using an all plastic, trace metal clean system. Water for the bioassay experiments was drawn from nutrient-replete waters having comparatively moderate-to-low iron concentrations. Seawater was pumped through the system for several hours to rinse the tubing and pump assembly before collecting a homogenized surface (5 m) sample in a 50 L acid-cleaned polyethylene carboy.

The homogenized surface sample without filtration was distributed into 1000 mL polycarbonate bottles and specific quantities of artificial ligand (Desferal (DFB) or rhodotorulic acid (RA)) or iron (as $FeCl_3$). Triplicate bottles were prepared for daily sampling. Amended cultures were immediately placed in an on-deck, flowing seawater incubator. At the appropriate intervals, bottles were cleanly sampled for nutrients, viruses, bacteria and phytoplankton. Phytoplankton communities were analyzed immediately, without initial preservation, using a Becton Dickinson FACSCalibur flow cytometer equipped with a low argon laser and CellQuest software. In order to normalize the spectrum of cell responses, the software was calibrated using the following: 1, 2, 4, 10, 16 μm non-fluorescent beads for cell size based calibration and 10 μm fluorescent beads to standardized fluorescence corresponding to chlorophyll and phycocyanin.

Results

The yield and growth rate of each of the cultures was influenced by the total amount of iron in the medium (Fig. 1). The yield of all the cultures, except the diatom, were maximal when total iron added was greater than 10^{-6} M, but higher concentrations were required to achieve maximum yield in the diatom culture. As iron levels in the medium were reduced, the yield of the two flagellate cultures dropped quickly with little accumulated biomass when iron levels were less than 10^{-7} M. These flagellates did show an initial but unsustainable growth rate at these low iron levels, indicating that the low level of yield was a function of satiating the iron requirement of the cells, and not an issue of diffusion limitation.

The cyanobacterium and the diatom cultures contrast the growth kinetics of the two flagellates. In the case of the cyanobacterium, there was a rapid loss of cell yield and growth rate with a reduction of iron in the medium. The diatom culture remained active in growth and in the acquisition of iron throughout the different levels of iron, indicating that either more "available" iron was available for this cell or that the quota of this cell was considerably more "plastic" than the other cultures and the cell could maintain a growth rate at low iron concentrations.

If DFB was added to artificially reduce the level of "available" iron in the culture, the cells behaved differently than if the inorganic iron alone was reduced (Fig. 2). The flagellate strains had a more effective ability to remove iron from the complex than the cyanobacterium, whereas the diatom obtained sufficient iron for growth over the entire chelation range, even though the rate of iron transport was dramatically reduced (Fig. 3).

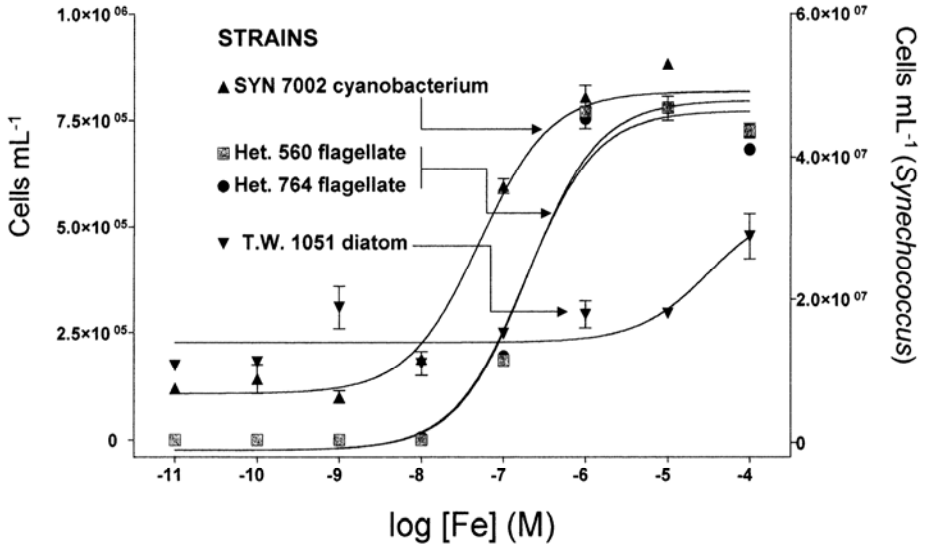

Fig. 1 The yield of the four phytoplankton cultures grown in media with different levels of total iron added.

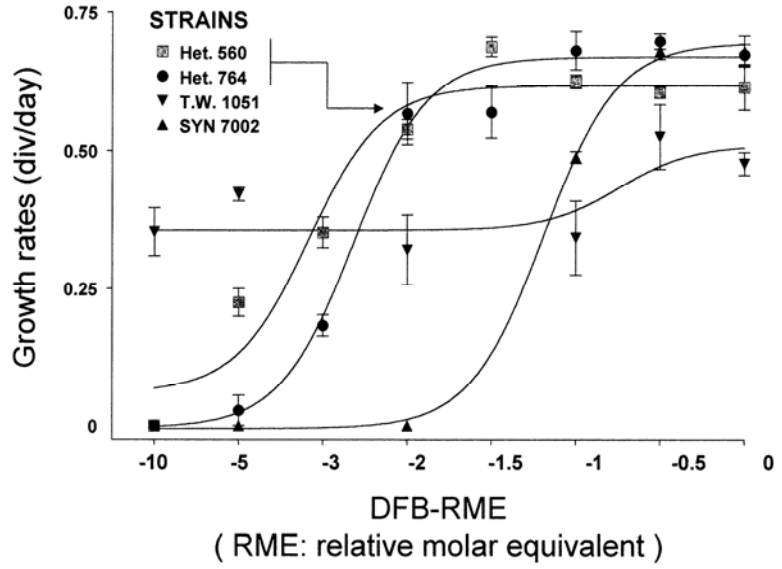

Fig. 2 The maximum growth rate of the laboratory cultures inoculated into media containing 1 µM Fe and the indicated level of DFB (Desferal). Growth rates are the maximum rates observed over a 10-day sampling period.

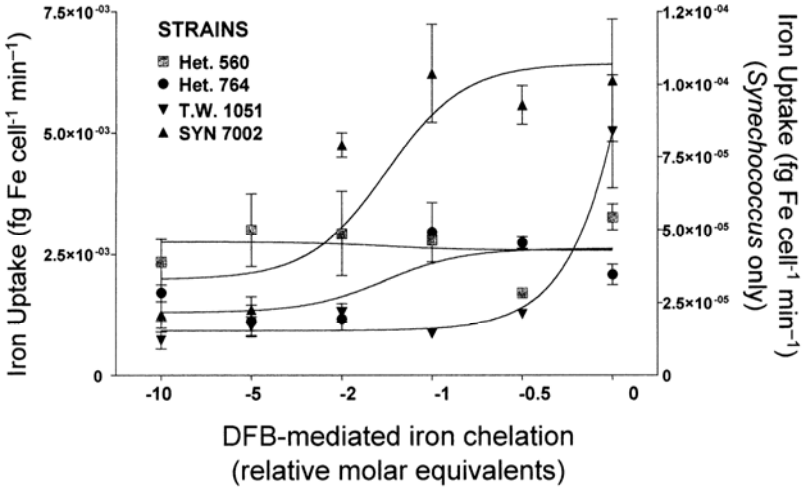

Fig. 3 The rates of iron accumulation mediated by DBF when the cells are exposed to an increasing level of xenosiderophore in the laboratory flask. Iron adsorbed to the cells was removed using the Ti-citrate wash.

Contrasting the addition of DFB to chelate the available iron, the addition of RA was stimulatory to the cyanobacterium and the diatom, while being as limiting to the two flagellates as the addition of the DFB (Fig. 4).

The addition of DFB to the natural population from the HNLC region southeast of the Galapagos Islands almost completely reduced the ability of the population to transform the available nutrients in the water mass. The water contained ~12 nM nitrate, ~9 nM silicate, and ~1.5 nM of phosphate. With the addition of iron to the sample, the final yield of the grow-out experiments was stimulated proportional to the amount of iron added. This stimulation only lasted for 3 days as the system was modified by grazers after Day 3 (Fig. 5).

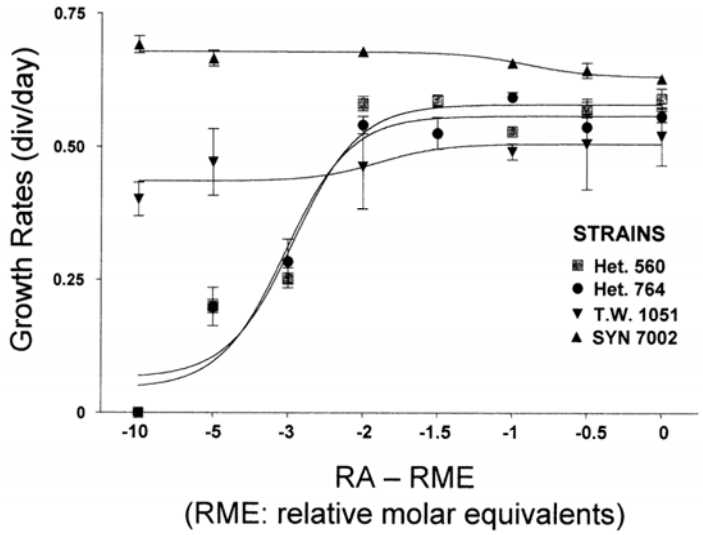

Fig. 4 The growth rates of the four laboratory cultures when the medium contained 1 μM $FeCl_3$ and the level of rhodotorulic acid (RA) was added. The *x*-axis is calculated based on a 2:3 ligand:iron binding ratio for RA.

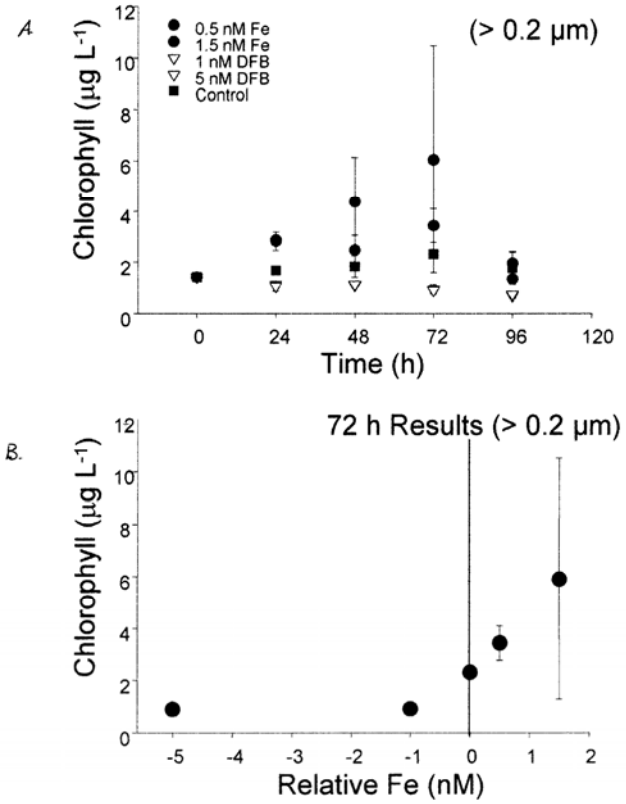

Fig. 5 The growth response of the natural population to the addition of (A) iron (as $FeC1_3$) and (B) DFB to chelate any other iron in the environment. The value of "0" indicated the non-supplemented waters.

The yield was proportional to the level of available iron in the system (Fig. 5B) but not all cells responded identically to the addition or removal of iron (Fig. 6). Figure 7 illustrates the response of four different types of photosynthetic organisms in the grow-out bioassays. In general, all the cells grew in response to the level of predictable iron, with the dramatic exception of the nanoeukaryotic cells (5–20 μm cells). These cells could compete for the available nutrients at low concentrations as the other cells were suitably inhibited by the lack of available iron. The nanoflagellates were growing in the low-iron waters in spite of having a dramatic reduction in the amount of chlorophyll per cell (Fig. 8).

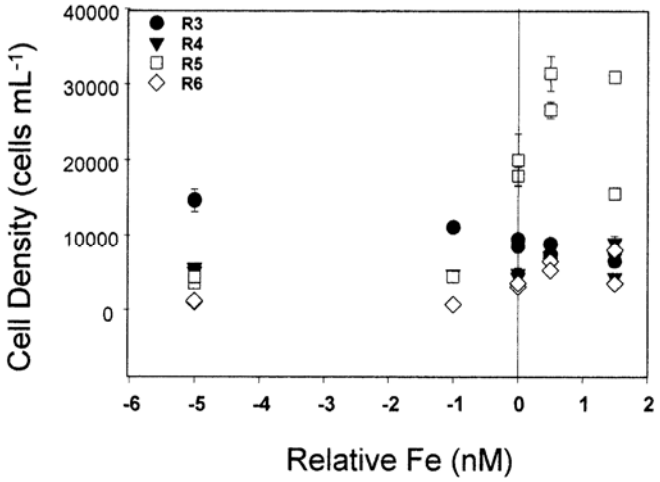

Fig. 6 The different responses of the community to the addition of either iron or the xenosiderophore. R5 is a PC-rich cyanobacterum. R6 is a PE-rich cyanobacterium. R3 is the response of the nanoflagellates in the system.

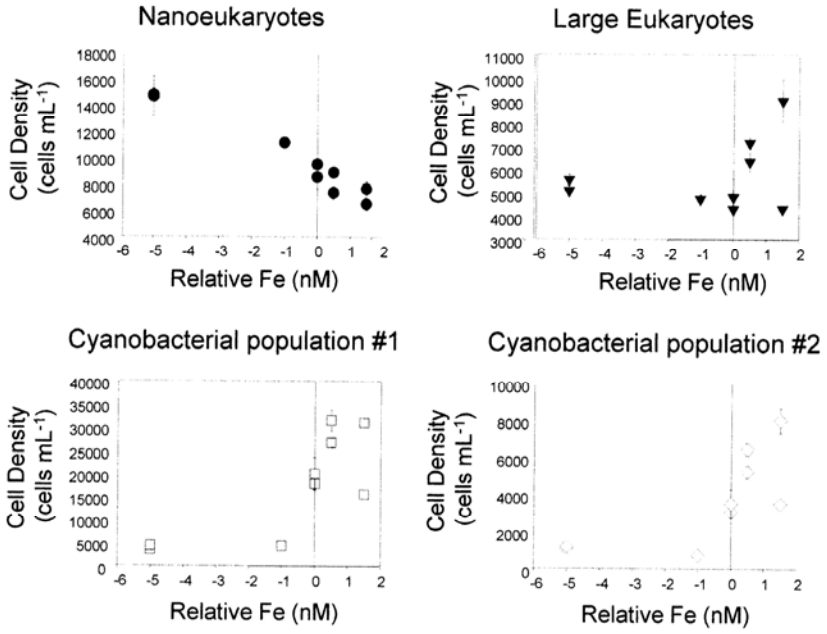

Fig. 7 A detailed look at the different cell populations in response to added iron or chelator.

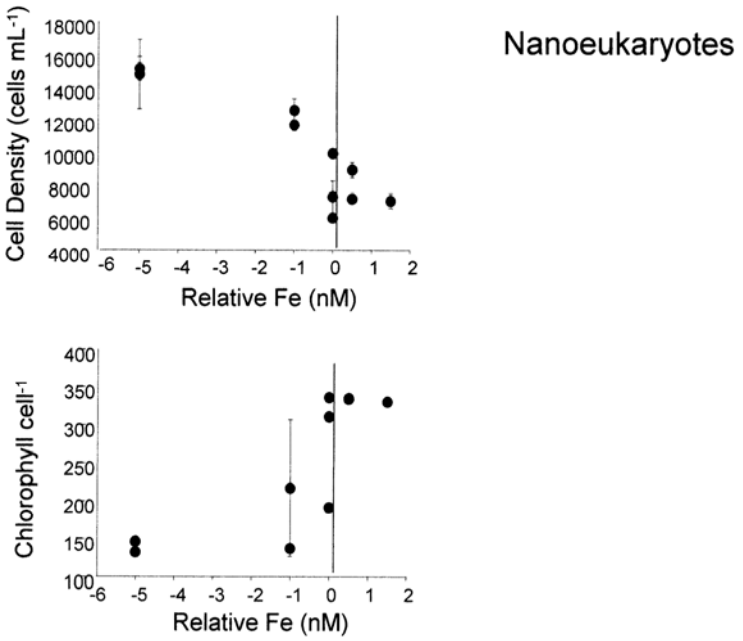

Fig. 8 The response of the nanoeukaryote community to the level of available iron. Even though the population continues to grow when iron levels are low, the lower panel indicates the level of chlorophyll within each surviving cell is dramatically reduced.

Discussion and conclusions

The importance of siderophores in cyanobacteria and the lack of extracellular "siderophores" from diatoms have created an artificial and unwelcome view of how iron is shared among members of the photosynthetic community. There are several points to bring forward:

1. Cyanobacteria are excellent producers of siderophores, and these may be the source of the natural ligand. But in non-marine systems, eukaryotes such as fungi, yeasts, and protests (photosynthetic and non-photosynthetic) are all active producers of iron-binding ligands (some of which have the low-iron inducible ligand–iron transport system and are thus "siderophores"; others are iron-binding "ligands"). Production of natural ligands by eukaryotic microorganisms remains under-appreciated.
2. Production of ligands from heterotrophic bacteria remains a possibility. While recent papers have indicated that carbon limitation remains the primary controlling factor even in HNLC regions, work by Price and by Cochlan (later in the workshop) should provide a new insight.
3. Field and laboratory observations indicate that cyanobacteria perform somewhat better than the larger eukaryotes when the xenosiderophore concentration is only in slight excess to the available iron. The growth of larger eukaryotes is very sensitive to the availability of the free iron in the system and there is no indication that any ability to obtain iron from the xenosiderophore–iron complex results in a competitive advantage of the cells.
4. The group that fills the void when the free iron levels drop and the ligand concentration increases over the natural levels of iron is the "nanoeukaryotes".

The reason for this dominance is not known at present but we could ask the simple question: Is it because they are "nano" or is it because they are mostly flagellates? We can pose several mechanisms. First, like many of the other photosynthetic protists, the photosynthetic system is reduced at higher ligand:iron concentrations. This is evident in chlorophyll/cell and parameters of photosynthetic efficacy. Since many of the observed cells are flagellates without predominant coccoliths (*Phaeocystis*, small dinoflagellates, *etc.*), iron acquisition through phagotrophy is a

possibility, thus circumventing the FIT/LIT model for the origin of available iron. Alternatively, there have been reports to suggest that the adsorption of small colloids to the complex surface of some flagellates will allow for a semi-portable iron pool, accessed through membrane-based reduction physiologies. If we can use our understanding from studies on coastal flagellates as examples, we conclude that the flagellates may have a higher level of adsorbed iron to the cell surface and a means to solubilize and utilize this iron pool.

Acknowledgements

Funding for this work was provided by the Natural Sciences and Engineering Research Council of Canada (NSERCC) and seed funding from The Center for Environmental BioInorganic Chemistry (CEBIC) to CGT.

References

Harrison, P.J., Waters, R. and Taylor, F.J.R. 1980. A broad spectrum artificial seawater medium for coastal and open ocean phytoplankton. *J. Phycol.* **16**: 28–35.

Macrellis, H.M., Trick, C.G., Rue, E.L., Smith, G.J. and Bruland, K.W. 2001. Isolation of natural iron-binding ligands from seawater. *Mar. Chem.* **76**: 175–187.

Rue, E. and Bruland, K.W. Dissolved iron speciation in seawater. This workshop.

In situ testing of iron limitation in the Southern Ocean: An overview of the Southern Ocean Iron Enrichment Experiment (SOIREE)

Cliff S. Law[1] and Phillip W. Boyd[2]

[1] Plymouth Marine Laboratory, Prospect Place, The Hoe, Plymouth, UK, PL1 3 DH. E-mail: csl@pml.ac.uk

[2] Centre of Excellence for Chemical and Physical Oceanography, University of Otago, Dunedin, NZ

Introduction

The HNLC (high nutrient, low chlorophyll) regions account for approximately 30% of the ocean, of which the Southern Ocean occupies the largest surface area and represents the largest repository of excess nutrients. The role of iron as a limiting micronutrient of phytoplankton growth was suggested as early as the 1930s (see de Baar, 1994). Dissolved iron levels at sub-nanomolar concentrations and increases in phytoplankton biomass in response to iron addition have been confirmed for Southern Ocean waters (Martin *et al*., 1990a,b), and circumstantial evidence of iron-limited phytoplankton growth has been obtained in the Polar Front (PF) region (de Baar *et al.*, 1995). However, extrapolation from *in vivo* experiments is limited, due to the exclusion of grazing and physical controls (Banse, 1991), and causality in observational studies is difficult to prove. An alternative approach to establishing the relationship between iron supply and phytoplankton growth was achieved by mesoscale iron enrichment of surface waters in the equatorial Pacific (IronEx I), with tracking of the fertilised waters using a conservative tracer, sulphur hexafluoride (Martin *et al*., 1994; Law *et al*., 1998). A second study, IronEx II, unequivocally confirmed iron limitation in this region, with increased iron availability stimulating phytoplankton growth biomass and production despite increased grazing (Coale *et al*., 1996). Macronutrient concentrations declined in association with a drawdown of surface pCO_2 as inorganic carbon was fixed by the phytoplankton (Cooper *et al*., 1996).

These observations lent support to the "iron hypothesis" (Martin, 1990) that iron-mediated increases in export production may influence atmospheric CO_2. Yet, despite the 90-µatm decrease in surface CO_2 during IronEx II, the equatorial Pacific is not considered an important region for iron-mediated carbon sequestration, due to its limited capacity for transfer of fixed carbon into the deep ocean (Sarmiento and Orr, 1991). Instead, the Southern Ocean is considered to have the greatest potential to influence the oceanic CO_2 sink, due to the significant deep-water formation in this region. Indeed, 3-D ocean models predict that whatever limits nutrient uptake in the Southern Ocean constrains global atmospheric CO_2 on timescales of hundreds of years, with complete nutrient utilisation potentially resulting in a 6–21% decline in atmospheric CO_2 (Sarmiento and Orr, 1991).

However, the results of IronEx II cannot be extrapolated to the Southern Ocean, as factors such as light limitation (Sunda and Huntsman, 1997), co-limitation of diatoms by silicate availability (Boyd *et al*., 1999), and reduced physiological growth rates at lower temperatures may complicate the response to increased iron availability. Similarly, the response of biogeochemical cycling in the surface mixed layer to iron enrichment cannot be extrapolated from *in vivo* studies. Modelling simulations (Sarmiento and Orr, 1991) predict that iron enrichment would result in the complete utilisation of surface ocean macronutrients, yet significant variation has been observed in *in vitro* iron enrichments (de Baar and Boyd, 1999) and the open Southern Ocean (Comiso *et al*., 1993; Moore *et al*., 1999). The results of IronEx II confirmed the requirement for an *in situ* iron fertilisation experiment in open Southern Ocean waters to address the controls of the magnitude of phytoplankton stocks and the implications for atmospheric CO_2. The following discussion describes the results of the **S**outhern **O**cean **IR**on **E**nrichment **E**xperiment (SOIREE) which took place in February 1999 in the Austalasian sector of the Southern Ocean.

Methods

Site selection

Executing an *in situ* experiment, with the requirement to create and track a coherent body of surface water over a 2-week period was logistically and scientifically challenging in the dynamic environment of the Southern Ocean. Site selection for the experiment was critical to the success of the experiment and subsequent extrapolation of the dataset, and so site criteria were identified. The site had to be representative of a broad region of circumpolar HNLC waters, but with low current shear to maximise the timescale of patch tracking. The depth of the surface mixed layer had been regionally representative (see Fig. 1), but shallow enough to avoid iron/light co-limitation (Sunda and Huntsman, 1997), or over-dilution of the iron/SF_6. The pre-cruise desktop survey of bathymetry, sea surface temperature, mean mixed layer depth, wind speed, buoy drift trajectories from climatological datasets of WOA (World Ocean Atlas), JGOFS (Joint Global Ocean Flux Study) and satellite data, is described in Trull *et al.* (2001). Two regions were initially identified (Fig. 1), with 61°S 141°E chosen as the favoured site, partly because it was bounded by two major survey transect lines — R/V *Astrolab* and WOCE SR3 — which provided information on the major features in this region. The site was considered to be dynamically more stable due to a widening between the Polar Front and the southern Antarctic Circumpolar Current. The primary concern relating to the position of the site was the de-coupling of the silicate front from the Polar Front with the southerly migration of the former during summer. Bottle experiments in HNLC regions, IronEx II and observations from the Polar Front all suggest that diatoms were most likely to respond to iron addition, and silicate availability was therefore an important consideration. A 72-h pre-survey of the region confirmed that conditions were representative of polar open waters in summer (Table 1), and stable enough to initiate and maintain an iron-fertilised patch.

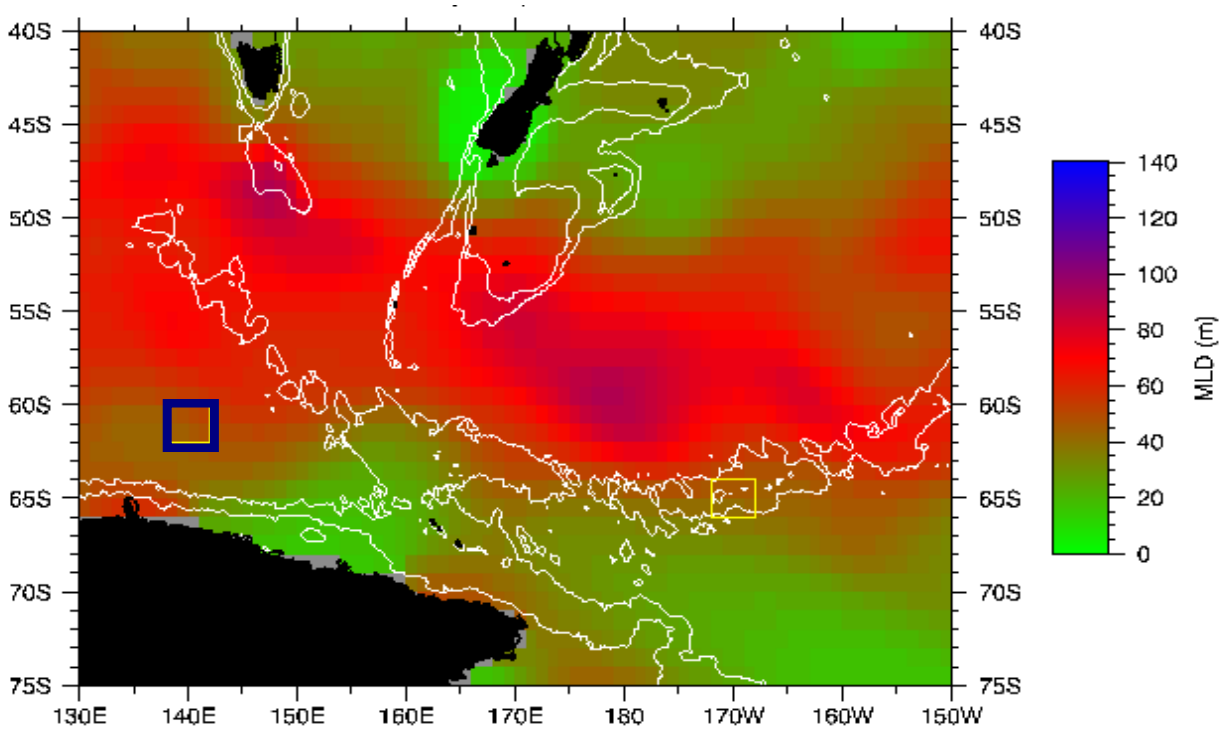

Fig. 1 The SOIREE site (blue box) at 61°S 141°E on a composite image of average mixed layer depth in summer (World Ocean Atlas).

Release

The release of 3.8 tonnes of acidified $FeSO_4$ and 164 g of tracer SF_6 took place on February 9, 1999 over approximately 50 km^2. The release was achieved by an expanding hexagonal track in a Lagrangian frame of reference around a central drifter buoy which updated its position every 10 min, allowing correction for surface water advection. Subsequent iron additions were initiated in response to low dissolved iron levels in the surface waters of the patch. The three subsequent infusions of iron on Days 3, 5 and 7 at the tracer patch centre were smaller (~1.6–1.8 tonnes) than the initial release and were not accompanied by SF_6, as the tracer signal remained high and the patch clearly defined throughout the experiment.

Methodologies are briefly described in Boyd *et al.* (2000) and in detail in the associated references for the following measurements: SF_6 (Law *et al.*, 1998); iron (Bowie *et al.*, 2001); Chlorophyll/ Production (Gall *et al.*, 2001b); DMS/DMSP (Turner *et al.*, 2004); CO_2/DIC (Watson *et al.*, 2000; Bakker *et al.*, 2001).

Table 1 Pre-infusion conditions at the SOIREE site (from Boyd *et al.*, 2001).

Property	
Temperature (C)	2.0±0.05
Density (kg m^{-3})	27.0±0.05
Mixed layer depth (m)	65.0±2.0
Chlorophyll *a* (μg L^{-1})	0.25±0.03
Nitrate (μM)	25.0±1
Silicate (μM)	10±0.4
Phosphate (μM)	1.5±0.2
Dissolved iron (nM)	0.08±0.03
Iron-binding ligands (nM)*	3.8±0.4
Algal community structure	Picophytoplankton-dominated
F_v/F_m	0.22±0.02
Diatom iron stress – (flavodoxin)	High
Euphotic zone depth (m, 1%Io)	84
Community primary production (0–65 m, mg C m^{-2} d^{-1})	150±17
Mesozooplankton stocks (0–70 m, g C m^{-2})	1.6 ± 0.86
Heterotrophic bacterial abundance (× 10^8 cells L^{-1})	3 ± 0.1

Results and discussion

Tracer and iron distribution

The patch drifted approximately 80 km east-southeast during the 13-day experiment and increased in surface area to 200–250 km^2. The tracer patch remained coherent throughout with the cross-patch width remaining constant at ~4–5 km and the along-patch length extending along its transit axis to ~30 km. The coherence of the patch enabled identification of the patch centre and borders and so ease positioning of the IN and OUT stations for vertical hydrocasts. The vertical structure of the patch did not vary significantly although transient structure developed within the 65-m surface mixed layer in the latter part of the experiment in response to improved meteorological conditions.

Iron was measured underway in surface waters and on vertical hydrocasts as dissolved iron (DFe – Fe(II) and Fe(III) that passed through a 0.2-μm filter) and total dissolvable iron (TFe) (Bowie *et al.*, 2001). The mean DFe during the initial mapping was 2.8 nM, close to the predicted release concentration, and observed concentrations in the Polar Front region (de Baar *et al.*, 1994). DFe fell

to 0.3 nM within 2 days to background pre-infusion levels (0.2 nM) due to rapid oxidation to Fe(III) to oxyhydroxides and soft colloids with subsequent aggregation. A similar trend was observed with the re-infusions, with DFe declining towards background levels, although TFe loss decreased prior to the final re-infusion on Day 7. After elevation to 2 nM on Day 7, DFe did not subsequently fall below 0.8 nM for the last 5 days of the experiment. The persistence of the elevated DFe was surprising and it appears that slower precipitation of the insoluble Fe(III) in the colder water of the Southern Ocean, combined with increased potential for photoreduction of Fe(III) to Fe(II), contributed. Furthermore, ~80% of the iron was in the reduced Fe(II) phase at the end of the experiment. This may have been associated with a doubling in the concentration of the Fe(III) ligands which was observed after the final re-infusion (Boyd *et al*., 2000; Croot *et al.*, 2001), leading to an increase in iron complexation capacity. The results indicate that biological mechanisms maintained iron availability in the surface waters of the Southern Ocean, leading to the persistence of the bloom.

Biological response

The response to increased iron availability was significantly slower than in the IronEx studies. This was expected due to the lower physiological rates at lower temperatures and lower light availability in the deeper surface mixed layer. The first biological response was recorded on Day 4 with an increase in F_v/F_m (see Fig. 2), a measure of the quantum efficiency of photosystem II and indicator of the general health of the phytoplankton (Boyd and Abraham, 2001). From Day 4, there was a steady increase in surface F_v/F_m during SOIREE, with an increase to the theoretical maximum of 0.65 in the lower surface mixed layer. Unlike IronEx II, there was no decrease in F_v/F_m after the last iron infusion.

This was followed by other physiological indictors, including decreases in iron stress (decreased flavodoxin expression) and decreased sinking rates (Boyd *et al*., 2000). There was a 5-fold increase in Chlorophyll *a* (Chl-*a*), from 0.4 mg/m^3 to 2 mg/m^3 by 13 days (Gall *et al*., 2001a,b), with an associated increase in column-integrated primary production from 0.2 g/m^2/d to 1.5 g/m^2/d. This exceeded the increase in biomass observed during IronEx I, but was less than the 30-fold increase during the Ironex II study (Coale *et al*., 1996). The elevated Chl-*a* concentrations observed were of similar magnitude to that associated with elevated iron concentrations in the Polar Front region (de Baar *et al*., 1995). C:chlorophyll ratios decreased from 90, prior to the experiment, to ~45 by Day 13, with phytoplankton carbon increasing by 3-fold. Silicate utilisation in the presence of iron was more efficient, with Si:C uptake ratios decreasing from 0.17 in surrounding waters to 0.09 in the iron-enriched patch (Watson *et al*., 2000).

The increase in chlorophyll was interpreted as an increase in chlorophyll per cell in the smaller size classes followed by floristic shifts with an increase in the number of large cells. Size fractionation of the Chl-*a* confirms that the smaller groups responded first, possibly reflecting their capacity to sequester iron faster (Gall *et al*., 2001a). However, by Day 8 the smallest size fraction, <2 µm, crashed in response to an increase in zooplankton grazing (Hall and Safi, 2001). The 5- to 20-µm size class was dominated by the flagellates and increased around Day 7–8 and plateaued towards the end of the experiment. The largest size class, consisting primarily of diatoms, dominated and accounted for 75% of primary production during the experiment. The diatoms were predominately *Fragilariopsis kerguelensis*, a common Southern Ocean bloom-forming species with a high silicate requirement. The increase observed in all size classes indicates that community structure was determined by iron availability, with dominance by the larger diatoms confirming previous observations.

Biogeochemical response

Macronutrient concentration did not exhibit a decrease until Day 5, with nitrate, phosphate and silicate decreasing by 3, 0.22 and 2.5 µM, respectively, by Day 13 (Boyd *et al*., 2000). As in IronEx II, inorganic carbon uptake was significant with CO_2 drawdown in the surface waters of the iron/tracer patch. Continuous measurement of the surface fCO_2 signal patch indicated a clear divergence between the iron-fertilised patch and surrounding waters with a small temperature-related increase in fCO_2 outside the patch and a decrease of ~30 µatm inside (Watson *et al*.,

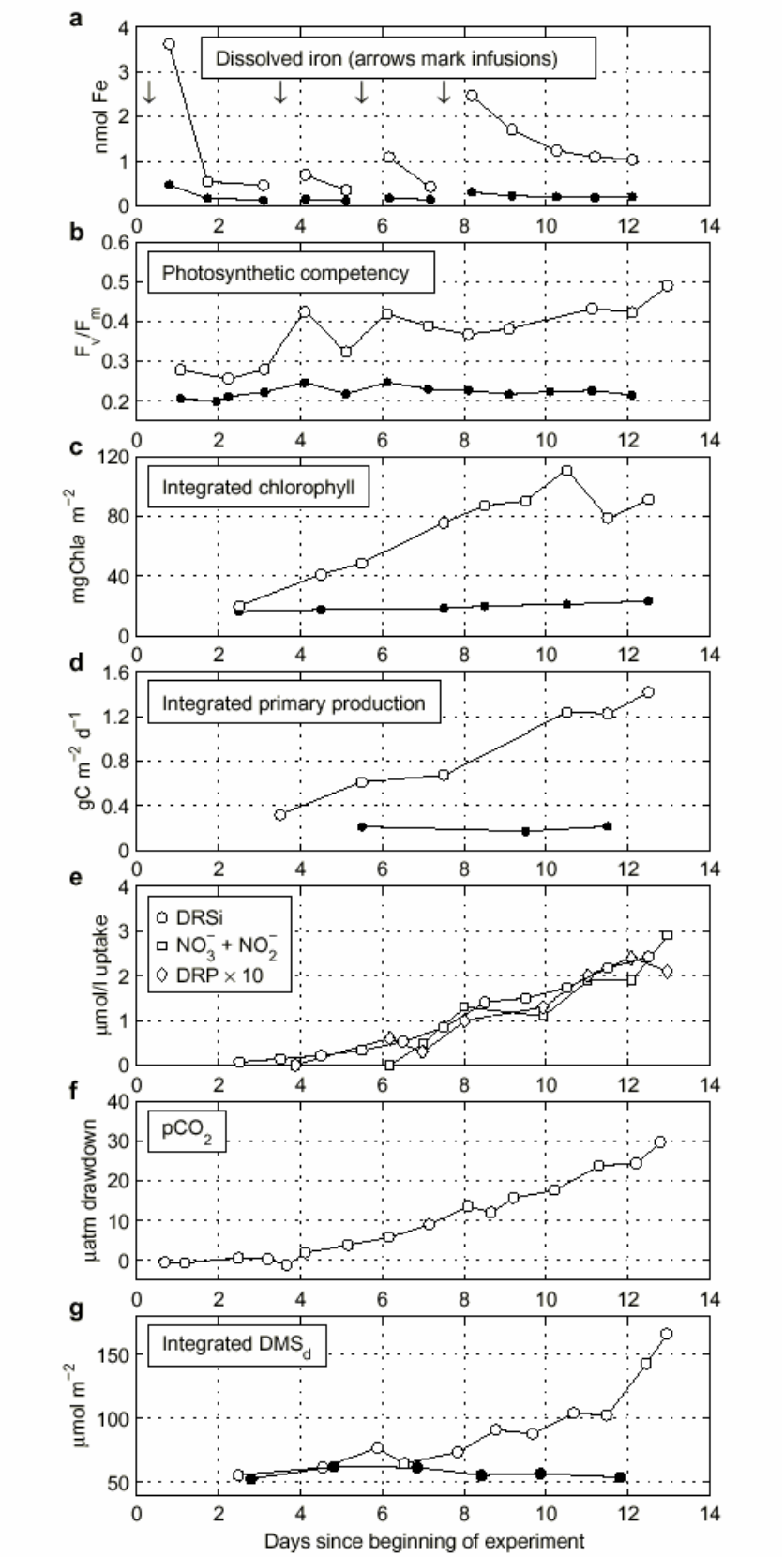

Fig. 2 Biological and biogeochemical response to iron fertilisation during SOIREE (Boyd *et al*., 2000).

2000; see Fig. 3). The drawdown of CO_2 was similar in magnitude to that associated with elevated iron in the Polar Front (de Baar, 1994). DIC decreased by ~15–18 µmol/kg, consistent with the fCO_2 and nitrate drawdown (Bakker *et al.*, 2001).

The increase in phytoplankton production and a shift in community structure stimulated dimethyl suphide (DMS) production during IronEx II (Turner *et al.*, 1996). DMS accounts for a significant proportion of the biogenic sulphur flux to the atmosphere, particularly in remote regions such as the Southern Ocean where it is oxidised to sulphate aerosols, and subsequently influences reflectance and cloud albedo (Charlson *et al.*, 1987). DMS derives from the precursor dimethyl-sulfionproprionate (DMSP) which is an intracellular osmolyte used by certain species of phytoplankton. During SOIREE, particulate DMSP increased to Day 8–9, and then declined, mirroring the 5- to 20-µm phytoplankton size fraction, and suggesting that the primary source of DMSP was the flagellates. DMS levels increased from Day 7, coincident with increased herbivory by the microzooplankton, and were still increasing on Day 13. It is speculative as to whether the DMS would have continued to increase, as diatoms are not generally regarded as significant sources of DMSP. The DMS increase observed during SOIREE was greater than that of IronEx II (7-fold compared with 3-fold compared with initial DMS concentrations, Turner *et al.*, 2004). The SOIREE results support the contention that an increase in iron flux to the Southern Ocean could stimulate DMS flux and impact atmospheric albedo in this region.

The results indicated potential for enhanced export into the deep ocean, with an increase in the biological pump. However, the phytoplankton were relatively healthy on departure (Boyd *et al.*, 2000), and the mesozooplankton response to the increased phytoplankton biomass was limited (Zeldis, 2001). The latter may be attributable to the heavily silicified *F. kergulensis*. Thorium-234 measurements, particulate organic carbon, and biogenic silicate collection in free-drifting sediment traps at 100 m all suggested that no significant export occurred during the 13-day experiment (Charette and Buessler, 2000; Nodder *et al.*, 2001). The accumulation of algal carbon (~4.1 g C/m^2) accounted for ~70% of iron-mediated algal C fixation (6.1 g C/m^2). However, there was evidence of increasing iron stress, aggregation and sinking rates towards the end of the experiment (Boyd *et al.*, 2000).

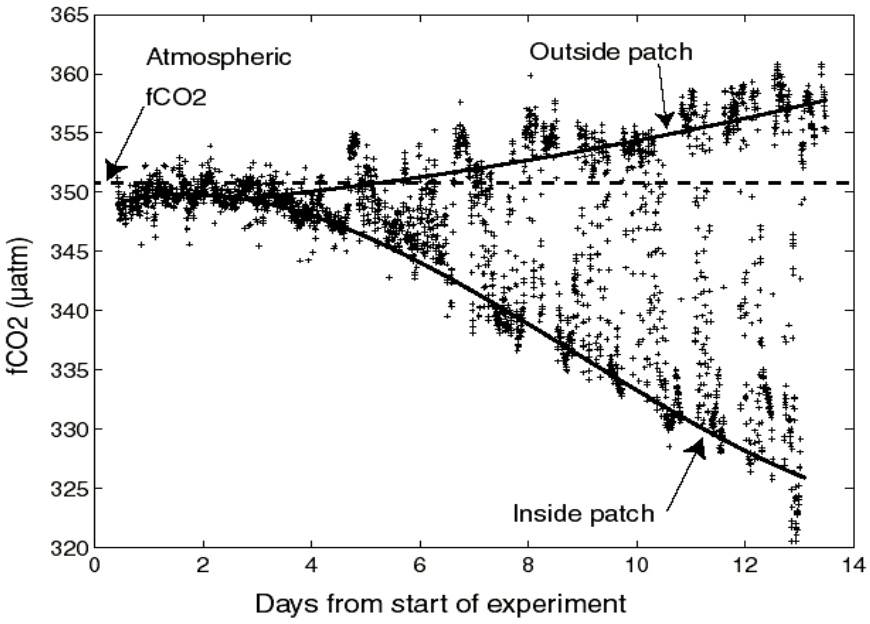

Fig. 3 Response of surface fCO_2 to iron fertilisation during SOIREE (Watson *et al.*, 2000)

Bakker *et al.* (2001) estimate that an additional 1350 tonnes of carbon would be transported into ocean interior on subduction, although Trull *et al.* (2001) suggest that subduction in this region would be unlikely. The persistence of the bloom, as evidenced by elevated Chl-*a* levels in satellite images of the region, confirm that subduction did not occur, and suggests that export was not significant for the 6- to 7-week period following SOIREE (Abraham *et al*., 2000). An elliptical feature of length ~150 km and surface area ~100 km^2 was observed with Chl-*a* levels exceeding 3 mg/m^3, which exceeds the maximum concentrations recorded for this region. Evolution of the bloom into a filament indicates that stirring not only controlled the dispersion but also the development of phytoplankton blooms. Analysis indicates that the patch was spreading at a low enough rate for phytoplankton growth to accumulate biomass and for the iron to remain above a critical level, but high enough to maintain silicate entrainment for diatom growth. Furthermore, the persistence of the bloom indicates that the majority of the iron that remained in the surface waters on Day 13 was still available 6 weeks later (Abraham *et al*., 2000).

Conclusions

SOIREE has successfully demonstrated that the significance of iron in water was broadly representative of 75% of polar waters during the austral summer in this region of the Southern Ocean. The results indicate that iron controls the magnitude of production and community composition, and further support the link between iron, phytoplankton and climate, although the ultimate fate of the iron-mediated bloom is speculative. The observations have raised fundamental questions relating to iron biogeochemistry and retention in the surface ocean, and identified the importance of stirring to the maintenance of phytoplankton blooms.

References

Abraham, E., Law, C.S., Boyd, P.W., Lavendar, S., Maldonado, M. and Bowie, A.R. 2000. The dispersal of an isolated phytoplankton bloom. *Nature* **407**: 727–730

Bakker, D.C.E., Watson, A.J. and Law, C.S. 2001. Southern Ocean Iron Enrichment promotes inorganic carbon drawdown. *Deep-Sea Res. II* **48**: 2483–2507.

Banse, K. 1990. Does iron really limit phytoplankton production in the offshore subarctic Pacific? *Limnol. Oceanogr.* **35**: 772–775.

Banse, K. 1991. Iron availability, nitrate uptake and exportable new production in the subarctic Pacific. *J. Geophys. Res.* **96**: 741–748.

Bowie, A.R., Maldonado, M.T., Frew, R.D., Croot, P.L., Achterberg, E.P., Mantoura, P.J., Worsfold, R.F.C., Law, C.S. and Boyd, P.W. 2001. The fate of added iron during a mesoscale fertilisation in the polar Southern Ocean. *Deep-Sea Res. II* **48**: 2703–2743.

Boyd, P.W. and Abraham, E.R. 2001. Iron-mediated changes in phytoplankton photosynthetic competence during SOIREE. *Deep-Sea Res. II* **48**: 2529–2550.

Boyd, P.W., La Roche, J., Gall, M., Frew, R. and McKay, R.M.L. 1999. The role of iron, light and silicate in controlling algal biomass in sub-Antarctic waters SE of New Zealand *J. Geophys. Res.* **104**: 13,395–13,408.

Boyd, P.W., Watson, A.J., Law, C.S. *et al.* 2000. A mesoscale phytoplankton bloom in the polar Southern Ocean stimulated by iron fertilization. *Nature* **407**: 695–702.

Charette M.A. and Buesseler, K.O. 2000. Does iron-fertilisation lead to rapid carbon export in the Southern Ocean? *Geochem. Geophys. Geosyst.* 2000GC000069.

Charlson, R.J, Lovelock, J.E., Andreae, M.O. and Warren, S.G. 1987. Oceanic phytoplankton, atmospheric sulphur, cloud albedo and climate. *Nature* **326**: 655–661.

Coale, K.H., Johnson, K.S., Fitzwater, S.E. *et al*. 1996. A massive phytoplankton bloom induced by an ecosystem-scale iron fertilization experiment in the equatorial Pacific Ocean. *Nature* **383**: 495–501.

Comiso, J.C., McClain, C.R., Sullivan, C.W., Ryan, J.P. and Leonard, C.L. 1993. Coastal Zone Color Scanner Pigment concentrations in the Southern Ocean and relationships to geophysical surface features. *J. Geophys. Res.* **98**: 2419–2451.

Cooper, D.J., Watson, A.J. and Nightingale, P.D. 1996. Large decrease in ocean-surface CO_2 fugacity in response to *in situ* iron fertilisation. *Nature* **383**: 511–513.

Croot, P.L., Bowie, A., Frew, R.D., Maldonado, M., McKay, M., LaRoche, J. and Boyd, P.W. 2001. Retention of dissolved iron and Fe(II) in an iron induced Southern Ocean phytoplankton bloom. *Geophys. Res. Lett.* **28**: 3425–3428.

de Baar, H.J.W. 1994. Von Liebig's law of the minimum and plankton ecology (1899–1991). *Prog. Oceanogr.* **33**: 347–386.

de Baar, H.J.W. and Boyd, P.W. 1999. The role of iron in plankton ecology and carbon dioxide transfer of the global oceans. pp. 61–140. *In* The Dynamic Ocean Carbon Cycle: A Midterm Synthesis of the Joint

Global Ocean Flux Study, Chapter 4, International Geosphere Biosphere Programme Book Series. *Edited by* R.B. Hanson, H.W. Ducklow and J.G. Field, Cambridge University Press, Cambridge.

de Baar, H.J.W., Buma, A.G.J., Jacques, G., Nolting, R.F. and Trequer, P.J. 1989. Trace metals – Iron and manganese effects on phytoplankton growth. *Berichte zur Polarforschung* **65**: 34–44.

de Baar, H.J.W., de Jong, J.T.M, Bakker, D.C.E., Löscher, B.M., Veth, C., Bathmann, U. and Smetacek, V. 1995. Importance of iron for plankton blooms and carbon dioxide drawdown in the Southern Ocean. *Nature* **373**: 412–415.

de Baar, H.J.W., de Jong, J.T.M, Nolting, R.F., van Leeuwe, M.A., Timmermans, K.R., Bathmann, U., Rutgers van der Loeff, M. and Sildam, J. 1999. Low dissolved Fe and the absence of diatom blooms in remote Pacific waters of the Southern Ocean. *Mar. Chem.* **66**: 1–34.

Frost, B.W. 1996. Phytoplankton blooms on iron rations. *Nature* **383**: 475–476.

Gall, M., Boyd, P.W., Hall, J., Safi, K. and Chang, H. 2001a. Phytoplankton processes. Part 1: Community structure in the Southern Ocean Iron Release Experiment. *Deep-Sea Res. II* **48**: 2551–2570.

Gall, M., Strezpek, R., Maldonado, M. and Boyd, P.W. 2001b. Phytoplankton processes. Part 2: Rates of primary production and factors controlling algal growth during the Southern Ocean Iron RElease Experiment (SOIREE). *Deep-Sea Res. II* **48**: 2571–2590.

Hall, J. and Safi, K. 2001. The impact of Fe addition on the microbial food web. *Deep-Sea Res. II* **48**: 2591–2613.

Law, C.S., Watson, A.J., Liddicoat, M.I. and Stanton, T. 1998. Sulphur hexafluoride as a tracer of biogeochemical and physical processes in an open-ocean iron fertilisation experiment. *Deep-Sea Res. II* **45**: 977–994.

Martin, J.H. 1990. Glacial-interglacial CO_2 change: The iron hypothesis. *Paleoceanography* **5**: 1–13.

Martin, J.H., Gordon, R.M and Fitzwater, S.E. 1990a. Iron in Antarctic waters. *Nature* **345**: 156–158.

Martin, J.H., Gordon, R.M and Fitzwater, S.E. 1990b. Iron deficiency limits phytoplankton growth in Antarctic waters. *Global Biogeochem. Cycles* **4**: 5–12.

Martin, J.H., Coale, K.H., Johnson, K.S. *et al*. 1994. Testing the iron hypothesis in ecosystems of the equatorial Pacific Ocean. *Nature* **371**: 123–129.

Mitchell, B.G., Brody, E.A., Holm-Hansen, O., McClain, C. and Bishop J. 1991. Light limitation of phytoplankton biomass and macronutrient utilization in the Southern Ocean. *Limnol. Oceanogr.* **36**: 1662–1677.

Moore, J.K., Abbott, M.R., Richman, J.G., Smith, W.O., Cowles, T.J., Coale, K.H., Gardner, W.D. and Barber, R.T. 1999. SeaWiFS satellite ocean color data from the Southern Ocean. *Geophys. Res. Lett.* **26**: 1465–1468.

Nodder, S.D. and Waite, A.M. 2001. Is Southern Ocean organic carbon and biogenic silica export enhanced by iron-stimulated increases in biological production? Sediment trap results from SOIREE. *Deep-Sea Res. II* **48**: 2681–270.

Sarmiento, J.L. and Orr, J.C. 1991. Three-dimensional simulations of the impact of Southern Ocean nutrient depletion on atmospheric CO_2 and ocean chemistry. *Limnol. Oceanogr.* **36**: 1928–1950.

Sunda, W.G. and Huntsman, S.A. 1997. Interrelated influence of iron, light and cell size on marine phytoplankton growth. *Nature* **390**: 389–392.

Trull, T.W., Rintoul, S.R., Hadfield, M. and Abraham, E.R. 2001. Circulation and seasonal evolution of polar waters south of Australia: Implications for iron fertilization of the Southern Ocean. *Deep-Sea Res. II* **48**: 2439–2466.

Turner, S.M., Nightingale, P.D., Spokes, L.M., Liddicoat, M.I. and Liss, P.S. 1996. Increased dimethyl sulphide concentrations in sea water from *in situ* iron enrichment. *Nature* **383**: 513–517.

Turner, S., Harvey, M.J., Law, C.S., Nightingale, P.D. and Liss, P.S. 2004. Iron-induced changes in oceanic sulfur biogeochemistry. *Geophys. Res. Lett.* **31**: doi:10.1029/ 2004GL020296.

Watson, A.J., Bakker, D.C.E., Boyd, P.W., Ridgwell, A.J. and Law, C.S. 2000. Effect of iron supply on Southern Ocean CO_2 uptake and implications for glacial atmospheric CO_2. *Nature* **407**: 730–732.

Zeldis J. 2001. Mesozooplankton community composition, grazing, nutrition, and export production at the SOIREE site. *Deep-Sea Res. II* **48**: 2615–2634.

A1.2.2 Chemistry in the North Pacific and IronEx

Iron distribution in the Northeast Pacific Ocean

C.S. Wong[1], Shigenobu Takeda[2], Jun Nishioka[2], W. Keith Johnson[1] and Nes Sutherland[1]

[1] Climate Chemistry Laboratory, Institute of Ocean Sciences, Department of Fsiheries and Oceans, 9860 West Saanich Road, Sidney, BC, Canada V8L 4B2. E-mail: wongcs@pac.dfo-mpo.gc.ca
[2] Biology Department, Central Research Institute of Electric Power Industry, Abiko-city, Chiba, Japan 270-1194

Introduction

This paper describes the preliminary results on the spatial description of iron in the Northeast Pacific Ocean, being conducted on board the CCGS *John P. Tully* for a joint project between the Climate Chemistry Laboratory of the Institute of Ocean Sciences (IOS, Canada) and the Biology Department of the Central Research Institute of the Electric Power Industry (CRIEPI, Japan).

The upper waters of the subarctic Pacific Ocean, equatorial Pacific and Southern Ocean are the three major HNLC (high nutrients, low chlorophyll) regimes in the world oceans. They are characterized by a shortage of iron as a micronutrient, thus inhibiting the growth of diatoms and limiting the full utilization of the macronutrients available in the surface mixed layer. The seasonal and spatial distributions of iron are therefore, fundamental to understanding the availability and utilization of this essential micronutrient by diatoms in HNLC waters.

Iron in seawater is difficult to measure due to the ubiquitous presence of iron as a contaminant in the sampling and measuring procedures, with dust in the air and rust from ship and oceanographic sampling gears and wires. Extreme care is required in all phases of shipboard sampling and analysis to ensure data integrity. This paper describes the salient points in the detection of iron in seawater, results of recent measurements from IOS cruises on Line P and Station P, and a project to study mesoscale eddies in the Northeast Pacific Ocean. Nishioka *et al*. (2001) describes the distribution of soluble and small colloidal iron for these cruises.

The definitions used to distinguish different forms of dissolved iron are: (1) labile, unfiltered seawater, (2) dissolved, <0.45µm, (3) labile particulate, (1) minus (2), (4) colloidal, between 0.1 and 0.45 µm, and (5) soluble plus small colloidal, <0.1 µm. In this study, the main form discussed here is labile (sometimes called total dissolvable) iron.

Methods

Samples for iron analyses were collected under two separate projects: (1) a Station P/Line P monitoring study and (2) an eddy study in the Northeast Pacific Ocean. For project (1), iron distribution on Line P from the west coast of Vancouver Island to Station P (*i.e.*, P26) is shown in Figure 1, with sampling stations at regular oceanographic stations of P04 (48º 29′N, 126º 40'W), P12 (48º 58′N, 130º 40′W), P16 (49º 17′N, 134º 40′W), P20 (49º 34′N, 138º 40′W) and P26 (50º 00′N, 145º 00′W). At these stations, hydro-casts for iron samples were made for depths of 10, 25, 75, 100, 200, 300, 400 and 600 m as well as 800 and 1000 m in more recent expeditions. Surface sampling was done from a Zodiac rubber boat. For the Eddy Project (project 2), iron sampling was made during special cruises to monitor the water properties at the edge and inside the eddy as it moved from the coastal ocean towards the vicinity of Station P. Similar profiles for iron were made, as described for the regular Station P/Line P monitoring project.

Sampling of seawater for the iron study was done in several ways. At hydro-stations, 30 Go-flow™ samplers were pre-cleaned in the laboratory by sequential soaking with 5% Extran for about 1 day, then 0.1% HCl or dilute 0.1M ascobic acid, or a mixture of both, for a few days with DMQ rinses in between. At sea the samplers were filled with seawater at low iron levels for about 1 day for soaking.

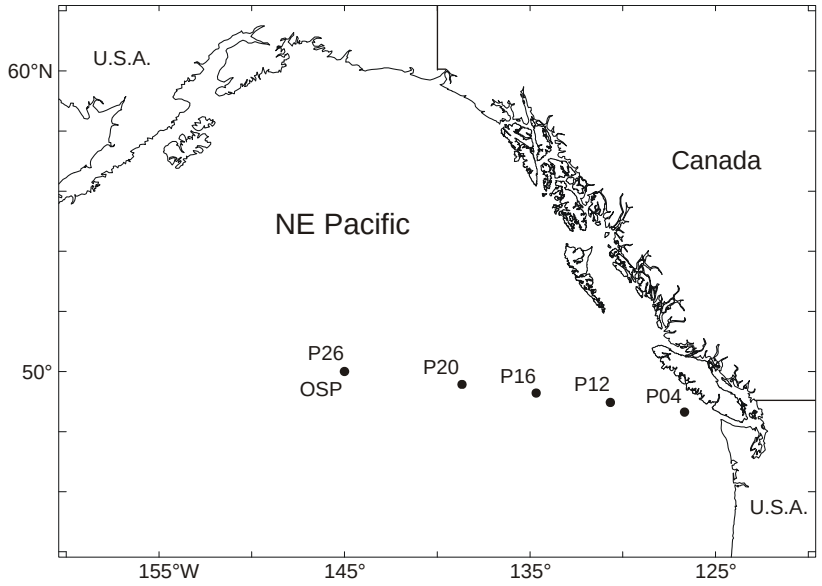

Fig. 1 Position of stations along Line P.

Samples from 75 m and below were collected using 30 L (or 10 L for Station P04 only) bottles on a 1,000-m Kevlar line spliced to the hydrowire on a hydro winch, with a layer of plastic separating the Kevlar from the steel line. Lead weights, freshly encased in epoxy resin, were attached to the end of the Kevlar line. Shallow samples at 10, 25 and 40 m were also collected using an air-driven Teflon pump and Teflon sampling tube with handling done in a PVC HEPA clean hood on deck. Seawater samples were drawn from Go-flow™ samplers on deck using boxes with extended sides and roof to minimize air disturbance. A Teflon tube was attached to a Teflon valve on the Go-flow™ and on the other end, a bell jar covered the sample bottles during sub-sampling. Two to six 250-ml pre-cleaned CPE bottles, after rinsing three times, were immediately filled with seawater. Normally, two were unfiltered, and one each was filtered through a 90 mm 0.45 µm Durapore membrane filter, and a 0.1µm (0.22 µm used since June, 2000) Opticap cartridge by Millipore.

Analysis

Iron analyses were made inside a shipboard clean laboratory of about 10′ × 7′, constructed with polyethylene sheets with a small entry cubicle. A positive-pressure clean hood (Class 100 EACI laminar flow work station at ~360 cubic feet per minute) with a Class 100 HEPA filter created a clean space for reagent preparation and sample processing. A tacky mat at the entrance eliminated dirt on shoes and personnel entering the clean room wore clean plastic suits with hoods, boots and gloves. A milli-Q ultra-violet system inside the clean room supplied high purity water (DMQ) for reagents, standards and cleaning.

A chemiluminescence technique (Obata *et al*., 1993) with modifications (Obata *et al*., 1997) was used. A semi-automated system, constructed by the Climate Chemistry Laboratory, was used. The method is a combination of selective column extraction using chelating resin and chemiluminescence detection. Samples were buffered to pH 3.2 using a buffer solution of formic acid-ammonium formate. Samples were delivered to the system using an eight port valve (Hamilton MVP 8) and a peristaltic pump. About 4–16 ml were passed through a resin column of 8-hydroxyl quinnolin immobilized on silica gel at a flow rate of 4 ml per minute. The iron was then removed from the column using dilute HCl (0.3N). The resulting eluent was then mixed with luminol, aqueous ammonia and hydrogen peroxide, prior to entering the cell (Teflon tubing coiled on a mirror). A Hamamatsu photo multiplier tube measured the light emitted from the chemiluminescent reaction of the iron and luminol as the eluent passed through the cell with the resulting signal recorded on a laptop computer.

Reagents

The reagents were prepared as described in Obata *et al*. (1997): Seastar ultrapure grade HCl and NH_4OH, re-crystallized luminol and TETA (triethylene tetramine), K_2CO_3 (Merck Suprapure grade), H_2O_2 (Baker Ultrapure grade) and twice quartz distilled HCOOH. The 8-quinolinol immobilized chlelating resin was obtained from Dr. H. Obata. Reagents were prepared in advance to allow for degassing of the aerated DMQ between the feed source on the ship and the shipboard laboratory.

Standards

AAS Standard Fe(III) of 1,000 ppm solution commercially available was used to prepare a primary standard (1,000 ppb) and secondary standard (10 ppb), which were used to prepare fresh daily working standards. Seawater, collected from Station P surface waters and filtered through a 0.1 μm cartridge filter, was used to make up standards. The iron content was < 0.l nM.

Results and discussion

The study area covered Line P (48.5ºN, 126ºW to 50ºN, 145ºW) and Line Z (47°N, 145°W to 59.5°N, 145°W). At Station P, inter-calibrations (Fig. 2) were made between IOS and CRIEPI using basically the same technique and sampling equipment. John Martin's profile (Martin and Fitzwater, 1988) in 1987, using the atomic absorption technique, is also plotted in the figure for comparison. There was good agreement between IOS and CRIEPI for seawater at a depth lower than about 400 m, while in the upper ocean the CRIEPI values were slightly higher.

The vertical profiles (0–1,000 m) of unfiltered labile (LFe) iron for June 1998 (cruise #9815) on Line P (Fig. 3), showed relatively low (<0.1 to 0.4 nM) iron in the surface 50 m. At coastal station P04, iron increased rapidly to a high value of 4.5 nM at 600 m, then decreased slowly to 3.6 nM at 1,000 m. Station P12 showed a slightly higher value in the upper 100 m and below 500 m compared to the other offshore stations. For the offshore stations P16, P20 and P26 (Station P) in the HNLC waters, iron values were generally < 0.1 nM in the upper 100 m with a small increase to about 0.5 to 0.6 nM at depths from 400 to 1,000 m.

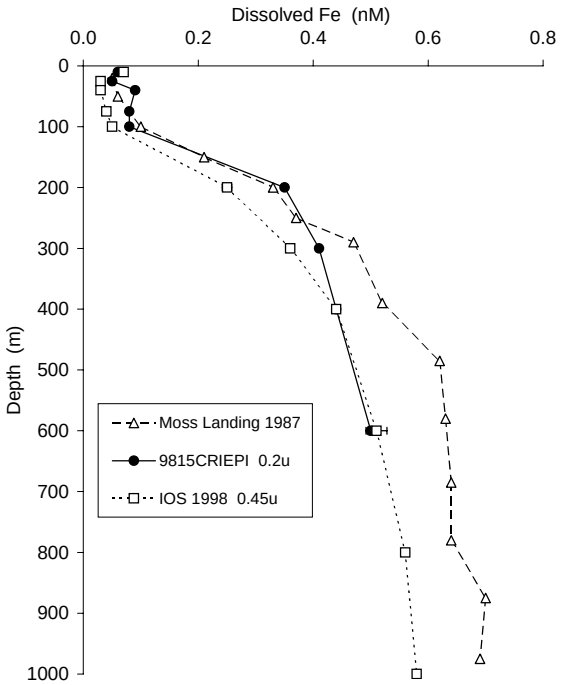

Fig. 2 Intercomparison of iron measurements done near Station P (P26) by IOS, CRIEPI and earlier, by Moss Landing Marine Laboratory (Martin and Fitzwater, 1988).

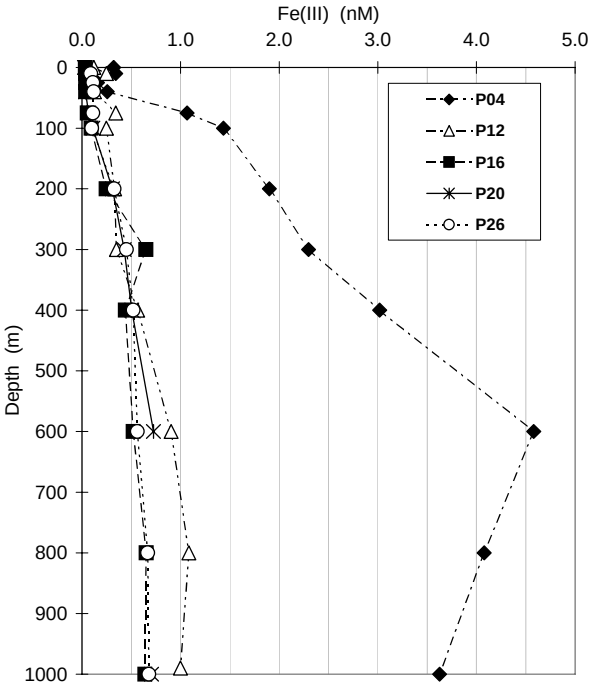

Fig. 3 Vertical distribution of unfiltered iron (Cruise 9815) at stations P04, P12, P16, P20 and P26 along Line P.

Horizontal surface iron distribution (labile and dissolved, 0.1 µm filtered) at depths of 10 and 20 m in September 1997 is shown in Figure. 4. There is a high coastal labile iron concentration at 0.75 nM and much lower distribution of <0.15 nM farther offshore from P19 to P26. At Station P17 (at 136°W), there is marked increase to 0.35 nM and for stations at 143°W and 145°W, a smaller increase to 0.2 nM, indicating possible transport of iron-rich waters either vertically or by eddies.

The Haida Eddy is a slow-moving eddy formed near the Queen Charlotte Islands, off the west coast of British Columbia. The eddy is anti-cyclonic, has a diameter of about 200–300 km, and moves at about 3–5 km per day to the west towards Station P. The Haida Eddy 1998, formed just outside Queen Charlotte Islands in February 1998, moved in a path opposite to the direction of the Alaskan arm of the eastern sub-arctic gyre, first southward along 134ºW to 48ºN 136ºW (February 1998), then southwestward towards 46ºN 141ºW (February, 2000). Iron measurements from the surface to a depth of 600 m were made at the centre, the edge and outside the eddy (Fig. 5) in Haida 2000. In the centre, labile iron in the surface mixed layer down to 50 m was about the same as at the edge of the eddy. To the south of the eddy, the labile iron was higher in the surface due to coastal seawater streaming from Hecate Strait.

Open ocean values are shown from P20 to demonstrate how much more iron is found in coastal and eddy seawater. Below the pycnocline at about 100–120 m, labile iron from the centre of the eddy was much higher than the values at the edge and outside the eddy. This indicated that the centre of the anti-cyclonic Haida Eddy conserved high iron after it left the coastal zone. The original depth of the Haida Eddy was thought to be 200 to 300 m, indicating that some iron was being transported to depth as the eddy aged. The iron content after filtration through a 0.22 µm Millipore/Durapore filter, was only 25% lower. The same is true for the stations at the centre and on the edge of the eddy. By September, the surface iron was probably approaching limits for the Haida Eddy when both labile and dissolved iron (<0.22 µm) in the whole upper 75 m were both below 0.05 nM while water below this was still more than double what was found at P20.

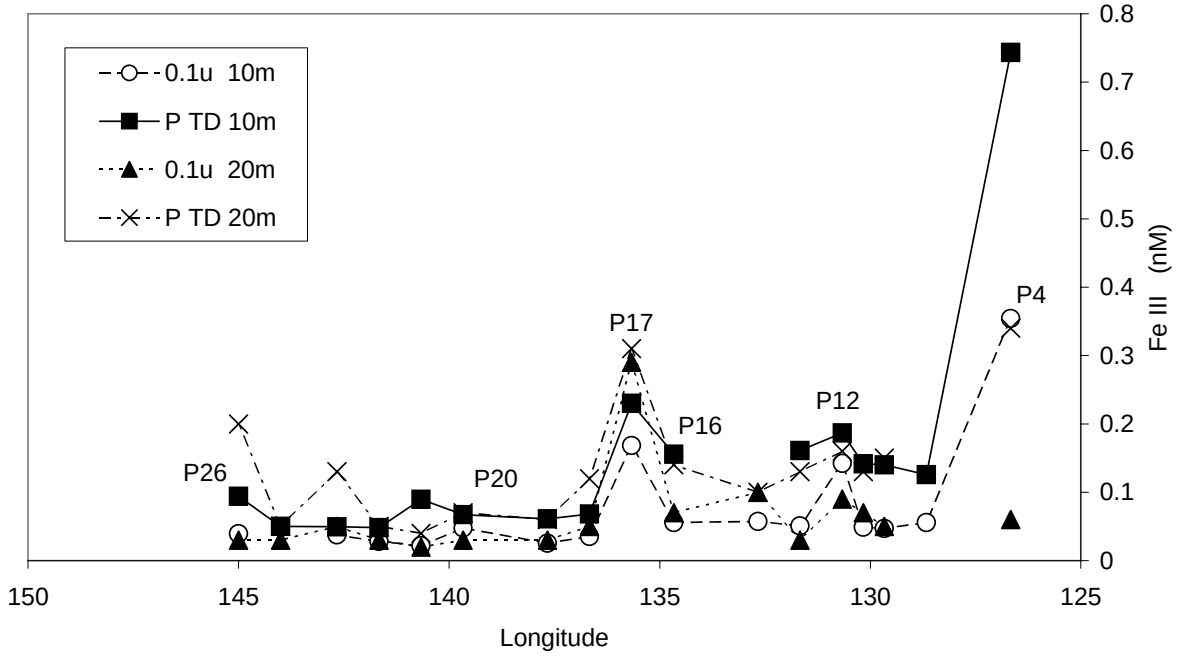

Fig. 4 Horizontal distribution of iron along Line P in September 1997.

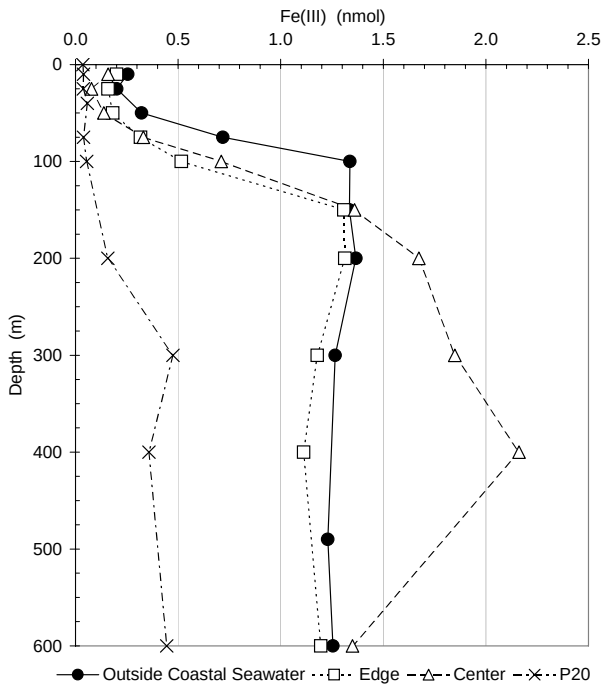

Fig. 5 Distribution of unfiltered buffered (labile) iron at the edge, inside and outside the Haida Eddy in June 2000.

Conclusions

1. Shipboard iron measurements by chemi-luminesence technique using clean reagents, sampling procedures and analytical environment are compatible between CRIEPI and IOS laboratories.

2. The vertical distribution of iron in HNLC waters in the Northeast Pacific showed very low surface values while in deep waters, iron was high but was prevented from reaching the surface mixed layer because of a strong pynocline at 100 m depth.

3. The horizontal distribution of iron in September, 1997, from coastal to open-ocean waters showed a progressive decrease, with high values of 0.8 nM just west of Vancouver Island to <0.1 nM at Station P (P26) with high values at Station P17 in between, suggesting the possibility of eddy transport of high iron from coastal waters to offshore.

4. In an eddy study in the Northeast Pacific to track the change in water properties, iron distribution was measured at the edge, outside and at the centre of the Haida Eddy. Coastal iron outside and at the edge of the eddy showed similar features with depth, but in the centre of the eddy below the pycnocline, iron was almost doubled, suggesting that iron was trapped inside the eddy. Compared with open ocean seawater, the eddy contained more than four times as much iron below 75 m.

References

Martin, J. and Fitzwater, S.E. 1988. Iron deficiency limits phytoplankton in the northeast Pacific subarctic. *Nature* **331**: 341–343.

Nishioka, J, Takeda, S., Wong, C.S. and Johnson, W.K. 2001. Size-fractionated iron concentrations in the northeast Pacific Ocean: distribution of soluble and small colloidal iron. *Mar. Chem.* **74**: 157–179.

Obata, H., Karatani, H. and Nakayama, E. 1993. Automated determination of iron in seawater by chelating resin concentration and chemi-luminescence detection. *Anal. Chem.* **65**: 1524–1528.

Obata, H., Karatani, H. and Nakayama, E. 1997. Fundamental studies for chemical speciation of iron in seawater with an improved analytical method. *Mar. Chem.* **56**: 97–106.

Iron and manganese distribution in the surface waters of the North Pacific Ocean and the Bering Sea

Hajime Obata[1], Eiichiro Nakayama[2], Masahiro Maruo[2], Michiaki Takano[2] and Yoshiyuki Nozaki[3]

[1] Oceanography Laboratories, University of Liverpool, Liverpool, UK L69 7Zl. E-mail: obata@liverpool.ac.uk
[2] School of Environmental Science, The University of Shiga Prefecture, Hassaka, Hikone, Shiga, Japan 522-8533
[3] Ocean Research Institute, University of Tokyo, Nakano-ku, Tokyo, Japan 164-8639

The distributions of iron and manganese in the surface layers were investigated in the North Pacific Ocean and the Bering Sea. Samples were collected during the research cruise of R/V *Hakuho-maru* (University of Tokyo), KH-99-3 (from June 25 to July 22, 1999). Iron and manganese concentrations were determined with automated chemiluminescence methods (Nakayama *et al*., 1989; Obata *et al*., 1993, 1997). Iron was depleted at 0–50 m all through the sampling stations, but iron concentrations below 50 m showed contrasting distributions between the western and the eastern sides of the North Pacific Ocean, and the Bering Sea. To discuss the difference in the iron sources between the stations, iron distributions were compared with those of manganese. As the residence time of manganese in the surface layer is relatively long (5–19 yr, Landing and Bruland, 1987), manganese is suitable as a tracer for the supply of a lithogenic substance. The relationship between nitrate and silicate in the surface layers also showed various patterns in each oceanic regime. Iron limitation is reported to affect the uptake ratio of silicate to nitrate by diatoms (Takeda, 1998), and the supply of iron may influence the relationship between nitrate and silicate in the surface layer.

References

Landing, W.M. and Bruland, K.W. 1987. The contrasting biogeochemistry of iron and manganese in the Pacific Ocean. *Geochim. Cosmochim. Acta* **51**: 29–43.

Nakayama, E. Isshiki, K., Sohrin, Y. and Karatina, H. 1989. Automated determination of manganese in seawater by electrolytic concentration and chemiluminescence detection. *Anal. Chem.* **61**: 1392–1396.

Obata, H., Karatani, H. and Nakayama, E. 1993. Automated determination of iron in seawater by chelating resin concentration and chemiluminescence detection. *Anal. Chem.* **65**: 1524–1528.

Obata, H., Karatani, H. and Nakayama, E. 1997. Fundamental studies for chemical speciation of iron in seawater with an improved analytical method. *Mar. Chem.* **56**: 97–106.

Takeda, S. 1998. Influence of iron availability on nutrient consumption ratio of diatoms in oceanic waters. *Nature* **393**: 774–777.

Assessment of the lower limit of iron addition required to initiate massive diatom blooms in the eastern equatorial Pacific

Mark L. Wells

School of Marine Sciences, University of Maine, Orono, ME, U.S.A. 04469. E-mail: mlwells@maine.edu

Introduction

The issue of iron limitation in the oceans has garnered rapidly increasing interest since the successful mesoscale iron enrichment experiment in the equatorial Pacific known as IronEx II. This experiment demonstrated unequivocally that iron is limiting diatom (and thus export) production in the eastern equatorial Pacific high nitrate, low chlorophyll (HNLC) regime (Coale *et al.*, 1996). Iron infusion transformed the oceanic picoplanktonic phytoplankton assemblage into a coastal-type pennate diatom-dominated assemblage, increasing total chlorophyll levels 20 times over levels outside the enriched patch. The accompanying macronutrient and TCO_2 depletion during the first 12 days of the bloom testify to the major geochemical impact that iron flux alone can have in this region (Steinberg *et al.*, 1998).

Although the IronEx II enrichment study clearly demonstrated iron limitation of phytoplankton production, the experiment was not designed to ascertain the minimum iron flux needed to generate large diatom blooms in equatorial Pacific waters. Iron concentrations generated within the infused patch (2 nM) were low by coastal standards but were massive in comparison to ambient levels, raising iron concentrations by two orders of magnitude. Assessing the lower limit of required iron enrichment is important because it provides insight to the scale of natural perturbations that could cause these types of bloom events. For example, if high iron flux is required, then significant iron-induced increases in export production could only be a response to climate change. However, if comparatively minor increases in iron flux are necessary, then increased export production might precede and contribute to global climate change.

Although there remains uncertainty about which iron species are available to phytoplankton in general, and diatoms in particular, iron uptake appears to be restricted to the truly soluble, or low molecular weight fraction in seawater (Wells *et al.*, 1995). Here, I present results from cross-flow filtration (CFF) studies during IronEx II where iron was partitioned into dissolved (< 0.4 µm), soluble (< 1 kDa) and colloidal (1 kDa to 0.4 µm) size fractions. The results demonstrate that the soluble iron fraction increased only minimally despite nanomolar iron additions, the bulk of added iron occurring in the colloidal size phase. Soluble iron concentrations changed in conjunction with chlorophyll increase and macronutrient drawdown. The relative drawdown of silicic acid and nitrate suggest the diatom population continued to experience iron stress throughout bloom development, despite calculations indicating the pennate diatoms were not diffusion limited at the concentrations of soluble iron measured. These findings help to constrain the magnitude of iron flux needed to initiate and sustain large phytoplankton blooms in equatorial HNLC waters.

Materials and methods

Samples were collected from various locations near the center of the enriched patch (marked by a drogue buoy) using Teflon®-lined 30 L GO-Flo bottles (General Oceanics) on a Kevlar line (Philadelphia Resins). M. Gordon (Moss Landing Marine Laboratory) kindly provided 20 L carboys of conventionally filtered (< 0.4 µm) samples for processing. These 20 L dissolved samples were then further size fractionated by CFF using a 1-kDa membrane (Filtron). Details of the steps used are given in Wells (2003). CFF processing was completed within ~ 5 h of sample collection. Samples were acidified with 4 ml of quartz-distilled 6 N HCl per liter and stored for several months before extraction and analysis.

The dissolved (< 0.4 µm), permeate (< 1 kDa) and retentate (1 kDa to 0.4 µm) samples were extracted before analysis using a new solid phase extraction procedure (Wells and Bruland, 1998). Sample

extracts were analyzed on a Finnigan MAT ELEMENT magnetic sector (high resolution) ICP-MS. Colloid concentrations were calculated using the concentration factor (*cf*) of the individual CFF run and the measured metal concentrations in the retentate and permeate fractions:

$$[colloid] = \frac{[retentate] - [permeate]}{cf}$$

This quantification of colloid concentrations is more robust than simply subtracting permeate (< 1 kDa) from total dissolved (< 0.2 μm) concentrations because: (1) the latter depends on accurately measuring the difference between two large numbers, and (2) the mass balance can be determined for each CFF run:

$$[< 0.2\mu m] = [permeate] + [colloid]$$

Good agreement between the sum of permeate and calculated colloid concentrations with dissolved values is strong evidence that CFF processing was not significantly influenced by contamination or sorptive losses of soluble or colloidal species to the membrane.

Results

Results from pre-release sampling indicate that ~85% of the ambient dissolved iron was soluble in nature, with ~3 pM Fe occurring in the colloidal phase. Reliable identification of such a small colloidal component within the dissolved phase would be impossible from the simple difference between dissolved (< 0.4 μm) and permeate (< 1 kDa) values. However, the comparatively high retentate concentration (152 ± 22 pM Fe), along with the good mass balance (104%), raises confidence that the extent of the soluble/colloidal partitioning is reasonably accurate.

Dissolved iron concentrations within the enriched patch cycled repeatedly from nanomolar to picomolar levels, with dissolved iron concentrations decreasing sharply after each infusion. The rate of this iron disappearance increased progressively from the first to third infusions. The vast majority of the added iron occurred in the colloidal phase, with soluble (< 1 kDa) concentrations increasing by only ~ 25 pM over ambient levels. The percentage of colloidal iron decreased from nearly 100% immediately following the first infusion to ~60% 9 days later. Colloidal-sized iron phases continued to dominate iron speciation even when total dissolved iron concentrations within the patch fell to near pre-release levels.

Soluble iron concentrations increased from 16 to ~ 40 pM Fe over the four days following the first infusion. This trend preceded increases in Chl-*a* concentrations by 2 full days. After biomass (as indicated by Chl-*a*) began to increase dramatically on Day 5–6, soluble iron concentrations dropped precipitously and then remained at near pre-release levels through Day 9, the final day of CFF sampling.

The relative drawdown rate of nitrate and silicic acid provides some insight to the level of iron stress experienced by diatoms within the patch. The silicic acid:nitrate ratio in surface waters was 0.5 before infusion began. Alleviation of iron limitation by infusion led to an initially balanced drawdown of nitrate and silicic acid. But approximately 1.5 days after the second infusion the Si:N drawdown ratio increased significantly, with the subsequent linear decrease in dissolved Si:N ratios being synchronous with decreased soluble iron concentrations and increases in Chl-*a*. A minimum dissolved silicic acid:nitrate ratio of 0.14 occurred on Day 13 after Chl-*a* concentrations peaked before beginning to increase again in conjunction with decreasing Chl-*a* concentrations.

Discussion

Some insight to the minimum level of iron needed to generate massive diatom blooms comes from size-fractionated analysis of iron within the infused patch during IronEx II. Although there remains uncertainty about which iron species are available to phytoplankton in general, and diatoms in particular, iron uptake appears to be restricted to the truly soluble, or low molecular weight fraction in seawater (Wells *et al*., 1995). The colloidal proportion of added iron was initially extremely high (99%) but decreased somewhat with each infusion (90% in the second infusion; 60% in the third infusion). However, this progressive change is largely due to the decreasing concentrations of total dissolved iron measured in the samples obtained after each infusion. This trend may be simply due to the non-homogeneous distribution of

iron within the patch, but it also is likely that the increasing iron demand by the rapidly growing population resulted in higher short-term rates of iron removal from the dissolved phase.

Soluble iron concentrations (or that containing the iron species known to be directly accessed by phytoplankton) doubled after the initial iron infusion and continued to increase over the first 4 days, reaching a maximum of ~ 40 pM Fe. During the same time, total Fe(III) complexing organic ligands increased by 400% to ~ 2 nM, with most of the increase attributed to the stronger ligand class (Rue and Bruland, 1997). The bulk of these iron–ligand complexes were colloidal in size, in contrast to pre-release conditions where the strong ligand–iron complexes were largely in the soluble phase. The increase in soluble iron concentrations during the first 4 days presumably reflects a small change in the size distribution of these ligands with time, through either the biotic release of low molecular weight iron complexing ligands or by the escape of low molecular weight ligands from colloidal polymer matrices (Chin *et al*., 1998).

A dramatic decrease in soluble iron concentrations was observed on Day 6, likely due to the rapidly increasing iron demand, as evidenced by the increasing Chl-*a* concentrations across this interval. The total iron demand can be estimated from Chl-*a* concentrations and cellular iron quotas measured for oceanic diatoms under controlled conditions. Chl-*a* increased within the patch by ~ 3 μg L^{-1} over the first 9 days, corresponding to an increase in cellular carbon of ~1.7 $\times 10^{-5}$ moles C L^{-1} (0.20 mmol Chl:mol C (Sunda and Huntsman, 1995)). Taking a lower value for the cellular Fe:C ratio for oceanic diatoms (5 μmol Fe:mol C, Sunda and Huntsman, 1995) yields a minimum cellular iron demand of ~90 pM Fe to fuel the increase in Chl-*a* measured. This value underestimates actual demand because neither grazing nor "luxury" uptake of iron by cells is taken into account. It is clear then that significant iron flux from the colloidal through the soluble phase was required to support bloom development.

Assessing what iron flux to surface waters is required to stimulate large diatom blooms like that generated by IronEx II reduces to two issues: (1) what is the lowest iron concentration whereby uptake still permits maximum cellular growth rates, and (2) what iron flux to surface waters is then needed to sustain high diatom productivity once this concentration threshold is surpassed? The distinction between concentration and flux is important because it constrains the magnitude of events needed to generate intense diatom blooms. The minimum iron concentration at which pennate diatom growth becomes diffusion limited was estimated as a function of cell length and cell shape. The parameters chosen for this calculation were a molecular diffusivity of 0.9×10^{-5} cm^2 s^{-1} (for iron species sized near inorganic complexes), a cellular iron content of 50 μmoles L^{-1} of cytoplasm (Sunda and Huntsman, 1995), a cellular aspect ratio of 20 (length/width) and a growth rate of 1 d^{-1} (K. Bares, pers. comm.). The result illustrates the extreme benefit pennate diatoms enjoy over their centric cousins with respect to diffusional constraints. To escape diffusion-limited growth conditions, centric diatoms 15 μm in diameter require > 160 times higher iron concentrations than pennate diatoms 15 μm in length. This difference might help explain why centric diatoms flourished in some bottle enrichment studies with equatorial Pacific waters (Maldonado and Price, 1996) while pennate species dominated in the mesoscale experiment; iron availability in the bottles would have remained comparatively high because iron was not lost from the system.

The question of the iron flux needed to sustain high diatom productivity (once diffusion limitation concentrations are surpassed) is more complex. While the iron flux used during IronEx II was massive (compared to ambient inputs), and the resultant diatom response dramatic, there is reason to suspect that growth rates in the patch remained below maximum levels. Growth rates of oceanic diatoms in controlled culture conditions reach ≥ 1.5 d^{-1} (Sunda and Huntsman, 1995; Maldonado and Price, 1996), significantly higher than the growth rate estimated during the bloom (1 d^{-1}, K. Bares, pers. comm.). Indeed, there is evidence that diatoms were experiencing iron stress in the midst of bloom development. It has been shown recently that diatoms draw down nitrate and silicic acid equally under iron-replete conditions, but iron stress causes a shift to the preferential removal of silicic acid (Hutchins and Bruland, 1998). By this measure, the low ambient nitrate:silicic acid ratio (~0.5) indicates the influence of iron limitation prior to the first iron infusion. The subsequent utilization of these nutrients begins equally shortly after infusion but the drawdown ratio then drops

sharply as Chl-*a* increases, and soluble iron concentrations decrease. These findings strongly indicate that the bloom organisms had become iron stressed despite the third iron infusion on Day 7. These data add further support to the finding that diatoms were unable to access all of the iron in the soluble phase. As a result, the geochemical impact of the bloom on nitrate drawdown and the carbon cycle was smaller that it would have been if silicic acid utilization had been more efficient.

Despite our uncertainty about the iron forms that phytoplankton access in seawater, the results here demonstrate that concentrations of soluble iron complexed by natural organic ligands need only increase slightly (≤ 25 pM) above ambient levels for large diatoms to grow rapidly. However, what is not clear is whether the increase in strong Fe(III) complexing organic ligand concentrations that accompany large influxes of iron ultimately result in lower effective supply of iron to diatoms and other large eukaryotic organisms. If so, then slow, persistent influxes of iron may not be able to maintain high diatom growth once the chemical speciation of iron again becomes dominated by complexation with strong organic chelators.

References

Chin, W.-C., Orellana, M.V. and Verdugo, P. 1998. Spontaneous assembly of marine dissolved organic matter into polymer gels. *Nature* **391**: 568–572.

Coale, K.H., Johnson, K.S., Fitzwater, S.E. *et al.* 1996. A massive phytoplankton bloom induced by an ecosystem-scale iron fertilization experiment in the equatorial Pacific. *Nature* **383**: 495–501.

Hutchins, D.A. and Bruland, K.W. 1998. Iron-limited diatom growth and Si:N uptake ratios in a coastal upwelling regime. *Nature* **393**: 561–564.

Maldonado, M.T. and Price, N.M. 1996. Influence of N substrate on Fe requirements of marine centric diatoms. *Mar. Ecol. Prog. Ser.* **141**: 161–172.

Rue, E.L. and Bruland, K.W. 1997. The role of organic complexation on ambient iron chemistry in the equatorial Pacific Ocean and the response of a mesoscale iron addition experiment. *Limnol. Oceanogr.* **42**: 901–910.

Steinberg, P.A., Millero, F.J. and Zhu, X.R. 1998. Carbonate system response to iron enrichment. *Mar. Chem.* **62**: 31–43.

Sunda, W.G. and Huntsman, S.A. 1995. Iron uptake and growth limitation in oceanic and coastal phytoplankton. *Mar. Chem.* **50**: 189–206.

Wells, M.L. 2003. The level of iron enrichment required to initiate diatom blooms in HNLC waters. *Mar. Chem.* **82**: 101–114.

Wells, M.L. and Bruland, K.W. 1998. An improved method for rapid preconcentration and determination of bioactive trace metals in seawater using solid phase extraction and high resolution inductively coupled mass spectrometry. *Mar. Chem.* **63**: 145–153.

Wells, M.L., Price, N.M. and Bruland, K.W. 1995. Iron chemistry in seawater and its relationship to phytoplankton: a progress report. *Mar. Chem.* **48**: 157–182.

Characteristic vertical profiles of Fe(III) hydroxide solubility in the northwestern North Pacific Ocean

Kenshi Kuma[1], Shigeto Nakabayashi[2], Isao Kudo[1] and Masashi Kusakabe[2]

[1] Graduate School of Fisheries Sciences, Hokkaido University, Hakodate, Japan 041-8611
E-mail: kuma@fish.hokudai.ac.jp
[2] Ocean Research Department, Japan Marine Science and Technology Center, 2-15 Natsushima, Yokosuka, Japan 237-0061

Recently, a number of studies pointed out that the Fe(III) complexation with natural organic ligands is possible in oceanic waters, but the detailed vertical distribution, origin and chemical identity of organic ligands are largely unknown. Here, we report the spatial vertical distributions of Fe(III) hydroxide solubility in subarctic and subtropical water masses and the boundary zone in the northwestern North Pacific Ocean. The detailed vertical profiles of Fe(III) hydroxide solubility have the following features in common:

- the solubility in the surface mixed layer (0–50–100 m) is generally high and variable (0.3–1.9 nM);
- the solubility minima (0.2–0.4 nM) occur at depths of 75–125 m, below the suface mixed layer;
- the subsequent solubility levels in middepth waters appear to increase with depth in association with the increase in nutrient concentrations in the subtropical and boundary zone (0.2–0.7 nM) or to vary little with high constant solubility (0.7 nM) and nutrient values in the subarctic zone (upwelling area);
- the solubility levels in deep waters (>1000–1500 m) tend to decrease a little to 0.4–0.5 nM with depth in association with the decrease in nutrient concentrations.

The higher Fe(III) hydroxide solubility in the surface mixed layer is probably due to higher concentration or stronger affinity of natural organic Fe(III) chelators, which were possibly released by phytoplankton or bacteria during their metabolism. There are significant correlations between the Fe(III) hydroxide solubility and the nutrient (PO_4, NO_3+NO_2) concentration in deeper waters below the depth of minimum solubility, suggesting the regenerative formation of organic Fe(III) chelators through oxidative decomposition and transformation of biogenic organic matter sinking into the deep waters.

A1.2.3 Biology in the North Pacific and IronEx

Station Papa time series: Insights into ecosystem dynamics

Paul J. Harrison

Department of Earth and Ocean Sciences, University of British Columbia, Vancouver, BC, Canada V6T 1Z4
E-mail: pharrison@eos.ubc.ca

Ocean Station Papa (OSP) in the subarctic NE Pacific at 50°N and 145°W, has been the site of open ocean research for the last 40 years, commencing with sampling conducted on board the Canadian weatherships from 1956–1981. Hydrocasts were carried out to a depth of 1200 m at OSP. In 1959, 5 stations were sampled along the line connecting OSP to the coast (Line P) and by 1964, 13 stations along Line P were established. During the 25-year weathership era, temperature, salinity, nutrients (nitrate, phosphate and silicate), Chl-*a* and zooplankton were sampled approximately weekly (but with considerable variability). This good temporal coverage firmly established the annual cycle at OSP. This cycle is provided in some detail by Whitney and Freeland (1999), and only the highlights are summarized here. The range in selected parameters is given in Table 1. In the winter, winds average 12 m s^{-1} and the surface waters are mixed to about 120 m (much shallower than the Atlantic Ocean where mixing occurs to about 300 m). Surface temperature reaches a minimum of 5–6°C, salinity increases to 32.7 and maximum winter nitrate and silicate are 15.8 ± 2.3 and 24.0 ± 3.4 µM, respectively. Winter Chl-*a* is approximately 0.2–0.3 µg L^{-1}. The mean irradiance levels received by cells traversing the mixed layer is 0.91 and 2.3 mol quanta m^{-2} d^{-1} in February and October, respectively (Maldonado *et al*., 1999). As incident irradiance increases and the mixed layer depth (MLD) decreases in spring, Chl-*a* increases from 0.2–0.4 µg L^{-1} (there is no spring bloom as observed in the Atlantic Ocean). It is interesting that nitrate drawdown begins in April, while silicate begins to decline in early June. Sediment traps at 200 m depth show the highest downward flux of Si from June to July, whereas N fluxes are high from May through September (Wong *et al*., 1999). In August/September, when the MLD is only 40 m and surface temperatures reach 12–13°C, nitrate and silicate reach minimal values of about 8–9 and 13 µM, respectively. This represents a drawdown in nitrate and silicate of 7 and 11 µM, respectively, and a Si:N drawdown ratio of 1.6:1. This ratio suggests iron limitation since it is higher than the normal 1:1 Si:N ratio (Hutchins *et al*., 1998).

At the end of the weathership era, three key observations were used to explain how the ecosystem functioned. Since there was no spring bloom and minimum summer nitrate values were 8–9 µM (not 0), it was suggested that the large copepods which migrated to the surface and grew quickly in size, controlled the phytoplankton standing crop via grazing (*i.e.*, top down control) and aided secondarily by low light (Parsons and Lalli, 1988). This conclusion was logical because it was before the realization of the importance of small phytoplankton (picoplankton) and microzooplankton, and the discovery of iron limitation.

In the mid-1980s, the Subarctic Pacific Ecosystem Research (SUPER) group challenged the "major grazer hypothesis" (Frost, 1987). They found that the main diet of these large copepods (*Neocalanus* spp. and others) was not phytoplankton. They were mainly carnivores and they consumed only small amounts of phytoplankton (Dagg, 1993). In addition, Booth *et al*. (1993) found that phytoplankton < 5 µm dominated the phyto-plankton standing stock. Just as the field work by SUPER was ending, Martin and his colleagues made the startling discovery that iron limited primary productivity at OSP (Martin and Fitzwater, 1988). Therefore, within a few years these three new key observations dramatically revised our ideas of how this ecosystem functioned.

Table 1 Range in various ecosystem parameters at OSP, with winter representing one extreme and late summer the other extreme. Most values are for surface water or integrated over the photic zone.

Parameter	Winter	Late summer	Reference
Light Extinction Coeff (k, m^{-1})	0.065	0.13	Sherry *et al.*, 1999
Wind (m s^{-1})	12	7	Whitney and Freeland, 1999
Temperature (°C)	5.5	13	Whitney and Freeland, 1999
Salinity	32.7	32.5	Whitney and Freeland, 1999
$Sigma_t$	25.7	24.5	Whitney and Freeland, 1999
Mixed Layer Depth (m)	120	40	Whitney and Freeland, 1999
Photic Zone (m)	80	30–40	Sherry *et al*., 1999
Nitrate (µM)	15.8	8.5	Whitney and Freeland, 1999
Silicate (µM)	24.0	13.0	Whitney and Freeland, 1999
Phosphate (µM)	0.8	1.3	Appendix, DSR II **46**: 3019
Ammonium (µM)	0.5	0.1	Varela and Harrison, 1999
Urea (µg-at L^{-1})	0.5	0.1	Varela and Harrison, 1999
Fe (nM)	~ 0.1	0.05	Nishioka, Wong and Tabata (unpubl. data)
chl (µg L^{-1})	0.2	0.4	Boyd and Harrison, 1999
chl (mg m^{-2})	13.5	20	Varela and Harrison, 1999
Phytoplankton Carbon (µg C L^{-1})	15	25	Denman and Putland (unpubl. data)
POC (µg C L^{-1})	50	70–90	Wong *et al.*, 1999
Particulate N (mg-at m^{-2})	52	95	Varela and Harrison, 1999
Primary Productivity (µg C L^{-1} d^{-1})	<10	35	Boyd and Harrison, 1999
Primary Productivity (mg C m^{-2} d^{-1})	300	400–850	Wong *et al*., 1995; Boyd and Harrison, 1999
f-ratio	0.25	0.25	Varela and Harrison, 1999
ρ NO_3 (mg-at m^{-2} d^{-1})	1.78	3.86	Varela and Harrison, 1999
ρ urea (mg-at m^{-2} d^{-1})	0.96	3.59	Varela and Harrison, 1999
ρ NH_4 (mg-at m^{-2} d^{-1})	3.23	5.80	Varela and Harrison, 1999
ρ total N (mg-at m^{-2} d^{-1})	5.96	13.35	Varela and Harrison, 1999
Bacterial Biomass (µg C L^{-1})	12	25	Sherry *et al*., 1999
Bacterial Productivity (µg C L^{-1} d^{-1})	0.4	2.2	Sherry *et al*., 1999
Mesozooplankton (mg C m^{-3})	3	20	Goldblatt *et al*., 1999

By the beginning of the Canadian JGOFS (Joint Global Ocean Flux Study) project in 1992, the issue of iron limitation was not resolved, specifically the iron limitation versus grazing debate, because the large grazers were usually excluded from the previous bottle experiments (Banse, 1990; Miller *et al*., 1991; Frost, 1991; Miller, 1993). During the early 1990s, further shipboard iron enrichment experiments by Boyd and colleagues confirmed that iron limitation did limit phytoplankton stocks despite the presence of mesozooplankton levels comparable to the highest *in situ* upper ocean levels observed at OSP (Boyd *et al*., 1999). Furthermore, the iron enrichment in carboy experiments facilitated the drawdown of nitrate in May and September (Boyd *et al*., 1996). When iron was added in their experiments, large predominately pennate diatoms (> 18 µm) grew, confirming Martin and Fitzwater's (1988) earlier observations. This result was surprising since oceanic pennate diatoms were usually considered to be a minor component of oceanic phytoplankton assemblages. Iron limitation was also confirmed by biophysical (F_v/F_m fluorescence ratio, Boyd *et al*., 1998a) and biochemical (an iron-mediated reduction in the expression of the molecular marker for iron limitation, flavodoxin; LaRoche *et al*., 1996) markers. In February, when Boyd added iron, little or no increase in Chl-*a* was observed after a 5-day incubation, and it was suggested that light may be a co-limiting factor along with iron (Boyd *et al*., 1996). This suggestion was later confirmed by Maldonado *et al*. (1999) who demonstrated co-limitation of phytoplankton growth by iron and light during winter at OSP.

Ammonium showed little seasonality with concentrations ranging from 0.1 to 0.5 µM

(Table 1). Urea concentrations were generally from 0.1 to 0.5 µg-at L^{-1}, except for May 1993 when surface urea was 0.8 and up to 2.0 µg-at L^{-1} at 40 m (Varela and Harrison, 1999). Nitrate, urea and ammonium uptake rates in winter (February/ March) were 1.8, 1.0, and 3.2 mg-at N m^{-2} d^{-1}, respectively; in spring (May) they were 2.7, 3.3 and 5.4 and in late summer (September) they were 3.9, 3.6 and 5.8 mg at N m^{-2} d^{-1}, respectively. The seasonally averaged depth- integrated absolute uptake rates were 27% nitrate, 23% urea and 50% ammonium. There was no significant difference in the annual trend for the depth-integrated *f*-ratio, and the seasonal average was 0.25. Phytoplankton utilized nitrogen in the following order; NH_4 >> NO_3 > urea. The *f*-ratio was overestimated by up to 36% when urea was excluded from the calculation (Varela and Harrison, 1999).

There is low seasonality in primary productivity with mean winter and spring/summer values of 300 and 800 mg C m^{-2} d^{-1}, respectively (Boyd and Harrison, 1999). Using Wong *et al.*'s (1995) fall values of 366 mg C m^{-2} d^{-1}, and the values by Boyd and Harrison (1999) above, yields an annual estimate of 215 g C m^{-2} y^{-1} which is somewhat higher than Wong *et al.*'s (1995) estimate of 140 g C m^{-2} y^{-1} and Welschmeyer *et al.*'s (1993) estimate of 170 g C m^{-2} y^{-1} (using Wong's winter values) (Harrison *et al.*, 1999). This annual primary productivity is quite high considering that OSP is similar to an oligotrophic gyre with nutrient (Fe) limitation, a phytoplankton assemblage dominated by small cells and the primary productivity based largely on regenerated nutrients (*f*-ratio = 0.25).

The dominant small phytoplankton grow at 0.1 to 0.8 d^{-1}, similar to the growth rate of many microzooplankton (Landry *et al.*, 1993; Boyd and Harrison, 1999). Therefore, it has been suggested that these small phytoplankton are controlled by microzooplankton grazing (Landry *et al.*, 1993), although results suggest that these micro-zooplankters preferentially ingest heterotrophic rather than autotrophic picoplankton (Rivkin *et al.*, 1999). The large copepods such as *Neocalanus* sp. are now known to be omnivores rather than herbivores (Dagg, 1993). In fact, when twice the maximum ambient number of *Neocalanus plumchrus* was added to a carboy enriched with iron, large pennate diatoms grew and they were not grazed down by high abundances (comparable to the maximum ambient levels) of the large copepods (Boyd *et al.*, 1999).

In contrast to the conceptual phytoplankton–mesozooplankton food chain previously reported (Frost, 1987; Parsons and Lalli, 1988), now it is necessary to have two nitrogen sources and two size fractions of phytoplankton to explain the ecosystem dynamics at OSP. The large phytoplankton are thought to exhibit bottom up control by iron (due to their higher iron cell quotas; Muggli *et al.*, 1997), while the small phytoplankton exhibit top down control by microzooplankton grazing. The large phytoplankton (mainly diatoms > 10 µm) increase in abunadance quickly when iron is added in carboy experiments and they are able to use up all the ambient nitrate. They are not eaten to any marked extent by *N. plumchrus*, and thus these large cells likely sink out after they consume the iron addition (Muggli *et al.*, 1996). The small phytoplankton (mainly prasinophytes and prymnesiophytes < 5 µm) utilize regenerated nitrogen (NH_4 and urea, Boyd *et al.*, 1996; Varela and Harrison, 1999) to decrease the iron demand associated with nitrate reduction to ammonium.

Microzooplankton span a wide size range and taxonomic group of organisms and, to date, they have not been well studied. They consume mostly small phytoplankton and bacteria (Landry *et al.*, 1993; Rivkin *et al.*, 1999). Their biomass shows little seasonality, unlike the 5- to 10-fold increase in mesozooplankton in May/June (mainly due to the increase in size of the C1 to C4 copepodites (Boyd *et al.*, 1995, see their Table 1). Therefore, the nearly 3-fold seasonal increase in primary productivity from winter to summer (Boyd and Harrison, 1999) is passed through the microzooplankton to provide part of the large increase in mesozooplankton biomass in May/June.

Mean monthly downward particle fluxes at 3800 m show a distinct seasonality. Flux rates of 38 mg m^{-2} d^{-1} (in February) have an annual minimum during winter months and a maximum of 150 mg m^{-2} d^{-1} during summer. The average downward mass flux at OSP is 52 g m^{-2} y^{-1} at 1000 m and 32 g m^{-2} y^{-1} at 3800 m (Wong *et al.*, 1999).

Interannaul variability

A warming of 1.2°C/century and freshening of 0.2 psu/century in the surface waters at OSP has been

estimated by Freeland *et al.* (1997). From these data, they calculated that the MLD has also decreased significantly ($p = 0.05$) from 130 m in the 1960s to 100 m in the late 1990s. This decrease in the MLD likely contributes to the decrease in the winter nutrient concentrations.

In addition to these longer-term changes, El Niño events have resulted in rapid, short-lived changes. One of the strongest El Niño events of the century happened in 1982/83. During that time the largest particle flux to sediment traps at 3800 m occurred and 90% of this flux was opal; the particle flux was > 400 mg m^{-2} d^{-1} during late summer (Wong and Matear, 1999).

During the transition from the La Niña in 1989 to the series of El Niños ending in 1994, the surface waters became warmer by 2°C, more saline by 0.3 psu and the winter nitrate concentrations were 30% lower (Whitney *et al*., 1998). In late summer, depletion of nitrate in the surface waters during the 1989 La Niña period extended 250 km offshore, but during the 1994 El Niño period, surface nitrate depletion extended 600 km offshore. This suggests that the boundary between the more coastal nitrate-limited area and the iron-limited offshore area can shift more offshore or onshore due to El Niño/La Niña events. The lower winter nitrate supply during El Niño is estimated to have reduced new production by 40% and possibly shifted phytoplankton community structure to smaller primary producers (and a longer food chain) which could, in turn, have affected higher trophic levels (Whitney *et al*., 1998).

Whitney and Freeland (1999) compared the nitrate and silicate concentrations of the 1970s to the 1990s and observed that the winter nitrate has decreased by 2.5 µM and silicate by 3.6 µM. Their nutrient utilization between February and September has declined from 7.8 to 6.5 µM NO_3 and from 8.5 to 6.0 µM Si (the $Si:NO_3$ ratio decreased from 1.08 to 0.92). The larger decrease in silicate uptake (29%) relative to the decrease in nitrate uptake (17%) suggests that the supply of iron may also have declined during these two decades because the Si:N uptake ratio for phytoplankton increases under iron limitation (Hutchins *et al*., 1998).

From 1956 to 1980 the mesozooplankton biomass has nearly doubled at OSP (Brodeur and Ware, 1992). An obvious question is: Has the phytoplankton biomass/productivity also increased? There has been no apparent increase in Chl-*a*, despite the fact that GF/F filters (0.8 µm nominal pore size) were used in the 1990s compared to GF/C filters (1.8 µm nominal pore size) in the 1960s–70s. However, early estimates of an annual primary productivity of 60 g C m^{-2} (McAllister *et al*., 1960) have increased to 140 g C m^{-2} (Wong *et al*., 1995) and recently to 215 g C m^{-2} (Harrison *et al*., 1999). This 2- to 3-fold increase in primary productivity may be due to the use of trace metal clean techniques in the 1980s and 90s, but the increase could be real and it could explain the doubling in the mesozooplankton biomass.

The other long-term change in mesozooplankton is the arrival time of *N. plumchrus* into surface waters 2 months earlier than in the 1960s–70s (Mackas *et al*., 1998). The peak biomass (late C4 copepodites) now occurs in early May versus early July. The reason for this earlier shift in this copepod's life cycle in unclear, but it may be linked to the presently warmer surface waters.

Interannual variation in nitrate and silicate was well documented in the 1970s due to the weekly sampling by weathership personnel. During the summers of 1972, 1976 and 1979, silicate was depleted to < 1 µM, indicating that productivity was high and dominated by diatoms (Wong and Matear, 1999). Both 1972 and 1976 were high silicate and nitrate utilization years, while 1976 had low nitrate utilization relative to silicate utilization ($Si:NO_3$ drawdown = 3.6); the only way to explain this high ratio at present is to suggest severe iron limitation. Unfortunately, during the decade of the 1970s no sediment traps were deployed to assess changes in export to depth.

During brief periods of 1964, 1965, 1969 and 1975, Chl-*a* concentrations were 10 times greater than ambient concentrations (*i.e.*, > 3 µg L^{-1}; Parslow 1981). One explanation for these Chl-*a* peaks is the episodic input of iron, based on the observations during iron addition experiments where pennate diatoms grow and draw down nitrate and silicate. Again, it would have been helpful to have had sediment traps to determine if this 10-fold increase in Chl-*a* resulted in increased particle fluxes (see Boyd *et al.* (1998b) for further discussion). Surprisingly, the detailed time series of nitrate and

silicate concentrations in 1975 do not show accompanying drawdowns in nitrate and silicate during the three peaks in chlorophyll.

Summary

The 40-year time series at OSP provides a valuable data set to resolve the ecosystem dynamics in this region. The range of various ecosystem parameters at OSP is summarized in Table 1. During 1956–81, the temporal resolution was excellent, however, the number of parameters that was measured was limited. There was no size-fractionated Chl-*a*, no microzooplankton biomass estimates, and no sediment traps deployed. The lack of these data limits the interpretation of unusual years. For example, during 1972, 1976 and 1979 when silicate was drawn down to < 1 µM in the summer, the accompanying nitrate drawdown varied considerably and the Si:NO_3 drawdown ratios were 1.4, 2.5 and 3.6, respectively. Accompanying phytoplankton species composition data could help to clarify why these Si/N ratios varied by so much.

In the 1980s–90s, the number of parameters that was measured increased, but the temporal resolution decreased to two or three cruises per year. This may explain why many of the episodic events that were observed in the 1960s–70s (*e.g.*, Chl-*a* peaks and silicate drawdowns to < 1 µM) have not been observed since that time, except for the possible episode in 1983 when the largest particle flux to 3800 m sampled to date at OSP, was measured (Wong *et al.*, 1999).

Future research should continue regular cruises to maintain the priceless time series and include moored instruments to increase the temporal resolution in order to determine if any episodic events are presently occurring. Since iron limits algal growth, the sources of iron for OSP must be determined and these sources may be linked to the episodic increases in Chl-*a* or nutrient drawdown that were observed in the 1960s–70s (Boyd *et al.*, 1998b).

References

Banse, K. 1990. Does iron really limit phytoplankton production in the offshore subarctic Pacific? *Limnol. Oceanogr.* **35**: 772–775.

Booth, B.C., Lewin, J. and Postel, J.R. 1993. Temporal variation in the structure of autotrophic and heterotrophic communities in the subarctic Pacific. *Prog. Oceanogr.* **32**: 57–99.

Boyd P. and Harrison, P.J. 1999. Phytoplankton dynamics in the NE subarctic Pacific. *Deep-Sea Res. II* **46**: 2405–2432.

Boyd, P.W., Strom, S., Whitney, F.A., Doherty, S., Wen, M.E., Harrison, P.J., Wong, C.S. and Varela, D.E. 1995. The NE subarctic Pacific in winter: I. Biological standing stocks. *Mar. Ecol. Prog. Series* **128**: 11–24.

Boyd, P.W., Muggli, D.L., Varela, D.E., Goldblatt, R.H., Chretian, R., Orians, K.J. and Harrison, P.J. 1996. *In vitro* iron enrichment experiments in the NE subarctic Pacific. *Mar. Ecol. Prog. Series* **136**: 179–193.

Boyd, P.W., Berges, J.A. and Harrison, P.J. 1998a. In vitro iron enrichment experiments at iron-rich and-poor sites in the NE subarctic Pacific. *J. Exper. Mar. Biol. Ecol.* **227**: 133–151.

Boyd, P.W., Wong, C.S., Merrill, J., Whitney, F., Snow, J., Harrison, P.J. and Gower, J. 1998b. Atmospheric iron supply and enhanced vertical carbon flux in the NE subarctic Pacific: Is there a connection? *Global Biogeochem. Cycles* **12**: 429–441.

Boyd, P.W., Goldblatt, R.H. and Harrison, P.J. 1999. Mesozooplankton grazing manipulations during in vitro iron enrichment studies in the NE subarctic Pacific. *Deep-Sea Res. II* **46**: 2645–2668.

Brodeur, R.D. and Ware, D.M. 1992. Interannual and interdecadal changes in zooplankton biomass in the subarctic Pacific Ocean. *Fish. Oceanogr.* **1**: 32–38.

Dagg, M.J. 1993. Grazing by the copepod community does not control phytoplankton production in the subarctic Pacific Ocean. *Prog. Oceanogr.* **40**: 1431–1445.

Freeland, H.J., Denman, K., Whitney, F. and Jacques, R. 1997. Evidence of change in the mixed layer in the northeast Pacific Ocean. *Deep-Sea Res. II* **44**: 2117–2129.

Frost, B.W. 1987. Grazing control of phytoplankton stock in the open subarctic Pacific Ocean: a model assessing the role of mesozooplankton, particularly the large calanoid copepods *Neocalanus* spp. *Mar. Ecol. Prog. Series* **39**: 49–68.

Frost, B.W. 1991. The role of grazing in nutrient-rich areas of the open sea. *Limnol. Oceanogr.* **36**: 1616–1630.

Goldblatt, R.H., Mackas, D.L. and Lewis, A.G. 1999. Mesozooplankton community characteristics in the NE subarctic Pacific. *Deep-Sea Res. II* **46**: 2619–2644.

Harrison, P.J., Boyd, P.W., Varela, D.E., Takeda, S., Shiomoto, A. and Odate, T. 1999. Comparison of factors controlling phytoplankton productivity in the NE and NW subarctic Pacific gyres. *Prog. Oceanogr.* **43**: 205–234.

Hutchins, D.A., DiTullio, G.R., Zhang, Y. and Bruland, K.W. 1998. An iron limitation mosaic in the

California upwelling regime. *Limnol. Oceanogr*. **43**: 1037–1054.

Landry, M.R., Monger, B.C. and Selph, K.E. 1993. Time-dependency of microzooplankton grazing and phytoplankton growth in the subarctic Pacific. *Prog. Oceanogr.* **32**: 205–222.

LaRoche J., Boyd, P.W., McKay, R.M.L. and Geider, R.J. 1996. Flavodoxin as *in situ* marker for iron stress in phytoplankton. *Nature* **382**: 802–805.

Mackas, D.L., Goldblatt, R.H. and Lewis, A.G. 1998. Interdecadal variation in development timing of *Neocalanus plumchrus* populations at Ocean Station P in the Subarctic North Pacific. *Can. J. Fish. Aquat. Sci.* **55**: 1878–1893.

Maldonado, M.T., Boyd, P.W., Harrison, P.J. and Price, N.M. 1999. Co-limitation of phytoplankton growth by light and Fe during winter in the subarctic Pacific Ocean. *Deep-Sea Res. II* **46**: 2475–2485.

Martin, J.H. and Fitzwater, S.E. 1988. Iron deficiency limits phytoplankton growth in the north-east Pacific subarctic. *Nature* **331**: 341–343.

McAllister, C.D., Parsons, T.R. and Strickland, J.D.H. 1960. Primary productivity and fertility at Station "P" in the north-east Pacific Ocean. *J. Conseil* **25**: 240–259.

Miller, C.B. 1993. Pelagic production processes in the subarctic Pacific. *Prog. Oceanogr.* **32**: 1–15.

Miller, C.B., Frost, B.W., Wheeler, P.A., Landry, M.L., Welschmeyer, N. and Powell, T.M. 1991. Ecological dynamics in the subarctic Pacific, a possibly iron-limited system. *Limnol. Oceanogr.* **33**: 1600–1615.

Muggli, D.L., Lecourt, M. and Harrison, P.J. 1996. Effects of iron and nitrogen source on the sinking rate, physiology and metal composition of an oceanic diatom from the subarctic Pacific. *Mar. Ecol. Prog. Series* **132**: 215–227.

Parslow, J.S. 1981. Phytoplankton-zooplankton interactions: data analysis and modelling (with particular reference to Ocean Station Papa (50°N 145°W) and controlled ecosystem experiments. Ph.D. thesis, University of British Columbia, Vancouver, Canada.

Parsons, T.R. and Lalli, C.M. 1988. Comparative oceanic ecology of plankton communities of the subarctic Atlantic and Pacific Oceans. *Oceanogr. Mar. Biol. Ann. Rev.* **26**: 317–359.

Rivkin, R.R., Putland, J.N., Anderson, M.R. and Deibel, D. 1999. Microzooplankton bacterivory and herbivory in the NE subarctic Pacific. *Deep-Sea Res. II* **46**: 2579–2618.

Sherry, N.D., Boyd, P.W., Sugiomoto, K. and Harrison, P.J. 1999. Seasonal and spatial patterns of heterotrophic bacterial production, respiration, and biomass in the subarctic NE Pacific. *Deep-Sea Res. II* **46**: 2557–2578.

Varela, D.E. and Harrison, P.J. 1999. Seasonal variability in nitrogenous nutrition of phytoplankton assemblages in the northeastern subarctic Pacific Ocean. *Deep-Sea Res. II* **46**: 2505–2538.

Welschmeyer, N.A., Strom, S., Goericke, R., Ditullio, G., Belvin, M. and Petersen, W. 1993. Primary production in the subarctic Pacific Ocean: Project SUPER. *Prog. Oceanogr.* **32**: 101–135.

Whitney, F.A. and Freeland, H.J. 1999. Variability in upper-ocean water properties in the NE Pacific Ocean. *Deep-Sea Res. II* **46**: 2351–2370.

Whitney, F.A., Wong, C.S. and Boyd, P.W. 1998. Interannual variability in nitrate supply to surface waters of the Northeast Pacific Ocean. *Mar. Ecol. Prog. Series* **170**: 15–23.

Wong, C.S. and Matear, R.J. 1999. Silicate limitation of phytoplankton productivity in the northeast subarctic Pacific. *Deep-Sea Res. II* **46**: 2539–2555.

Wong, C.S., Whitney, F.A., Iseki, K., Page, J.S. and Zeng, J. 1995. Analysis of trends in primary productivity and chlorophyll-a over two decades at Ocean Station P (50°N, 145°W) in the subarctic Northeast Pacific Ocean. *Can. Spec. Publ. Fish. Aquat. Sci.* **121**: 107–117.

Wong, C.S., Whitney, F.A., Crawford, D.W., Iseki, K., Matear, R.J., Johnson, W.K., Page, J.S. and Timothy, D. 1999. Seasonal and interannual variability in particle fluxes of carbon, nitrogen and silicon from time series of sediment traps at Ocean Station P, 1982–1993: Relationship to changes in subarctic primary productivity. *Deep-Sea Res. II* **46**: 2735–2760.

East–west variability of primary production in the subarctic North Pacific derived from multi-sensor remote sensing during 1996–2000

Sei-ichi Saitoh and Kosei Sasaoka

Laboratory of Marine Environment and Resource Sensing, Graduate School of Fisheries Science, Hokkaido University, 3-1-1 Minato-cho, Hakodate, Hokkaido, Japan 041-8611
E-mail: ssaitoh@salmon.fish.hokudai.ac.jp

The two gyres in the subarctic North Pacific are known as the Western Subarctic Gyre (WSG) and the Alaskan Gyre (AG). Comparative studies on the primary production of the WSG and AG have been carried out in order to understand the different effects of iron in these two regions. Satellite monitoring of temporal–saptial variability of the chlorophyll *a* (Chl-*a*) distribution is very important for understanding the role of iron fertilization in HNLC (high nutrients, low chlorophyll) waters.

Objectives of this study are: (1) to find out the temporal and spatial variability of Chl-*a* distribution and primary productivity in the subarctic North Pacific, and (2) to understand the mechanisms regulating Chl-*a* distribution during 1996–2000. We worked with several multi-sensor remote sensing data sets, including ocean color by OCTS and SeaWiFS, sea surface temperature (SST) by AVHRR, and sea surface height by TOPEX/Poseidon. Ocean color and SST images were used to study interannual variablity of primary productivity and front dynamics. Sea surface height data were applied to study circulation, transport and eddy distribution. In addition to these satellite data sets, we generated estimated nitrate maps by the algorithm which employs satellite Chl-*a* and SST values. We attempted to calculate primary productivity by the modified Vertically Generalized Production Model (VGPM) (Behrenfeld and Falkowski, 1997) using ocean color and SST satellite data sets. On the other hand, we examined the estimation error of the SeaWiFS in-water algorithm using bio-optical data gathered by the R/V *Mirai* and other research vessels. As a result, the SeaWiFS in-water algorithm is working well in these regions with the error of less than 40 percent. East–west differences and year-to-year differences of primary production in the study area will be discussed.

Reference

Behrenfeld, M.J. and Falkowski, P.G. 1997. Photosynthetic rates derived from satellite-based chlorophyll concentration. *Limnol. Oceanogr.* **42**: 1–20.

The planktonic nitrogen uptake and heterotrophic bacterial response during the second mesoscale Iron Enrichment Experiment (IronEx II) in the eastern equatorial Pacific Ocean

William P. Cochlan

Romberg Tiburon Center for Environmental Studies, San Francisco State University, 3152 Paradise Drive, Tiburon, CA, U.S.A. 94920-0855. E-mail: cochlan@sfsu.edu

The *in situ* responses of phytoplankton and hertertrophic bacteria were followed during the mesoscale iron enrichment experiment (IronEx II) conducted in the eastern equatorial Pacific during May–June, 1995. The rate of planktonic nitrogen (nitrate, ammonium and urea) uptake and the abundance and productivity of bacteria were measured within the fertilized patch and outside of the patch (control) at 15 m depth. Iron enrichment resulted in a dramatic increase in phytoplankton biomass (chlorophyll *a* concentration increased *ca*. 20-fold), but in contrast to long-term "grow-out" bottle experiments, the ambient nitrate concentration did not decrease to near zero, but declined by *ca*. 4–5 μM. Absolute uptake rates of nitrate increased *ca*. 15-fold as a result of iron enrichment, and post-incubation size-fractionation experiments demonstrate that larger phytoplankton (> 5 μm) were responsible for the enhanced nitrate utilization (> 85% of the NO_3 uptake). Iron enrichment shifted the size-structure of the phytoplankton community for picoplankton dominance to larger cells, and altered the relative utilization of new and regenerated N; the daytime *f*-ratio (*f*-ratio = NO_3 uptake/total N uptake) increased from *ca*. 0.65 to 0.91 (ratio uncorrected for isotopic dilution effects).

The carbon productivity and specific growth rate of heterotrophic bacteria increased 3-fold and 3- to 4-fold, respectively, resulting in the *in situ* accretion of bacteria (abundance increased 1.7-fold) within the iron patch. Although these results do not demonstrate a direct stimulatory response of hetertrophic bacteria to iron enrichment, they show that bacterial carbon demand can be potentially met by the increase in phytoplankton primary productivity.

Comparison of iron enrichment experiments on board in the NE and NW subarctic Pacific Ocean

Isao Kudo, Takeshi Yoshimura, Takaaki Nishida and Yoshiaki Maita

Graduate School of Fisheries Science, Hokkaido University, Minato3-1-1, Hakodate, Japan 041-8611
E-mail: ikudo@fish.hokudai.ac.jp

Introduction

It is recognized that iron plays a key role in controlling phytoplankton growth and primary productivity in the ocean, especially in HNLC (high nutrients, low chlorophyll) regions. The subarctic Pacific Ocean is one of them. We conducted three iron enrichment experiments on board in the summer of 1999 at Station Knot (NW) and Station P (NE) in the Pacific.

Materials and methods

Iron addition bioassays were conducted during the KH99-3 cruise (June 25 to August 25, 1999) of the R/V *Hakuho Maru*, University of Tokyo. Water samples were taken at two stations. The NW station (Stn K) and the NE station (Stn P) are located at the edge of the Western Subarctic Gyre (NW) and the edge of Alaskan Gyre (NE), respectively.

All necessary precautions were taken to prevent trace metal contamination throughout the preparation and handling. A specially designed bellows pump was used for pumping water from 5 m depth into Nalgene polycarbonate bottles (1 or 2 L).

The PC bottles were washed by a cleaning procedure. The samples were enriched iron as $FeCl_3$ at the final concentration of 0.3 or 1.0 nM. Some samples were also enriched zinc as $ZnCl_2$ at a final concentration of 1.0 nM. Nothing was added to the control bottles. The iron concentrations in the control bottles were confirmed to agree with that in the original seawater (Obata, pers. comm.). For the one experiment, five bottles were incubated for one treatment. The control incubation was conducted in duplicate while other treatments were single. The bottles were wrapped twice with plastic bags and incubated on board for 7 days in a water tank where water temperature was maintained to within 2ºC of the original temperature. All sample manupulations were conducted in a clean bench or clean room (Class 100) on board. Surface PAR (photosynthetically active radiation) was monitored with a 2 π sensor.

Nutrients and size-fractionated chlorophyll *a* (Chl-*a*) were measured every other day. Samples for bacteria and picoplankton counts were also taken at the same time. To prevent metal contamination, one bottle for each treatment was open for each sampling date to take subsamples for each measurement. Three different pore size nucleopore filters (10, 2 and 0.2 µm) were used for size fractionation of Chl-*a*. Nitrate reductase activity (NRA) and alkaline phosphatase activity (APA) were also assayed on Day 7.

Shipboard nutrient analyses were perfomed on a TRAACS 800 autoanalyzer, according to the methods of Grasshoff (1983). Chl-*a* was extracted with N-N, dimethylhormamide (Suzuki and Ishimaru, 1980) and measured with a Turner AU-10 fluorometer. NRA was assayed on board after Berges and Harrison (1995) in duplicate 500-ml samples on the initial day and on Day 7. Enzyme activity was expressed as a product of nitrite concentration per unit of volume and time (µmol NO_2 L^{-1} min^{-1}) or normalized to Chl-*a* concentration in the sample (µmol NO_2/µg Chl-a^{-1} min^{-1}). The APA was measured fluorometrically using 3-O-methylfluorescein phosphate as a substrate (Perry, 1972).

Phytoplankton cell counts were perfomed by light microscopy (larger cells: > 10 µm) and flow cytometry (smaller cells: < 10 µm). Samples for larger cells were preserved with formaldehyde at 5% of final concentration and stored at room temperature. Samples for smaller cells were preserved with paraformaldehide at 1% of final concentration and frozen immediately using liquid nitrogen and stored at –80ºC.

Results and discussion

Nitrate and phosphate concentrations at 5 m depth for both sites were almost the same, at 11 and 1.2 µM, while silicate was higher at Stn P (19 nM) than at Stn K (15nM). Total Chl-*a* concentration was slightly higher at Stn K than at Stn P, but both were below 0.5 µg L^{-1}, indicating both sites were at HNLC conditions at the time of the incubation. Light irradiance and temperature were not significantly different.

At both sites total Chl-*a* concentration increased sharply in the iron-enriched bottles after Day 3 (Fig. 1). At Stn K the highest Chl-*a* concentration of 8 µg L^{-1}, which was 17 times the initial value, was observed in the iron- and zinc-enriched bottle on Day 7. The increase in the bottle at 0.3 nM Fe was 4 µg L^{-1}, which was half of that at 1.0 nM Fe. The control bottles showed little increase in Chl-*a* in 7 days. The zinc-only addition did not affect Chl-*a* concentration as in the control. At Stn P the addition of iron also stimulated the Chl-*a* concentration to its highest concentration, at 14 µg L^{-1}, which was 52 times the initial value and observed in the iron- and zinc-enriched bottle on Day 7. The Chl-*a* concentration in the bottles at 0.3 nM Fe was almost a half of the 1.0 nM-enriched bottle. The control and Zn-only added bottles showed a slight increase in Chl-*a* of up to 3.5 µg L^{-1}. This increase was 18% of that in the 1.0 nM Fe-added bottles. These results strongly suggested that phytoplankton growth at both the NE and NW stations were limited by iron deficiency in the summer of 1999. This was supported by the evidence that dissolved iron was depleted in the surface at both stations (Obata, pers. comm.).

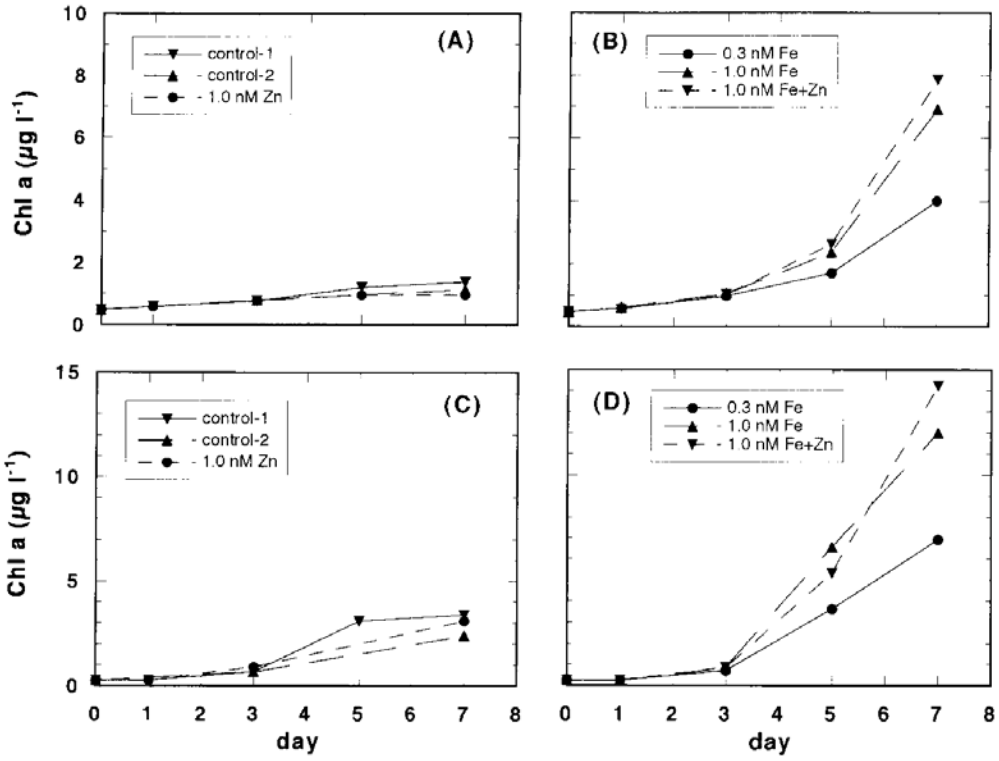

Fig. 1 Change in total Chl-*a* concentration with time in the incubation bottles. (A) two controls and 1.0 nM Zn-added bottles at Stn K (NW). (B) 0.3 and 1.0 nM Fe-added bottles and 1.0 nM Fe- and Zn-added bottles at Stn K. (C) same as in (A) except at Stn P (NE). (D) same as in (B) except at Stn P.

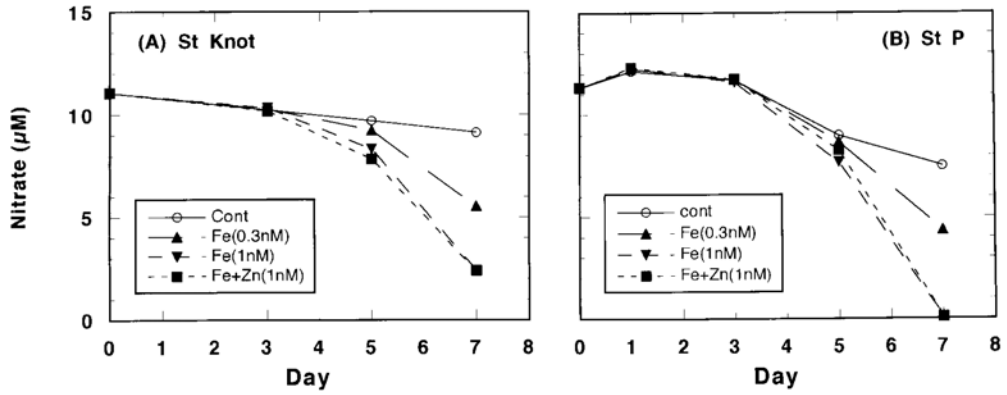

Fig. 2 Change in nitrate concentration with time in the incubation bottles. (A) Stn K (NW), (B) Stn P (NE).

Nutrient concentrations did not change until Day 3, but decreased after Day 5, especially for iron-added bottles (Fig. 2). The amounts of nutrient drawdown was higher for the 1.0 nM Fe addition than that for the 0.3 nM Fe addition and the control. No difference in phosphate and silicate concentrations on Day 7 was found between 1.0 nM Fe and 1.0 nM Fe plus 1.0 nM Zn-added bottles at Stn K, but iron- and zinc-added bottles showed higher utilization of nutrients at Stn P.

The consumed N:P ratio in the control bottles (12.5) was almost same in the iron-added bottles, but the Si:N ratio was 2.4 which was 2.2 times higher than in the iron-added bottles. The ratios in nutrient consumption were not different between the control and iron-added bottles at Stn P (Si:N ratio of 1.23 and 0.97 and N:P ratio of 8.8 and 10.5 in the control and the iron-added bottles). These differences in the consumption ratio of Si:N in the control bottles seemed to be derived from the different phytoplankton assemblages in each station: centric diatom dominance in the NW station and pennate diatom and coccolithophorids dominance in the NE station. The centric diatoms consumed silicate and nitrate at equimolar amounts under iron-replete conditions whereas they consumed more silicate than nitrate under iron-limited conditions (Takeda, 1998). *Emiliania huxleyi* are coccolithophorids that achieve their maximal growth rate even under iron-limited conditions (Muggli and Harrison, 1997). Thus, at Stn K dominant centric diatoms utilized much more silicate under iron limitation while at Stn P co-existing coccolithophorids and pennate diatoms utilized nutrients at a Si:N ratio of 1:1 even if the diatoms consumed excess silicate over nitrate, because coccolithophorids require only nitrate and phosphate as nutrients.

NRA measured on Day 0 at both stations was close to the detection limit. On Day 7, even after normalizing to Chl-*a* (biomass), NRA in the 1.0 nM Fe-added bottles showed 4 times higher activity than the control.

We also assayed APA which requires zinc for the same occasions as the NRA. None of the samples assayed showed detectable APA activity.

References

Berges, J.A. and Harrison, P.J. 1995. Nitrate reductase activity quantitatively predicts the rate of nitrate incorporation under steady state light limitation. A revised assay and characterization of the enzyme in three species of marine phytoplankton. *Limnol. Oceanogr.* **40**: 82–93.

Grasshoff, K. 1983. Automated chemical analysis. pp. 263–289. *In* Methods of Seawater Analysis, second edition. *Edited by* K. Grasshoff, M. Ehrhardt and K. Fremling, Verlag Chemie, Weinheim.

Muggli, D.L. and Harrison, P.J. 1997. Effects of iron on two oceanic phytoplankters grown in natural NE subarctic Pacific seawater with no artificial chelators present. *J. Exp. Mar. Biol. Ecol.* **212**: 225–237.

Perry M.J. 1972. Alkaline phosphatase activity in subtropical Central North Pacific waters using a sensitive fluorimetric method. *Mar. Biol.* **15**: 113–119.

Suzuki, R. and Ishimaru, T. 1980. An improved method for the determination of phytoplankton chlrorophyll using N,N-dimethylformamide. *J. Oceanogr. Soc. Jpn*. **46**: 190–194.

Takeda, S. 1998. Influence of iron availability on nutrient consumption ratio of diatoms in oceanic waters. *Nature* **293**: 774–777.

Iron-siderophore receptors of heterotrophic marine bacteria

Neil M. Price, Julie Granger and Evelyn Armstrong

Department of Biology, 1205 Ave. Docteur Penfield, McGill University, Montreal, QC, Canada H3A 1B1
E-mail: nprice@bio1.lan.mcgill.ca

Laboratory isolates of heterotrophic bacteria and field populations from low-iron waters of the ocean are able to take up ^{55}Fe from ferrioxamine B, a fungal siderophore (Granger and Price, 1999; Maldonado and Price, 1999). Rates of transport are up-regulated when ambient iron concentrations are low, suggesting that the use of siderophore-bound iron is an adaptation to overcome iron limitation. Using a non-denaturing PAGE (polyacrylamide gel electrophoresis) assay, we have discovered that the laboratory strains produce outer-membrane receptors that bind ferrioxamine B when iron is limiting growth. So far we have examined *Altermonas* sp., a clone isolated from waters near Station P in the subarctic Pacific Ocean, and PWF3, a clone from the Gulf of Mexico. The receptor is absent from cells cultured in a high-iron medium and is rapidly induced upon transfer to a low-iron medium. Its apparent molecular weight is roughly 80 kD, similar in the size to other siderophore receptors from terrestrial and pathogenic bacteria. We are now characterizing the specificity of the receptor(s) by examining binding of other siderophores and inorganic iron complexes. The method could be used to examine siderophore receptor expression in natural populations of bacteria before and during an iron fertilization experiment.

References

Granger, J. and Price, N.M. 1999. The importance of siderophores in iron nutrition of heterotrophic marine bacteria. *Limnol. Oceanogr.* **44**: 541–555.

Maldonado, M.T. and Price, N.M. 1999. Utilization of iron bound to strong organic ligands by phytoplankton communities in the subarctic Pacific Ocean. *Deep-Sea Res. II* **46**: 2447–2474.

The size-fraction of supplied iron and change in the concentration of iron in different size fractions in onboard bottle incubation experiments

Jun Nishioka[1], Shigenobu Takeda[1], C.S. Wong[2], W. Keith Johnson[2] and Frank A. Whitney[2]

[1] Central Research Institute of Electric Power Industry, 1646 Abiko-shi, Abiko, Chiba, Japan 270-1194
E-mail: nishioka@criepi.denken.or.jp

[2] Climate Chemistry Laboratory, Institute of Ocean Sciences, Department of Fisheries and Oceans, 9860 West Saanich Road, Sidney, BC, Canada V8L 4B2

Introduction

The relationship between iron dynamics and phytoplankton growth is important for the study of iron biogeochemistry after iron fertilization. Size-fractionated iron analysis will be one useful approach for the study of iron dynamics. Therefore, to investigate the size-fraction of supplied iron and changes in the concentration of different size fractions of iron during phytoplankton growth in open-ocean seawater, a combination of measurements of size-fractionated iron and concurrent incubation experiments was performed at Ocean Station PAPA (OSP) in September 1997. One of the objectives of this experiment was to investigate the difference in iron size fractions in seawater between artificial iron addition and by natural iron supply.

Previous laboratory studies suggested that small colloidal particles formed in traditionally dissolved fractions (< 0.2 μm) might be one of the available iron forms for oceanic phytoplankton, with some mechanisms such as cell-surface reduction (Wells and Mayer, 1991; Wells *et al*., 1991; Kuma and Matsunaga, 1995; Nishioka and Takeda, 2000). Therefore, we investigated changes of size-fractionated iron during ambient phytoplankton growth by using a combined trace metal clean filtration method, which uses a 0.2 μm-pore size Teflon membrane filter and a 200-kDa nominal molecular weight polyethlene hollow-fiber ultrafilter (Nishioka and Takeda, 2000), and ultra-clean onboard bottle incubation experiments.

Method

An onboard incubation experiment was conducted on board the R/V *J.P. Tully* at Ocean Station PAPA (OSP: 50°N, 145°W) in September 1997. Seawater samples for vertical profiles of size-fractionated iron were collected using Teflon-coated, modified 30-L Go-Flo bottles suspended on a Kevlar line on September 3, 1997. For the incubation experiment, a water sample with resident phytoplankton was collected on September 4 from the sea surface and transferred to two acid-cleaned 20-L polyethylene tanks by rubber boat sampling with clean technique. A deep seawater sample was collected from 600 m depth using the same method as for the vertical sample collection on September 5. Acid-cleaned polycarbonate bottles were used for the incubation experiments. Although the problem with wall adsorption and desorption was expected, we confirmed that determination of dissolved and size-fractionated total acid-labile Fe concentration in filtered seawater samples did not significantly change in acid-cleaned polycarbonate incubation bottles for more than 5 days (Takeda and Obata, 1995; Nishioka and Takeda, 2000). We prepared three treatments in this incubation experiment.

Control treatment

Surface water was homogenized in a 20-L polyethylene bottle, and the water sample for the control treatment was then dispensed into eight, acid-cleaned, replicate 1-L polycarbonate incubation bottles.

Iron addition treatment

The iron-enriched treatment was prepared from surface water enriched with a 0.7 nM $FeCl_3$ solution and dispensed in the same manner as the control treatment after homogenization.

Deep water mixed treatment

For the deep water mixed (DWM) treatment, the surface water sample was placed in a 20-L polyethylene bottle enriched with deep seawater (surface water: deep water = 1:2) and then immediately homogenized. This mixed seawater was dispensed in the same way as for the control

treatment. These preparation procedures were done in a clean-air tent. The 1-L bottles were sealed in three plastic bags and then incubated on deck in running surface seawater baths to maintain surface seawater temperatures for 6 days. The incubation baths were covered with neutral density screens, and incubation light intensity was 27% of the ambient light level.

During the course of the incubations, two bottles for each treatment were withdrawn from the incubation bath at Days 2, 4 and 6 and submitted to the measurements of nutrients and Chl-*a* concentrations. Size-fractionated iron in each treatment seawater sample was determined on the initial and final days. Measured total labile Fe (unfiltered, detectable at pH 3.2) concentrations were divided into three size fractions; large labile particles (> 0.2 µm), small colloidal particles (0.2 µm–200 kDa) and soluble species (< 200 kDa). Concentrations of Fe (III) in the unfiltered and filtered samples were determined with an automatic Fe (III) analyzer (Kimoto Electric Co. Ltd.) using chelating resin concentration and chemi-luminescence detection (Obata *et al*., 1993, 1997). Initial sample bottles (Day 0) were analyzed without incubation. The incubation bottles were not repetitively sampled in order to avoid contamination during the sub-sampling procedure.

Results and Discussion

Vertical distribution of size-fractionated iron

At OSP, vertical profiles of dissolved Fe (< 0.2 µm) exhibited nutrient-like distributions in September 1997. Concentrations of soluble Fe were low in the surface mixed layer and increased below 300 m depth (~ 0.34 nM, Nishioka *et al*., 2001). The concentrations of small colloidal Fe were generally low in the surface mixed layer (0.01–0.06 nM) with higher concentrations below 200 m depth (~ 0.22 nM). At 600 m depth, small colloidal Fe represented 39% of dissolved Fe (< 0.2 µm) (Nishioka *et al*., 2001).

Onboard incubation experiment

Initial concentrations of nutrients, total Chl-*a* and total labile Fe in each treatment incubation bottle are shown in Table 1. In the DWM treatment, iron was enriched to 0.35 nM with a high level of nutrients. Both additions of minute $FeCl_3$ and Fe in deep water to surface seawater samples containing excess nutrients increased the stocks of Chl-*a* in incubation bottles relative to the controls (Figs. 1 and 2). Total Chl-*a* concentration in the control treatment increased by only 2.2 times the initial concentrations during 6 days of incubation. In contrast, total Chl-*a* concentrations in the iron addition treatment and DWM treatment increased 15 and 27 times, respectively for the initial concentrations in the same periods (Fig. 1).

The increase in Chl-*a* concentrations was correlated with major nutrient consumption (Fig. 2). In the iron addition and DWM treatments, concentrations of major nutrients were reduced significantly more than that of the control treatment. Nitrate concentration decreased only 0.7 µM in the control treatment, while 6.8 µM and 4.6 µM, respectively, in the iron addition and DWM treatments. Obviously, the stock of Chl-*a* concentration and nitrate consumption by phytoplankton taken from the OSP water increased with added $FeCl_3$ and deep water. These results strongly suggest that ambient phytoplankton were under iron limitation in OSP surface waters. Also, deepwater addition to surface water disarms iron limitation of ambient phytoplankton. This result suggests that biologically available iron is included in deep water and stimulates phytoplankton growth if deep water is supplied from below the mixed layer to the surface by upwelling and vertical diffusion.

Table 1 Initial (Day 0) concentrations of nutrients, total labile Fe and total Chl-*a* in each of the treatment incubation bottles.

	Unit	Control	Fe addition	Deep water mixed
NO_3	µM	7.7	7.7	32.1
PO_4	µM	0.77	0.77	2.29
Si	µM	14.7	14.7	82.3
Total labile Fe	nM	0.15	0.64	0.35
Total Chl-*a*	µg/L	0.33	0.33	0.09

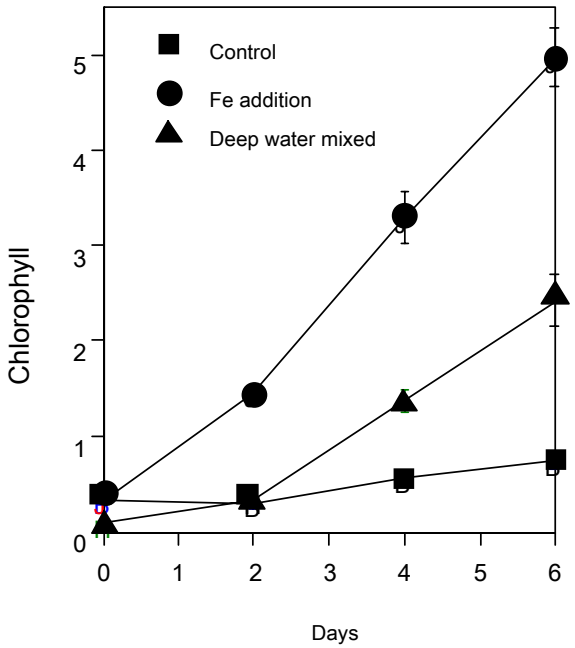

Fig. 1 The change of Chl-*a* concentration in each treatment.

Initial (Day 0) and final (Day 6) size-fractionated iron concentrations of all treatments are presented in Figure 3. In the control treatment, total labile Fe concentration decreased slightly (0.04 nM) during the 6 days, and significant iron remained in the only soluble species fraction (0.11 nM) in these bottles at end of the incubation. Total labile Fe concentration in the iron addition and DWM treatment samples showed large decreases during the 6 days' incubation. When the $FeCl_3$ solution was added to the OSP seawater in the iron addition treatment bottles, the iron concentration in small colloidal fraction increased significantly and comprised 85 % of the total labile Fe. Total labile Fe concentration decreased from 0.64 to 0.41 nM for the 6 days. Of the size-fractionated iron concentrations, small colloidal particles decreased significantly (0.43 nM) and 0.21 nM of this fraction converted to a large labile Fe fraction during incubation. Soluble Fe species did not significantly change on the final day (Fig. 3). While in DWM treatment, iron in the soluble species comprised 45.7 % of total labile Fe and total labile Fe concentration decreased 0.13 nM during 6 days of incubation. Of all the size fractions of iron, the soluble Fe species decreased most significantly by 0.11 nM. Comparing initial size-fractionated iron concentration in the iron addition treatment to the control treatment, the small colloidal Fe fraction decreased significantly during phytoplankton growth and some of the small colloidal Fe converted to the other fraction. The decrease in the small colloidal Fe concentration during the period of phytoplankton growth represented proportionally the greatest decrease in total labile Fe.

On the other hand, soluble Fe fraction increased in the DWM treatment at the initial stage of incubation and decreased during phytoplankton growth (Fig. 3). Comparing the iron addition treatment to the DWM treatment, the size fraction of supplied iron in seawater and its net change during phytoplankton growth were different. These results demonstrate that the size fraction of supplied iron in seawater and its net change during phytoplankton growth was different between different iron sources.

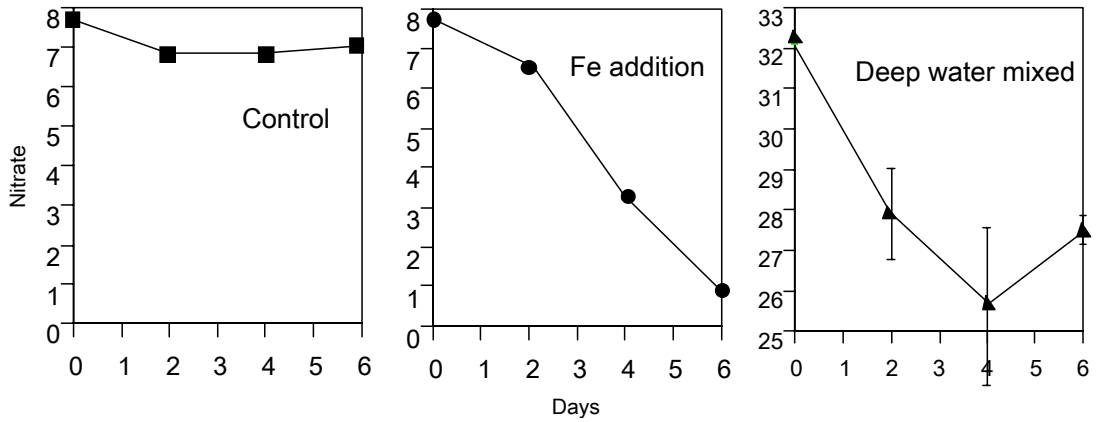

Fig. 2 The change of nitrate concentration in each treatment.

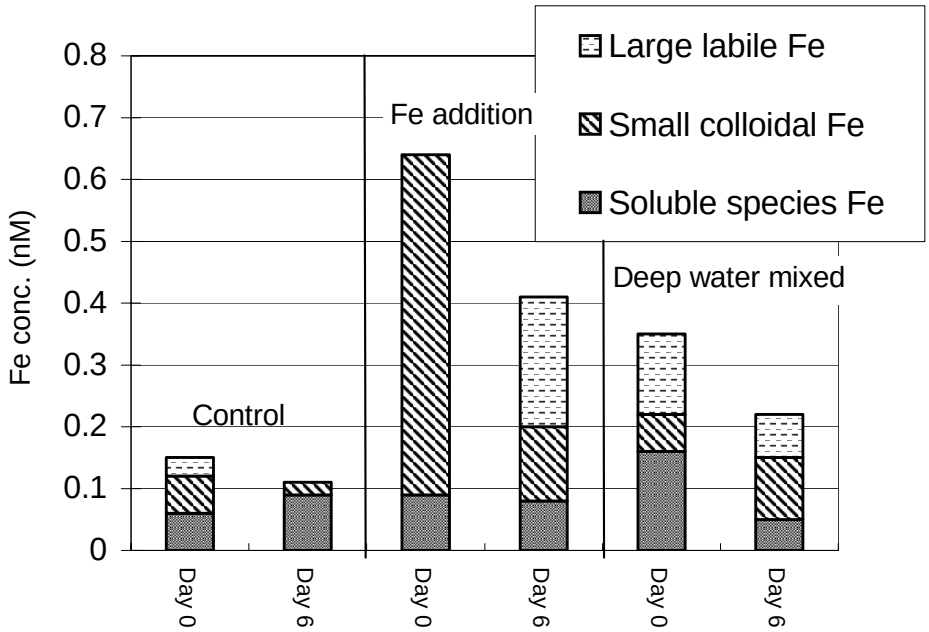

Fig. 3 Initial (Day 0) and final (Day 6) concentrations of size-fractionated Fe in each treatment.

Summary

- When the $FeCl_3$ solution was added to the surface seawater in the incubation bottle, the small colloidal Fe concentration increased significantly.
- The decrease in the small colloidal Fe concentration during the period of phytoplankton growth represented proportionally the greatest decrease in total labile Fe.
- Comparing the iron addition treatment to the DWM treatment, the size fraction of supplied iron in seawater and its net change during phytoplankton growth were different between different iron sources.
- The use of the size-fractionated iron analysis in iron fertilization experiments may provide important information for understanding iron dynamics after iron fertilization. Studies of iron dynamics in natural seawater should be focused on iron complexation with organic ligands as well as the relationship between changes in concentration of small colloidal Fe and phytoplankton growth.

Suggestions for iron fertilization experiments from this study

- Artificial iron additions result in different iron forms compared to the natural iron supply from deep water.
- Wet and dry deposition of atmospheric aerosols may have similar characteristics to the small colloidal Fe which is caused by artificial iron addition.
- The study of iron dynamics after iron fertilization should focus on iron complexation with organic ligands as well as small colloidal Fe.

References

Kuma, K. and Matsunaga, K. 1995. Availability of colloidal ferric oxides to coastal marine phytoplankton. *Mar. Biol.* **122**: 1–11.

Nishioka, J. and Takeda, S. 2000. Change in the concentrations of iron in different size fractions during growth of the oceanic diatom *Chaetoceros* sp.: importance of small colloidal iron. *Mar. Biol.* **137**: 231–238.

Nishioka, J., Takeda, S., Wong, C.S. and Johnson, W.K. 2001. Size-fractionated iron concentrations in the northeast Pacific Ocean: Distribution of soluble and small colloidal iron. *Mar. Chem.* **74**: 157–179.

Takeda, S. and Obata, H. 1995. Response of equatorial Pacific phytoplankton to subnanomolar Fe enrichment. *Mar. Chem.* **50**: 219–227.

Obata, H., Karatani, H. and Nakayama, E. 1993. Automated determination of iron in seawater by chelating resin concentration and chemi-luminescence detection. *Anal. Chem.* **65**: 1524–1528.

Obata, H., Karatani, H., Matsui, M. and Nakayama, E. 1997. Fundamental studies for chemical speciation of iron in seawater with an improved analytical method. *Mar. Chem.* **56**: 97–106.

Wells, M.L. and Mayer, L.M. 1991. The photoconversion of colloidal iron oxyhydroxides in seawater. *Deep-Sea Res.* **38**: 1379–1395.

Wells, M.L., Mayer, L.M., Donard, O.F.X., de Souza Sierra, M.M. and Ackelson, S.G. 1991. The photolysis of colloidal iron in the oceans. *Nature* **353**: 248–250.

Zooplankton response to nutrient input

Atsushi Tsuda[1] and Shigenobu Takeda[2]

[1] Hokkaido National Fisheries Research Institute, 116 Katsurakoi, Kushiro, Hokkaido, Japan 085-0802 E-mail: tsuda@hnf.affrc.go.jp

[2] Biology Department, Central Research Institute of Electric Power Industry, 1646 Abiko, Abiko-city, Chiba, Japan 270-1194

The roles of grazers (microzooplankton and mesozooplankton) and remineralizers (bacteria and heterotrophic nanoflagellates) were estimated during a nutrient enrichment experiment using a mesocosm. Primary production increased by about 11 times during the initial 3 days, and the grazing rate by zooplankton also increased by 7.4 times. During the initial 5 days, the primary production exceeded the grazing rate and after that, almost balanced rates were observed. The biomass peaks of bacteria and heterotrophic nanoflagellates (HNF) were observed after the phytoplankton bloom declined. Bacterial production and HNF grazing gradually increased from the beginning to the end of the experiment. The contribution of microzooplankton to grazing was greatest during the initial 7 days, and the response to phytoplankton growth was fastest during the same period. Heterotrophic dinoflagellates were the most dominant component of microzooplankton, but naked ciliates showed the fastest growth in response to phytoplankton production. Overall, microzooplankton grazing contributed the most to phytoplankton depletion. Their response to the phytoplankton growth was very quick, and they removed about 50% of the primary production constantly. Thus, naked ciliates and heterotrophic dinoflagellates were the most plausible organisms to realize the steady state of phytoplankton concentration in the ocean.

The western subarctic Pacific is characterized by relatively high standing stocks of phytoplankton and mesozooplankton. Moreover, the dominance of diatoms and the almost complete absence of haptophytes characterize the phytoplankton community of the western subarctic Pacific Ocean. The expected difference in response to iron addition by lower trophic organisms between the east and west will be discussed.

A.1.2.4 Physics in the North Pacific and iron addition techniques

Physical processes affecting the distribution of iron-fertilized ocean water in the North Pacific

Richard E. Thomson

Institute of Ocean Sciences, Fisheries and Oceans Canada, 9860 West Saanich Road, Sidney, BC, Canada V8L 4B2. E-mail: ThomsonR@pac.dfo-mpo.gc.ca

Modification of the upper ocean occurs through a variety of physical processes, including wind and buoyancy forcing, advection, and turbulent diffusion. Proposed iron fertilization sites in the northwest and northeast Pacific are regions of marked upper ocean startification, slow eastward-flowing surface currents, and moderately weak turbulent dissipation. Mean surface currents in the region range from 1–5 cm/s (approximately 1–4 km/day) while the mean horizontal eddy viscosity ranges from roughly 1.5×10^7 cm^2/s in the meridional direction to 2.5×10^7 cm^2/s in the zonal direction. Decorrelation time scales for mesoscale (10 to 100 km) motions are around 2 to 3 days over associated spatial scales of 15 to 30 km. Although tidal currents are weak (diurnal and semidiurnal velocities are of order 1 cm/s) passing atmospheric fronts can generate strong (up to roughly 50 cm/s), rapidly varying currents of 16-h periods that persist for several days to a week. These currents, combined with turbulent wind mixing and surface buoyancy (heat) flux, lead to short-term (< 1 day) variability in the surface mixed layer depth and to the formation of seasonal pycnoclines above the permanent pycnocline (approximately 100 m depth). The experimental sites may be impacted by packets of internal tidal waves formed near the Aleutian Islands and by the passage of westward propagating mesoscale eddies generated along the west coast of North America. Coupled ocean–atmosphere circulation models can assist in the retrospective analysis of the iron plume dispersion but presently lack the spatial and temporal resolution for accurate experimental design and prediction.

The application of SF_6 tracer Lagrangian studies in iron fertilisation experiments

Cliff S. Law

Plymouth Marine Laboratory, Prospect Place, The Hoe, Plymouth, Devon, UK PL1 3DH
E-mail: csl@pml.ac.uk

Introduction

The physical mechanisms that determine the dispersion of biological populations in the surface ocean confound the determination of the limiting parameters and processes. Interpretation of Eulerian time series data is hindered by a lack of knowledge of the physical forcing, as any temporal change may simply reflect the advection of different water bodies past the sampling point. This has been addressed in Lagrangian studies of upper ocean biogeochemistry using drifter buoys (Harris *et al*., 1997). However, wind slippage may reduce the correlation between buoy and water body with time (Stanton *et al*., 1998), and drifter buoys are also restricted to the air–sea interface and so cannot track in the event of subduction. Dyes have been used successfully in dispersion studies (Smart and Laidlaw, 1977), but adsorption onto particles, toxicity, and limited real-time analytical capability restrict their application to short-term coastal and shelf seas. Sulphur hexafluoride (SF_6) can be used for tracking water bodies at the surface over periods of 2 weeks (Wanninkhof *et al*., 1997; Law *et al*., 2001), and periods exceeding a year for sub-surface releases (Ledwell *et al*., 1993, 1998). The benefits of SF_6 include high analytical sensitivity, low oceanic and atmospheric background, inertness and relatively low price, providing a favourable combination for mesoscale tracer studies in the open ocean with minimal volumes of SF_6 (Law *et al*., 1998). Tagging with SF_6 permits the monitoring of temporal change in a discrete body of water, so providing an observational tool for constraining biological and biogeochemical cycling rates in a non-perturbated system (Wanninkhof *et al*., 1997; Law *et al*., 1998). This capability further permits *in situ* manipulation of the water body, and so ameliorates the limitations of marine experimentation experienced in *in vivo* studies. The use of the tracer in these manipulation experiments confirms causality, as initially suggested by Watson *et al.* (1991) and subsequently demonstrated in the IronEx and SOIREE (**S**outhern **O**cean **I**ron **RE**lease **E**xperiment) studies (Martin *et al*., 1994; Coale *et al*., 1996; Boyd *et al*., 2000). In the following discussion, the SF_6 Lagrangian framework will be described and the benefits and limitations of this approach discussed.

Methods

Analytical methodology

Analytical detection limits of 0.02 fmol/kg (1 femtomole = 10^{-15} mol) and an extremely low surface water background concentration of < 1.4 fmol/l permit mesoscale water mass tracking with modest releases of SF_6 (50–120 g). The SF_6 patch is monitored using two different analytical systems for continuous measurement of the lateral dispersion at the surface and for discrete water sampling of the vertical dispersion. Both analyses are achieved using automated systems incorporating sparge-cryogenic trapping and detection of SF_6 by ECD (electron capture detector). The discrete system includes pre-sparge vacuum injection to accelerate stripping and shorten analysis time, a single trapping system, and handles large volumes (350 ml) with increased precision (<1%) (Law *et al*., 1994). The mapping system runs continuously, using sample volumes of 180 ml and a dual trapping system, with a minor reduction in precision and sensitivity (Upstill-Goddard *et al*., 1991; Law *et al*., 1998). A surface measurement is obtained every 3 min which, at a ship speed of 5–10 kts, gives spatial sampling every 0.45–0.9 km. Concentration data are incorporated in near real-time into an uncorrected plot of the areal distribution of the patch by integrating the SF_6 data with the ship's GPS position. This enables rapid alteration to ship speed and direction in response to variation in the SF_6 signal and ensures resolution of patch boundaries for determination of the "IN" and "OUT" patch sampling stations. A Lagrangian correction accounting for the advection of surface waters during mapping is subsequently applied.

Tracer release

The SF_6 saturation, release and surveying techniques are described in Upstill-Goddard *et al.* (1991) and Law *et al.* (1998). Briefly, a saturated solution is prepared by sparging surface seawater in a steel tank with pure SF_6 at a rate of ~120 ml/min. SF_6 saturation is monitored by Thermal Conductivity Detector (TCD). During the release, the SF_6-saturated seawater is pumped out with replacement by water above a diaphragm in the top of the tank to prevent SF_6 dilution or degassing. It is then mixed with the iron solution and released at mid-depth of the surface mixed layer through the outlet of a re-enforced tube which is attached to a weighted depressor. The optimal distance of the outlet is ~12–15 m behind the ship, so that the tracer/iron solution will be mixed by the prop wash while immediate loss of SF_6 to the atmosphere, caused by entrapment of air in the prop wash, is minimised. The release period and ship speed are dependent upon length of release track and sea state but vary between 3–5 kts and 8–16 h, respectively.

The release is generally preceded by a large-scale site survey of at least 50 km^2 to determine the suitability for a tracer experiment. The site should be free from dynamic influences such as fronts, and physical, biological and biogeochemical variability should be minimal. Depth of the mixed layer is a critical issue, as gas exchange may reduce the SF_6 signal rapidly in a shallow mixed layer (<15 m), whereas a deep mixed layer may lead to over-dilution of the tracer.

Correction for surface water advection is essential for the creation of a coherent tracer patch with a clearly definable centre. A dead-reckoning strategy was used in the initial tracer release experiments (Upstill-Goddard *et al.*, 1991; Law *et al.*, 2001), but the advection of the centre-point has been monitored more recently using surface drifter buoys in more recent experiments. These drifter buoys are equipped with a VHF packet radio which communicates the buoy GPS position to the ship at short intervals, and the drifter buoy also subsequently functions as a locator for mapping during excursions outside the patch. The drifter buoys are generally tethered to holey-sock drogues centred mid-depth of the surface mixed layer to reduce wind-slippage. However, wind drift may still occur, with deviation of the patch and buoy tracks on relatively short timescales (Law *et al.*, 1998; Stanton *et al.*, 1998), although this effect may be minimal (Law *et al.*, 2001; Martin *et al.*, 2001) (see Fig. 1).

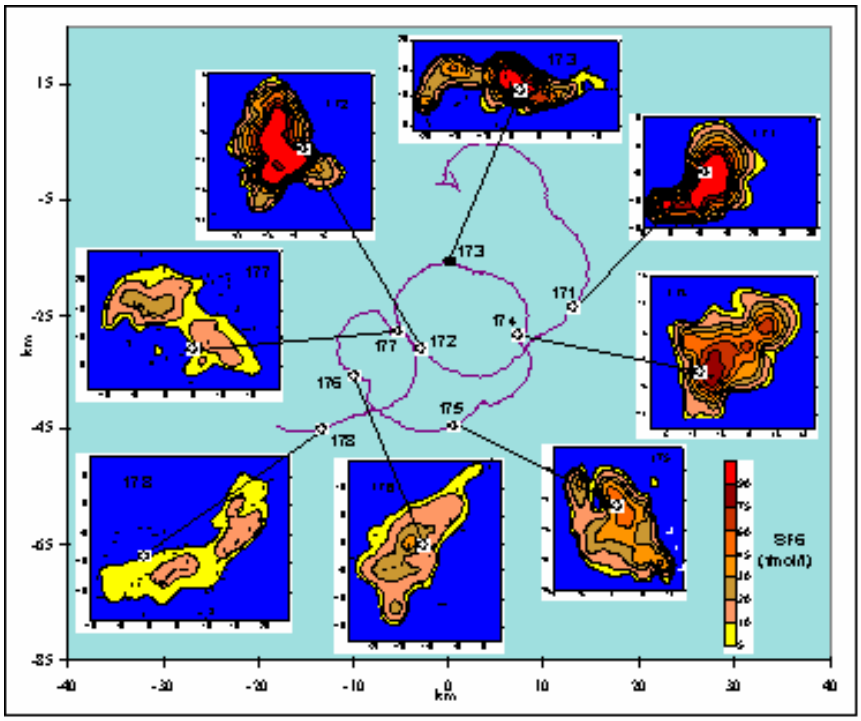

Fig. 1 GPS buoy track with transformed SF_6 contour plots for each day of survey referenced to the midday GPS buoy position from the UK PRIME Lagrangian experiment (Law *et al.*, 2001).

The SOIREE release was achieved by an expanding hexagonal track in a Lagrangian frame of reference around a central drifter buoy which updated its position every 10 min, with distances of 0.5–0.6 km between the expanding tracks (see Fig. 2). Re-infusion of iron was achieved using ADCP-derived velocities to inform the release track, with the SF_6 signal providing an indicator that the iron was added within the patch boundaries. This worked successfully during SOIREE as there was no need to add further SF_6 because the signal remained high. It is possible to use this approach during re-infusion of both SF_6 and iron (P. Nightingale, pers. comm.), although this runs the risk of contamination of the analytical mapping system.

Results and discussion

The Lagrangian tracer framework provides an "unbounded mesocosm" *in situ*, so that temporal variation can be determined within the same body of water, by comparison of the ecosystem response to the perturbation at the IN station with the control unperturbated OUT station. In addition, biogeochemical budgets benefit from concurrent determination of physical exchange rates in the water column and across the air–sea interface, accounting for loss processes and dilution.

Air–sea exchange rates

A minor disadvantage in the use of SF_6 as a tracer is its volatility, which reduces the time frame within which a surface release can be followed. The loss rate of SF_6 across the air–sea interface is well documented (Wanninkhof, 1992; Nightingale *et al*., 2000a), and can be estimated prior to release. Determination of the transfer velocity, k, in shelf seas and the open ocean has been achieved using a dual tracer approach of SF_6 and Helium-3 (Nightingale *et al*., 2000a). Estimates of k, obtained from wind-speed parameterisations (Liss and Merlivat, 1986; Wanninkhof, 1992) can differ by more than than 50%, and so lead to considerable variation in the calculated fluxes. The reliability of air–sea fluxes can be improved by concurrent determination of k and ΔC gradients for dissolved gases, as the k obtained will be representative of *in situ* conditions. In addition, constraining the volatile loss of SF_6 through the dual tracer approach will reduce the errors in the SF_6 budget and so improve dispersal and biogeochemical budgets. Furthermore, the addition of He-3 with SF_6 provides insight into the impact of other factors which influence k. For example, Nightingale *et al*. (2000b) have inferred from the IronEx II observations that the influence of algal blooms upon k is negligible.

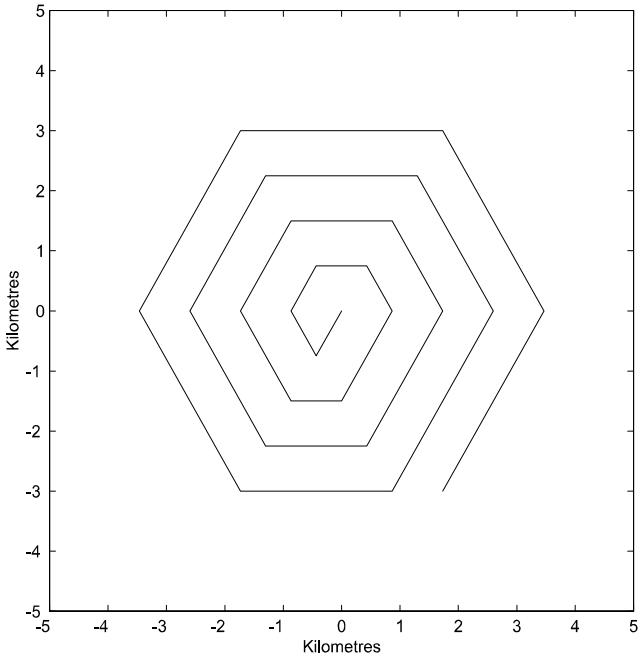

Fig. 2 Hexagonal release track around patch centre. Release pattern has a track spacing of 0.75 km. Patch area = 39 km^2, tacklength =52 km.

Lateral mixing and dispersion

Following the release, the total surface area occupied by the tracer initially expands rapidly as it mixes at the edges with water outside the patch. After this initial adjustment, the tracer will be normally distributed around the centre, and disperses at a slower rate. Calculation of the weighted second moment provides an estimate of the radial width of the tracer patch and, assuming Fickian diffusion, the lateral diffusivity Ky is then equal to half the gradient of the linear increase in W^2 with time (see Fig. 3). A recent estimate of Ky of 4 ± 2 m^2 s^{-1} during SOIREE in the Australasian sector of the Antarctic Circumpolar Current (Abraham *et al*., 2000) was within the range of 2–16 m^2 s^{-1} found at length-scale 8 km in dye release experiments in shelf seas (Okubo, 1980). However, this is lower than observed in previous open-ocean surface SF_6 releases, with a Ky of 22 ± 10 m^2 s^{-1} obtained within an eddy in the North Atlantic (Martin *et al*., 2001) and 25 m^2 s^{-1} in the equatorial Pacific (recalculated from Stanton *et al*., 1998).

Dispersion of the tracer is not just determined by diffusion. The spreading rate of a tracer patch in the streamline of an anti-cyclonic eddy exceeded that calculated from the radial effective horizontal diffusivity (Martin *et al*., 2001), due to shear-augmented along-streamline dispersion. The tracer patch area was estimated to increase by 5–26 km^2 d^{-1}, exceeding the surface area of 1.9 ± 0.86 km^2 d^{-1} which would result from an effectively diffuse dispersion in all directions.

In addition, the patch becomes influenced by strain and the length of the patch increases exponentially at the rate whereas the width of the patch stabilizes at a steady value. Stretching of the tracer patch results from the balance between the thinning effect of the strain and the widening tendency of diffusion. In ocean flows the strain is not constant, but an effective strain rate may be defined from the exponential growth in the length of a patch of tracer. The strength of the stirring in a two-dimensional flow can be estimated from the dispersion of the tracer, with calculation of an effective strain rate $\gamma = (8 \pm 3)\ 10^{-7}$ s^{-1} during SOIREE. This agreed with estimates of $\gamma = 5.8 \times 10^{-7}$ s^{-1} obtained from the subsequent dispersal of the patch as indicated by the chlorophyll distribution in satellite images (Abraham *et al*., 2000).

Dispersion will also influence any biological and biogeochemical variable within the patch the lateral and vertical transfer of the tracer provides a correction for this dilution. This was used to correct for the decrease in iron concentration due to dilution during SOIREE, thereby providing a constraint of the non-conservative losses of iron (Bowie *et al*., 2001).

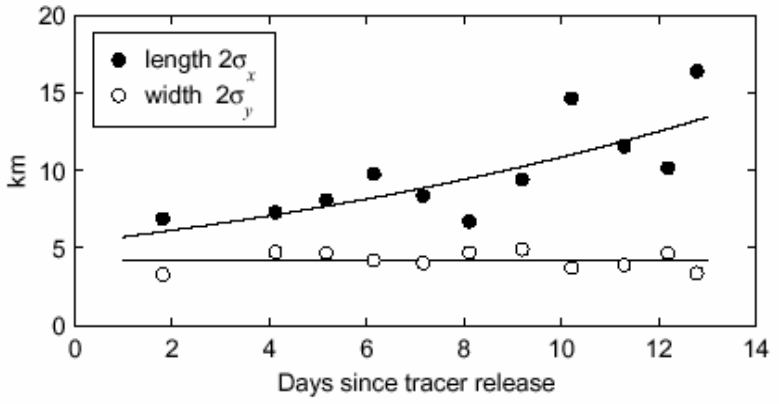

Fig. 3 Changes in the size and shape of the tracer patch during SOIREE. The width and length of the patch were determined by fitting a Gaussian ellipsoid using a least-squares fitting procedure. A best-fit to the length and width of the patch after Day 4 was used to estimate the strain rate and the diffusivity (Abraham *et al*., 2000).

Vertical diffusivity rates

The rate of transfer of SF_6 across isopycnals at the base of the mixed layer can provide a temporally and spatially integrated estimate of the vertical eddy diffusivity, K_z (Ledwell *et al.*, 1993, 1998; Law *et al*., 1998, 2001). The transfer of SF_6 across isopycnals results from the dissipation of turbulent kinetic energy by the breaking of internal waves and shear instability. As diapycnal diffusion of SF_6 is assumed to be Fickian, the distribution of SF_6 at the base of the mixed layer may be described by a one-sided Gaussian curve. K_z is then estimated from the increase of the second moment, the square of the mean width of each profile, with time. This approach is dependent upon the low variability across the patch and little variability in the density profile. The propagation of internal waves causes variation in the SF_6 profiles and the tracer distribution is referenced to the average density-depth profile for the survey period to correct for the isopycnal variation. K_z estimates derived from SF_6 tracer distributions vary by almost an order of magnitude. The K_z obtained from the subducted tracer patch during IronEx I was 0.25 $cm^2\ s^{-1}$ at a stable pycnocline (Law *et al*., 1998), whereas it was greater (1.95 $cm^2\ s^{-1}$) at the weaker pycnocline in a North Atlantic anti-cyclonic eddy (Law *et al*., 2000).

The vertical exchange of nutrients and gases may be determined by application of the derived K_z to the gradient at the base of the mixed layer. This approach provides an independent estimate of new production by constraining the transfer of nitrate from deep waters, which can be compared with new production estimates from *in vivo* stable isotope incubations (Law *et al*., 1998). In the Southern Ocean, vertical diffusion represents a source of dissolved iron, and preliminary estimates of K_z from SOIREE suggest that this pathway is more significant than atmospheric input in this region (Bowie *et al*., 2001).

Three-dimensional tracking

IronEx I demonstrated the utility of the SF_6 tracer in that, following subduction beneath a low-salinity front, the iron-enriched patch was still tracked by the tracer signal. Although sampling capability was reduced, as surface mapping was no longer practical and the patch has to be located by vertical profiling, this response to the iron could still be monitored.

Limitations

The SF_6 Lagrangian framework places certain logistical limitations, although these are minor compared with the benefits. Determination of the patch boundaries and identification of the centre dominate the programme and prevent continuous profiling at the patch centre, although this can be resolved by a two-ship exercise. Site selection may be biased by the need to identify a site in which a tracer Lagrangian experiment will be sustained, and so dynamic regions, such as fronts should be avoided. Similarly, surface mixed layers which are too deep, or too shallow, may potentially shorten the lifetime of the tracer patch.

A consideration of SF_6 tracer applications is the infrared activity of the SF_6 molecule, although the volume required for a mesoscale surface release is minimal when compared with total global SF_6 production (2000 tonnes p.a., Ko *et al*., 1993). It is estimated that the total SF_6 for a surface tracer experiment (including that released during saturation) has a radiative forcing equivalent to the CO_2 produced during 1–2 days research ship on passage.

Whereas the contribution of surface releases to the atmospheric signal is negligible, the background SF_6 signal in the ocean may be influenced in the event of subduction. SF_6 has considerable potential as a transient tracer of water mass ventilation and, following the stabilisation of the atmospheric CFC (chlorofluorocarbon) concentrations (Walker *et al.*, 2000), offers an alternative approach for tracking transport of recently-formed water into the deep ocean (Law *et al.*, 1994; Law *et al.*, 2001). However, even if subduction of a surface tracer patch occurs immediately after release, the impact of an additional 50–120 g upon sub-thermocline tracer concentrations will be minor, following dilution.

References

Abraham, E., Law, C.S., Boyd, P.W., Lavendar, S., Maldonado, M. and Bowie, A.R. 2000. The dispersal of an isolated phytoplankton bloom. *Nature* **407**: 727–730.

Bowie, A.R., Maldonado, M.T., Frew, R.C., Croot, P.L., Achterberg, E.P, Mantoura, R.F.C., Worsfold, P.J., Law, C.S. and Boyd, P.W. 2001. The fate of added iron during a mesoscale fertilisation experiment in the polar Southern Ocean. *Deep-Sea Res. II* **48**: 2703–2473.

Boyd, P.W., Watson, A.J., Law, C.S., *et al.* 2000. A mesoscale phytoplankton bloom in the polar Southern Ocean stimulated by iron fertilization. *Nature* **407**: 695–702.

Coale, K.H., Johnson, K.S., Fitzwater, S.E. *et al.* 1996. A massive phytoplankton bloom induced by an ecosystem-scale iron fertilisation experiment in the equatorial Pacific Ocean. *Nature* **383**: 495–501.

Harris, R.P., Boyd, P., Harbour, D.S., Head, R.N., Pingree, R.D. and Pomroy, A.J. 1997. Physical, chemical and biological features of a cyclonic eddy in the region of 61°10'N 19°50'W in the North Atlantic. *Deep-Sea Res I* **44**: 1815–1839.

Ko, M.K.W., Sze, N.D., Wang, W.-C., Shia, G., Goldman, A., Murcray, D.G. and Rinsland, C.P. 1993. Atmospheric sulfur hexafluoride: sources, sinks and greenhouse warming. *J. Geophys. Res.* (Atmos.) **98**: 10,499–10,507.

Law, C.S. and Watson, A.J. 2001. Determination of Persian Gulf Water transport and oxygen utilization rates using SF_6 as a novel transient tracer. *Geophys. Res. Lett.* **28**: 815–818.

Law, C.S., Watson, A.J. and Liddicoat, M.I. 1994. Automated vacuum analysis of sulphur hexafluoride in seawater; derivation of the atmospheric trend (1970–1993) and potential as a transient tracer. *Mar. Chem.* **48**: 57–69.

Law, C.S., Watson, A.J., Liddicoat, M.I. and Stanton, T. 1998. Sulphur hexafluoride as a tracer of biogeochemical and physical processes in an open-ocean iron fertilisation experiment. *Deep-Sea Res. II* **45**: 977–994.

Law, C.S., Martin, A.P., Liddicoat, M.I., Watson, Richards, K.J. and Woodward, E.M.S. 2001. A Lagrangian SF_6 tracer study of an anticyclonic eddy in the North Atlantic: patch evolution, vertical mixing and nutrient supply to the mixed layer. *Deep-Sea Res. II* **48**: 705–724.

Ledwell, J.R. and Watson, A.J. 1991. The Santa Monica Basin Tracer Experiment: a study of diapycnal and isopycnal mixing. *J. Geophys. Res.* **96**: 8695–8718.

Ledwell, J.R., Watson, A.J. and Law, C.S. 1993. Evidence for slow mixing across the pycnocline from an open-ocean tracer-release experiment. *Nature* **364**: 701–703.

Ledwell, J.R., Watson, A.J. and Law, C.S. 1998. Mixing of a tracer in the pycnocline. *J. Geophys. Res.* **103**: 21,499–21,529.

Liss, P.S. and Merlivat, L. 1986. Air-sea gas exchange rates: Introduction and synthesis. pp. 113–129. *In* The Role of Air-Sea Exchange in Geochemical Cycling. *Edited by* P. Buat-Menard, D. Reidel, Mass.

Martin, J.H., Coale, K.H., Johnson, K.S., Fitzwater, S.E. *et al.* 1994. Testing the iron hypothesis in ecosystems of the equatorial Pacific Ocean. *Nature* **371**: 123–129.

Martin, A.P., Richards, K.J., Law, C.S. and Liddicoat, M.I. 2001. Horizontal dispersion of an anticyclonic mesoscale eddy. *Deep-Sea Res. II* **48**: 739–755.

Nightingale, P.D., Malin, G., Law, C.S., Watson, A.J., Liss, P.S., Liddicoat, M.I. and Upstill-Goddard, R.C. 2000a. In-situ evaluation of air-sea gas exchange parameterisations using novel conservative and volatile tracers. *Global Biogeochem. Cycles* **14**: 373–388.

Nightingale, P.D., Liss, P.S. and Schlosser, P. 2000b. Measurements of air-sea transfer during an open ocean algal bloom. *Geophys. Res. Lett.* **27**: 2117–2120.

Okubo, A. 1980. Diffusion and ecological problems: Mathematical models. Biomathematics, Vol. 10, Springer, Berlin.

Smart, P.L. and Laidlaw, I.M.S. 1997. An evaluation of some fluorescent dyes for water tracing. *Water Res.* **13**: 15–33.

Stanton, T.P., Law, C.S., and Watson, A.J. 1998. Physical evolution of the IronEx-I open ocean tracer patch. *Deep-Sea Res. II* **45**: 947–975.

Upstill-Goddard, R.C., Watson, A.J., Wood, J. and Liddicoat, M.I. 1991. Sulfur hexafluoride and He-3 as seawater tracers: deployment techniques and continuous underway analysis for sulfur hexfluoride. *Anal. Chim. Acta* **249**: 555–562.

Wanninkhof, R. 1992. Relationship between wind speed and gas exchange over the ocean. *J. Geophys. Res.* **97**: 7373–7382.

Watson, A.J., Liss, P.S. and Duce, R.A. 1991. Design of a small scale iron enrichment experiment. *Limnol. Oceanogr.* **36**: 1960–1965.

Walker S.J., Weiss, R.F. and Salameh, P.K. 2000. Reconstructed histories of the annual mean atmospheric mole fractions for the halocarbons CFC-11, CFC-12, CFC-113 and carbon tetrachloride. *J. Geophys. Res.* **105**: 14,285–14,296.

Wanninkhof, R., Hitchcock, G., Wiseman, W.J., Vargo, G., Ortner, P.B., Asher, W., Ho, D.T., Schlosser, P., Dickson, M.-L., Masserin, R., Fanning, K. and Zhang, J.-Z. 1997. Gas exchange, dispersion, and biological productivity on the west Florida shelf: Results from a Lagrangian tracer study. *Geophys. Res. Lett.* **24**: 1767–1770.

Prediction of the physical behavior of released iron by random walk simulation during the iron fertilization experiment in the North Pacific

Daisuke Tsumune, Norikazu Nakashiki, Shigenobu Takeda and Jun Nishioka

Environmental Science Department, Central Research Institute of Electric Power Industry, 1646 Abiko, Abiko-shi Chiba, Japan 270-1194. E-mail: tsumune@criepi.denken.or.jp

At an iron fertilization experiment, it is important to predict the behavior of released iron in the surface water. Its behavior is complex because both physical and biogeochemical processes are involved. Simulations of a sulfur hexafluoride (SF_6) tracer release experiment is useful for understanding the physical behavior of released iron. The behavior of SF_6 is controlled by only physical processes.

A random walk simulation was employed to predict the physical behavior of released SF_6 in seawater. The random walk simulation is one of a number of particle tracking methods. Particles move by advection and diffusion in a random walk simulation. Stratification, oceanic currents and a diffusion coefficient were the physical conditions considered in this simulation. These conditions were set by typical values observed in the northwest and northeast Pacific. The influence of initial patterns of released SF_6 on the behavior of iron was also considered in the simulation in order to find an efficient release pattern of iron and SF_6. Time scales of this study were 4–5 days, 2 weeks and 1 month. This simulation acquired spatial scales that depend on time scales. As a result of this simulation, we would like to propose items of observation for simultaneous SF_6 tracer release experiments. We also performed a random walk simulation on the ocean general circulation model in the North Pacific. We found that the water mass moved from the northwest Pacific to the northeast Pacific by advection over several years. It suggests that the release of large amounts of iron and SF_6 in the northwest Pacific affects conditions in the northeast Pacific in several years.

Influence of Cape St. James on currents and eddies in the Gulf of Alaska

William R. Crawford, Josef Cherniawsky and James Gower

Institute of Ocean Sciences, Fisheries and Oceans Canada, 9860 West Saanich Road, Sidney, BC, Canada V8L 4B2. E-mail: crawfordb@pac.dfo-mpo.gc

Cape St. James lies at the southern tip of the Queen Charlotte Islands off the West Coast of British Columbia. The swift tidal streams and strong prevailing outflow currents at this cape contribute to the Haida Eddies in the Gulf of Alaska, and to outflow jets and plumes in the neighboring coastal waters. The waters at the cape itself are rich in marine life, and nutrients including iron, due to outflow of coastal water, and intense tidal mixing that stirs deep nutrient-rich water to the surface. Thomson and Wilson (1987) described an anti-cyclonic eddy that forms to the southwest of this cape, due to tidally rectified outflow currents. Crawford *et al.* (1995) found that wind-forced currents enhanced this outflow, especially in winter when storms are most intense and frequent. Satellite altimetry and infrared temperature observations provide additional insight into this region. We have re-processed the TOPEX/ Poseidon (T/P) and ERS-2 altimetry data using tidal constants based on regional tidal models (Foreman *et al.*, 2000), and on T/P data themselves (Cherniawsky *et al*., 2001.) We have also searched through 10 years of AVHRR measurements from NOAA satellites. In winter, the eddies that form to the southwest of Cape St. James often advect northward along the West Coast of the Queen Charlotte Islands with the prevailing winter coastal current. These anticyclonic eddies eventually separate from shore, forming the Haida Eddies, which can drift for several years in the Gulf of Alaska. Normally one or two such eddies form every winter, with larger eddies forming in major El Niño winters. We also find that Haida Eddies may originate along the Northwest Coast of the Queen Charlotte Islands, far from Cape St. James, supporting the hypothesis that local baroclinic instability of coastal currents is another generating mechanism for this class of eddies.

References

Crawford, W.R., Woodward, M.J., Foreman, M.G.G. and Thomson, R.E. 1995. Oceanographic features of Queen Charlotte Sound and Hecate Strait in summer. *Atmos.-Ocean* **33**: 639–681.

Foreman, M.G.G., Crawford, W.R., Cherniawsky, J.Y., Henry, R.F. and Tarbotton, M.R. 2000. A high-resolution assimilating tidal model for the northeast Pacific Ocean. *J. Geophys. Res.* **105**: 28,629–28,651.

Cherniawsky, J.Y., Foreman, M.G.G., Crawford, W.R. and Henry, R.F. 2001. Ocean tides from TOPEX/ Poseidon sea level data. *J. Atmos. Oceanic Tech*. **18**: 649–664.

Thomson, R.E. and Wilson, R.E. 1987. Coastal countercurrent and mesoscale eddy formation by tidal rectification near an oceanic cape. *J. Phys. Oceanogr.* **17**: 2096–2126.

A1.3 LIST OF PARTICIPANTS FOR THE 2000 IFEP PLANNING WORKSHOP

CANADA (9)

Crawford, William R.
Institute of Ocean Sciences
Fisheries and Oceans Canada
P.O. Box 6000
Sidney, BC
Canada V8L 4B2
E-mail: CrawfordB@pac.dfo-mpo.gc.ca

Denman, Kenneth L.
Institute of Ocean Sciences
Fisheries and Oceans Canada
P.O. Box 6000
Sidney, BC
Canada V8L 4B2
E-mail: denmank@pac.dfo-mpo.gc.ca

Harrison, Paul J.
Department of Earth and Ocean Sciences
University of British Columbia
6270 University Boulevard
Vancouver, BC
Canada V6T 1Z4
E-mail: pharrison@eos.ubc.ca

Johnson, W. Keith
Climate Chemistry Laboratory
Institute of Ocean Sciences
Fisheries and Oceans Canada
P.O. Box 6000
Sidney, BC
Canada V8L 4B2
E-mail: JohnsonK@pac.dfo-mpo.gc.ca

Levasseur, Maurice
Maurice Lamontagne Institute
P.O. Box 1000
Mont-Joli, QC
Canada G5H 3Z4
E-mail: Levasseurm@dfo-mpo.gc.ca

Peña, Angelica M.
Institute of Ocean Sciences
Fisheries and Oceans Canada
P.O. Box 6000
Sidney, BC
Canada V8L 4B2
E-mail: PenaA@pac.dfo-mpo.gc.ca

Price, Neil M.
Department of Biology
McGill University
1205 Docteur Penfield
Montreal, QC
Canada H3A 1B1
E-mail: nprice@bio1.lan.mcgill.ca

Trick, Charles G.
Department of Plant Sciences
University of Western Ontario
London, ON
Canada N6A 5B7
E-mail: cyano@julian.uwo.ca

Wong, C.S.
Climate Chemistry Laboratory
Institute of Ocean Sciences
Fisheries and Oceans Canada
P.O. Box 6000
Sidney, BC
Canada V8L 4B2
E-mail: wongcs@pac.dfo-mpo.gc.ca

JAPAN (21)

Furuya, Ken
Department of Aquatic Bioscience
University of Tokyo
1-1-1 Yayoi, Bunkyo-ku
Tokyo
Japan 113-8657
E-mail: furaya@fs.a.u-tokyo.ac.jp

Kadoyu, Masatake
Central Research Institute of Electric Power Industry
1646 Abiko
Abiko-shi, Chiba
Japan 270-1194
E-mail: kadoyu@criepi.denken.or.jp

Kimoto, Hideshi
Kimoto Electric Company Ltd.
Tennnoji, Osaka, Osaka 543-0024
Japan 543-0024
E-mail: hkimoto@Kimoto-electric.co.jp

Kiyono, Michiyasu
Central Research Institute of Electric Power Industry
1646 Abiko
Abiko-shi, Chiba
Japan 270-1194
E-mail: kiyono@criepi.denken.or.jp

Koike, Isao
Ocean Research Institute
University of Tokyo
1-15-1 Minamidai
Tokyo, Nakano-ku
Japan 164-8639
E-mail: koike@ori.u-tokyo.ac.jp

Kudo, Isao
Graduate School of Fisheries Sciences
Hokkaido University
3-1-1 Minato-cho
Hakodate, Hokkaido
Japan 041-8611
E-mail: ikudo@fish.hokudai.ac.jp

Kuma, Kenshi
Graduate School of Fisheries Sciences
Hokkaido University
3-1-1 Minato-cho
Hakodate, Hokkaido
Japan 041-8611
E-mail: kuma@fish.hokudai.ac.jp

Le Luo, Guan
Marine Biotechnology Institute
1900 Sodeshichou
Shimizu City, Shizuoka
Japan 424-0037
E-mail: lguan@shimizu.mbio.co.jp

Nakashiki, Norikazu
Central Research Institute of Electric Power Industry
1646 Abiko
Abiko-shi, Chiba
Japan 270-1194
E-mail: nakasiki@criepi.denken.or.jp

Nakata, Hitoshi
Kobe Steel, Ltd.
9-12, Kitashinagawa 5-chome
Shinagawa-ku, Tokyo
Japan 141-0001
E-mail: aa14971@steel.kobelco.co.jp

Nishioka, Jun
Central Research Institute of Electric Power Industry
1646 Abiko
Abiko-shi, Chiba
Japan 270-1194
E-mail: nishioka@criepi.denken.or.jp

Saitoh, Sei-ichi
Graduate School of Fisheries Science
Hokkaido University
3-1-1 Minato-cho
Hakodate, Hokkaido
Japan 041-8611
E-mail: ssaitoh@salmon.fish.hokudai.ac.jp

Saito, Hiroaki
Hokkaido National Fisheries Research Institute
116 Katsurakoi
Kushiro, Hokkaido
Japan 085-0802
E-mail: hsaito@hnf.affrc.go.jp

Senno, Yasunori
Toyo Glass Co. Ltd.
3-2-3 Yako, Kawasaki-ku
Kawasaki-shi, Kanagawa
Japan 210-0863
E-mail: yasunori_sennoh@toyo-glass.co.jp

Sourin, Yosiki
Institute for Chemical Research
Kyoto University
Uji, Kyoto
Japan 611-0011
E-mail: sohrin@scl.kyoto-u.ac.jp

Takahashi, Masayuki Mac
Department of Biology
University of Tokyo
3-8-1 Komaba, Meguro-ku
Tokyo
Japan 153-890
E-mail: ctkmac@mail.ecc.u-tokyo.ac.jp

Takeda, Shigenobu
Central Research Institute of Electric Power Industry
1646 Abiko
Abiko-shi, Chiba
Japan 270-1194
E-mail: s-takeda@criepi.denken.or.jp

Tsuda, Atsushi
Hokkaido National Fisheries Research Institute
116 Katsurakoi
Kushiro, Hokkaido
Japan 085-0802
E-mail: tsuda@hnf.affrc.go.jp

Tsumune, Daisuke
Central Research Institute of Electric Power Industry
1646 Abiko
Abiko-shi, Chiba
Japan 270-1194
E-mail: tsumune@criepi.denken.or.jp

Uematsu, Mitsuo
Ocean Research Institute
University of Tokyo
1-15-1 Minamidai
Tokyo, Nakano-ku
Japan 164-8639
E-mail: uematsu@ori.u-tokyo.ac.jp

Watanuki, Akira
Tetra Co., Ltd.
Shinjuku I-Land Wing
6-3-1, Nishi Shinjyuku, Shinjuku-ku
Tokyo
Japan 160-8350
E-mail: watanuki@tetra.co.jp

RUSSIA (1)

Gramm-Osipov, Lev M.
Pacific Oceanological Institute, FEB RAS
43, Baltiyskaya Street
Vladivostok
Russia 690041
E-mail: lmgramm@nettaxi.com

U.K. (2)

Law, Cliff S.
Plymouth Marine Laboratory
Prospect Place, The Hoe
Plymouth
U.K. PL1 3 DH
E-mail: csl@pml.ac.uk

Obata, Hajime
Oceanography Laboratories
University of Liverpool
U.K. L69 7ZL
E-mail: obata@liverpool.ac.uk

U.S.A. (5)

Chai, Fei
School of Marine Sciences
University of Maine
5741 Libby Hall
Orono, ME
U.S.A. 04469
E-mail: fchai@maine.edu

Coale, Kenneth H.
Moss Landing Marine Laboratories
California State University
8272 Moss Landing Road
Moss Landing, CA
U.S.A. 95039
E-mail: coale@mlml.calstate.edu

Cochlan, William P.
Romberg Tiburon Center for Environmental Studies
San Francisco State University
3152 Paradise Drive
Tiburon, CA
U.S.A. 94920-1205
E-mail: cochlan@sfsu.edu

Rue, Eden L.
Institute for Marine Sciences
University of California, Santa Cruz
1156 High Street
Santa Cruz, CA
U.S.A. 95064
E-mail: elrue@cats.ucsc.edu

Wells, Mark L.
School of Marine Sciences
University of Maine
5741 Libby Hall
Orono, ME
U.S.A. 04469
E-mail: mlwells@maine.edu

PICES (1)

Bychkov, Alexander
c/o Institute of Ocean Sciences
P.O. Box 6000
Sidney, BC
Canada V8L 4B2
E-mail: Bychkov@pices.int